THE ASTROPHYSICAL JOURNAL

AN INTERNATIONAL REVIEW OF SPECTROSCOPY AND
ASTRONOMICAL PHYSICS

VOLUME 89 JUNE 1939 NUMBER 5

THE RELATIONS BETWEEN ERUPTIONS AND SUNSPOTS

R. G. GIOVANELLI

ABSTRACT

In this paper a preliminary examination is made of the statistical relationships between sunspots and the solar eruptions that are associated with them. The analysis deals with the probability of an eruption in relation to the size, type, and development of the associated spot group.

MATERIAL

The material available at present consists of the following:

a) The lists of eruptions published in the *Bulletin for Character Figures of Solar Phenomena*. These first appeared in 1935, and the data for 1935–37, involving 1399 eruptions, have been used.

b) The areas of spots published in the *Monthly Weather Review*. It would have been desirable to use the Greenwich values, but these are not yet at hand. Since the foregoing areas have been contributed by different observatories, they do not form a consistent set. To eliminate systematic errors for each observatory, comparisons with Greenwich areas (umbra + penumbra) were made for several hundred individual spots selected at random throughout 1928–34. The mean factors obtained to reduce the areas to standard Greenwich values were as follows:

U.S. Naval (1935, 1936)	1.37
U.S. Naval (1937)	0.875
Mount Wilson	1.10
Harvard	1.01

Since the United States Naval Observatory increased their areas from January 1, 1937, by a factor of 1.57,[1] the reduction factor has, in this case, been changed to 0.875 since that date.

c) The types, and maximum magnetic fields, of spot groups published in the *Publications of the Astronomical Society of the Pacific.*

From the spot and eruption co-ordinates, most eruptions can be associated with particular spot groups. Many spot groups, however, have not been accompanied by observed eruptions, and these groups have been omitted. Although this affects the analysis to a certain extent, it has been necessary in order to allow the inclusion of the three years of observations with reasonable consistency. In the early period comparatively few observatories were co-operating, and consequently most eruptions passed unreported. However, the average daily number of hours of effective observations from October, 1936, to December, 1937, was 9.3,[2] and so approximately 39 per cent of all eruptions during this period would be observed. The foregoing limitations of groups enables a much higher degree of consistency to be obtained in the ratios of eruptions to spot areas throughout the period under discussion. Estimated corrections will be considered later.

For each spot group satisfying the foregoing condition the following information was tabulated: (*a*) date, (*b*) corrected area, (*c*) increase in area during the next twenty-four hours, (*d*) eruptions observed during the day, (*e*) type of spot group, and (*f*) maximum magnetic field associated with the group.

The areas were measured about 16:00 U.T. and may well be taken as the mean areas during the day. They were interpolated where necessary.

CORRELATIONS

In what follows, the probability of an eruption, P', is defined as the average number of eruptions observed per day per spot group (as distinct from those which occur whether observed or not).

a) *Spot areas.*—The daily areas were first separated into conveniently small ranges, and the probability of an eruption was obtained for groups lying in each range. The results are given in Table 1.

---

[1] *Monthly Weather Review,* **65,** 65, 1937.

[2] *Zs. f. Ap.,* **16,** 286, 1938.

The probability P' was then plotted against the mean areas, as in Figure 1. The graph through the points can be represented fairly well by a straight line. Although eruptions can occur in a spot-free area, this is a comparatively rare event, and the probability that an eruption will occur in any particular spot-free neighborhood is negligible. The graph in Figure 1, however, does not pass through the origin. The explanation of this is to be found in the method of selection of spot groups. Since, from Figure 1, it appears that eruptions are much more probable with large than with small groups, it follows that in the foregoing analysis small spot groups will often be neglected. Sample counts of the more homogeneous 1937 data show that if these had been included the graph would pass through the origin. On the other hand, since it is almost certain that all large spot groups have had eruptions associated with them, the probabilities for large groups require little or no correction. The graph has

TABLE 1

Area Range*	Mean Area	Total Groups†	Total Eruptions	P'
1– 25	12	215	34	0.158
26– 50	38	268	37	0.138
51– 75	62	190	46	0.242
76– 100	88	228	59	0.259
101– 150	125	348	83	0.239
151– 200	175	266	90	0.338
201– 250	225	209	80	0.383
251– 300	275	244	101	0.415
301– 350	325	155	69	0.445
351– 400	375	127	57	0.449
401– 500	450	218	124	0.570
501– 600	550	168	101	0.601
601– 700	650	110	78	0.709
701– 800	750	63	73	1.16
801– 900	850	84	76	0.903
901–1000	950	40	42	1.05
1001–1100	1050	40	41	1.02
1101–1200	1150	22	23	1.04
1201–1300	1250	19	28	1.47
1301–1500	1400	23	26	1.23
>1500	1925	52	124	2.38

* Millionths of the sun's hemisphere.

† A group is counted once for each day it is present on the sun's disk.

therefore been corrected to pass through the origin, as is shown in Figure 1.

From the graph we are led to the conclusion that the probability that an eruption will be observed in the neighborhood of a spot group is directly proportional to the area of the group.

To investigate possible variations in activity with type, the same procedure was repeated for the spot groups of each type. Straight-line graphs, similar to Figure 1, were obtained in all cases except for types α and αf, for which insufficient data were available. Except for the very active type γ, the graphs required slight corrections to pass through the origin. The slopes of these graphs give k, the probability of an eruption per unit area (one-millionth of the sun's hemisphere) for the different types, and these are given in Table 2.

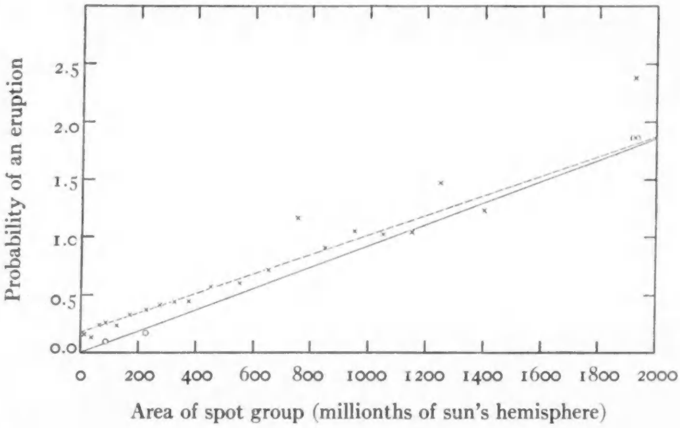

FIG. 1.—Crosses give values of P', the probability of an eruption per spot group per day, uncorrected for the arbitrary selection of spot groups; these are represented by the broken line. Circles represent sample counts including all spot groups, using 1937 data. Corrected values are given by the smooth line. The bracketed point for spots of mean area 1925 is obtained by omitting the extremely active group No. 4 in *Bulletin* No. 40.

It must be remembered that k refers to the probability that an eruption was observed in the neighborhood of a spot group. To obtain the probability that an eruption occurred, whether it was observed or not, a factor of 2.6 must be applied to k. During the latter part of the period under discussion, an effective observing period of

9.3 hours per day would result in 39 per cent of all eruptions being observed. Now, the majority of the eruptions used occurred during this period; the results for the earlier period have been rendered more homogeneous by our selection of spot groups, and the correction for a nonuniform selection of spot groups has been applied. In view of this, the use of the factor of 2.6 in conjunction with the results for the whole three years seems to be justifiable.

The αp, or unipolar type, is least active, and the activity increases as we proceed through the β to $\beta\gamma$ and γ types. It is interesting to note that the β, βf, and βp types all have the same activity, the equality between the latter two merely indicating that the orientation of the group has no influence on its activity.

TABLE 2

Type	No. of Groups	No. of Eruptions	k Probability of an Eruption per Area of One-millionth of the Sun's Hemisphere
αf	11	1	....
α	68	6	....
αp	508	130	0.81×10^{-3}
βf	246	110	0.96×10^{-3}
β	589	255	0.96×10^{-3}
βp	1124	416	0.96×10^{-3}
$\beta\gamma$	286	314	1.20×10^{-3}
γ	73	117	2.05×10^{-3}
Weighted mean	....	....	0.96×10^{-3}

It will be noticed that in Figure 1 the point for the largest group lies well off the curve. This irregularity can now be explained. One very large group of the γ type crossed the central meridian on October 4, 1937. Associated with this was the exceptional number of fifty-nine eruptions, of which forty-four occurred on nine days when the area was greater than 1500. If we neglect this group entirely, the bracketed point in Figure 1 is obtained, lying well on the graph. It is apparent that the exceptional position of the point is due to a fluctuation in the representation of the different types of groups introduced by this one group. No such discrepancy was found on the γ-type graph.

b) *Spot changes.*—It appears to be generally accepted that eruptions are most frequent during the growth of spots. To investigate this the life of a spot was separated into the following periods: (1) early growth, comprising the period up to half the maximum size of a spot; (2) late growth, up to the maximum size; (3) maturity, the period during which the spot area remains near its maximum; (4) early decay, from maturity down to half the maximum size; and (5) late decay, the final stages of the life of the spot.

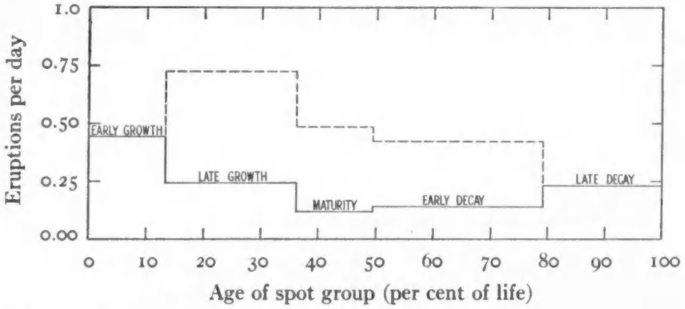

FIG. 2.—The probability of an eruption during the various stages of the life of a group is given by the broken curve, while the smooth curve represents the probability divided by the area as given in Table 3.

The duration assigned to each period was proportional to the number of times groups were placed in that period.

The average number of eruptions per day was plotted against the phase of growth, the mean duration of the latter being represented as a fraction of the total life of the group (Fig. 2). To detect variations in activity during these stages a simple correction for area was made by assigning to the mean areas during each period the relative values shown in Table 3.

The eruptions per unit area per day are also plotted in Figure 2. It is seen that the probability of an eruption per unit area, which may be called the intrinsic activity, is greatest around early growth, with a smaller maximum around late decay and a minimum at maturity, although the greatest number of eruptions occur during late growth. Sixty-two per cent, or nearly two-thirds of the eruptions, occur during the growth to the end of the mature stage, i.e., in the first half of the life of the group, while only 38 per cent occur during the second half.

The probability of an eruption was next plotted against the rate of increase of area. With the material available this graph was derived as follows: The probability was plotted against the change of area in the period (*a*) 24–0 hours before the eruption and (*b*) 0–24 hours after the eruption.

For these purposes the eruptions were presumed to take place at the time the area was measured on the day of the eruption. The plots show close resemblances and are shown in Figure 3, together with their mean curve; this represents the probability associated with the rate of change of area at the time of the eruption.

TABLE 3

Phase	Duration (Per Cent of Life)	Mean Area
Early growth	13.5	1
Late growth	23.0	3
Maturity	13.0	4
Early decay	30.0	3
Late decay	20.5	1

So far no attempt has been made to separate the effect due to the growth from that due to the area; to do this the following procedure was adopted:

Suppose the probability of an eruption, P', to be dependent upon the area a and upon the rate of change of area i, and that it takes the form

$$P' = F(a) \cdot f(i) ,$$

where $F(a)$ and $f(i)$ are functions of a and i, respectively. Let $N(a, i)\,\delta a\delta i$ be the number of groups with areas in the range $a - \frac{1}{2}\delta a$ to $a + \frac{1}{2}\delta a$ whose rates of change of area lie between $i - \frac{1}{2}\delta i$ and $i + \frac{1}{2}\delta i$. The total number of groups whose rates of change of area lie within these limits is thus

$$\sum^{a} N(a, i)\delta a\delta i ,$$

and the corresponding number of eruptions will be

$$\sum^{a} N(a,\, i)\delta a\delta i \cdot F(a) \cdot f(i)\,.$$

Hence, the probability of an eruption associated with an area change i, that is, $P'(i)$, is given by

$$P'(i) = \frac{\sum^{a} N(a,\, i)\delta a\delta i\, F(a) \cdot f(i)}{\sum^{a} N(a,\, i)\delta a\delta i}$$

and

$$f(i) = \frac{P'(i)}{A(i)}\,,$$

where

$$A(i) = \frac{\sum^{a} N(a,\, i)\delta a\delta i \cdot F(a)}{\sum^{a} N(a,\, i)\delta a\delta i}\,.$$

Given $F(a)$ and the distribution $N(a,i)\delta a\delta i$, together with the function $P'(i)$, the values of $f(i)$ can now be calculated. Now, it has already been shown that the probability is directly proportional to the area, so that $F(a)$ should take the form $k \cdot a$. However, it must be remembered that in the analysis there has been a restriction on the spot groups used. For the evaluation of $A(i)$ then, $F(a)$ is to be given by the uncorrected curve in Figure 1. As the rates of change of area at the actual time of the eruption are not immediately available, it is necessary to use the changes in area for the twenty-four hours before and after the eruption (assumed to take place at the time the area was measured on that day). The simplest procedure was considered to be as follows.

The two sets of values of $N(a,i)\delta a\delta i$ for $a = 25, 75, 125$, etc., and $i = \pm 25, \pm 75, \pm 125$, etc., with $\delta a = 50$ and $\delta i = 50$ (i here referring to the change of area [*a*] on the day preceding the eruption, [*b*] on the day following the eruption), were obtained and two sets of corresponding values $A(i)$ were derived. These were respectively combined with values of $P'(i)$ referring to the same periods, given in Figure 3. Two sets of $f(i)$ were then calculated and are given in Table 4.

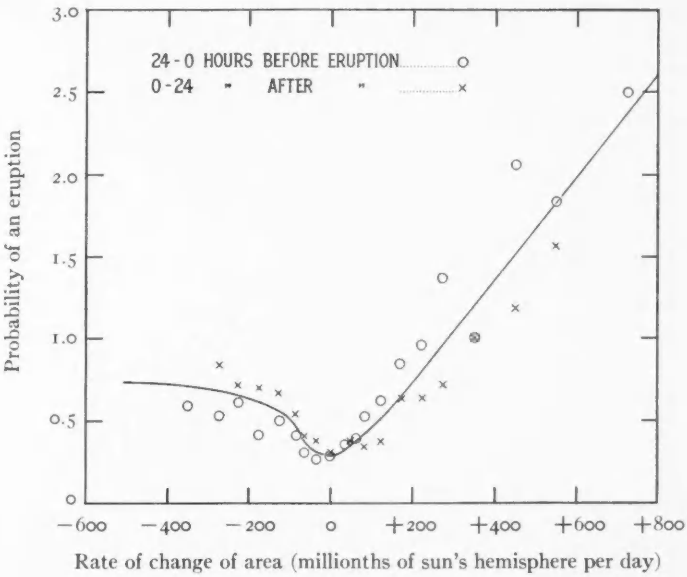

FIG. 3.—The probabilities of an eruption associated with changes in area during the days preceding and following the eruption are given by circles and crosses, respectively. The probability associated with the rate of change of area at the time of the eruption is given by the smooth curve through their means.

The mean value of $f(i)$ was plotted against the area change, as in Figure 4. It may be said to represent the effect of spot growth on eruption probability.

It is seen that for decreases of area and for small increases of area the eruption probability is independent of area change, while for large increases of area the probability increases uniformly. The graph may be fairly well represented by the two lines

$$f(i) = 0.90 \text{ for } i < +75 ,$$

$$f(i) = (0.70 + .0025i) \text{ for } i > +75 .$$

TABLE 4

i	*f(i)*		
Increase of Area in Millionths of the Sun's Hemisphere Per Day	Preceding Day	Following Day	Mean
−475	0.79	0.74	0.77
−275	0.83	0.89	0.86
−225	0.89	0.95	0.92
−175	1.02	1.11	1.06
−125	0.94	1.03	0.98
− 75	0.86	0.94	0.90
− 25	0.77	1.04	0.90
+ 25	0.89	0.86	0.88
+ 75	1.02	0.74	0.88
+125	1.25	0.85	1.05
+175	1.32	1.09	1.20
+225	1.26	1.10	1.18
+275	1.44	1.56	1.50
+325	1.60	1.72	1.66
+375	1.81	2.06	1.93
+475	1.48	1.86	1.67
+675	1.83	2.31	2.07

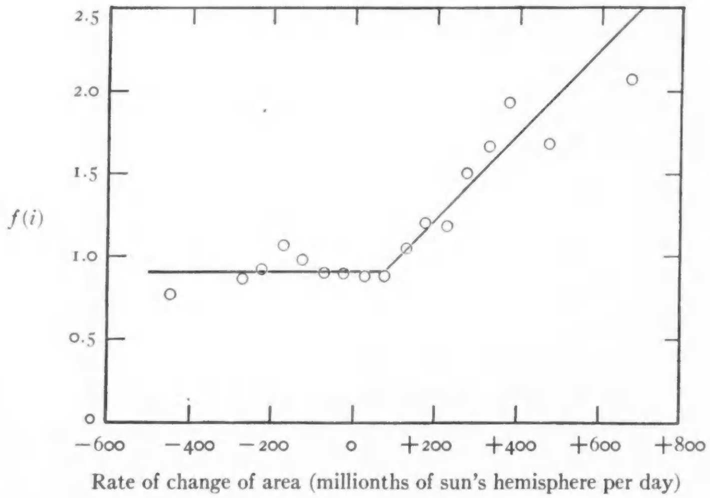

FIG. 4.—The function, *f*(*i*), representing the effect of spot growth on eruption probability is plotted as a function of *i*, the rate of change of spot area at the time of the eruption. The graph has been represented by two straight lines.

It is now possible to offer, in part, an explanation of the graph in Figure 2. Although curves are not available giving the mean areas of a spot group throughout its life, growth curves of "leader" spots are available.[3] If we assume that the groups have a similar behavior, the growth may be generally stated as follows: first, a rapid increase in area, followed by a slower increase; then, after passing through its maximum stage, a decrease, becoming less rapid toward the end of the life of the group. From Figure 4 we see that at the stage of early growth, with a rapid increase in area, a high probability will result; as the increase becomes slower, and, after a stationary period, a decrease takes place, the eruption probability, corrected for area, decreases and reaches a steady value.

This description is much the same as the graph in Figure 2, and there seems little doubt that the graph may be for the most part explained in this manner. It is only with the increase in activity in the final stages of decay that the age of the group seems to have any significance. Even then it must be remembered that the correction applied for area in Table 3 is only approximate, and it is quite possible that the apparent increase in intrinsic activity during late decay may be largely due to this approximation.

c) *Magnetic fields.*—The possibility of large magnetic fields present in spots playing an important part in eruptions has been investigated. Unfortunately, daily measurements of fields are not available, and only maximum values are published. The probability of an eruption was first plotted against the maximum magnetic field. Here again, although a straight-line graph was indicated, the magnetic field bears a statistical relation to the size of the group; and, in order to obtain more definite information, groups with a maximum area between three and four hundred millionths of the sun's hemisphere were selected. A plot was made (Fig. 5) in which individual points are shown. It is clear that there is no close relation between the maximum magnitude of the magnetic field and the probability of an eruption.

d) *Importance of eruptions.*—In the foregoing investigations the eruptions were all taken as of equal importance; no attempt has been made to weight them according to area, brightness, or duration.

---

[3] *Greenwich Photoheliographic Results*, 1924.

As a point of interest, the ratio of eruptions of importance 3 to the total number of eruptions has been obtained for the various types of spot groups (Table 5).

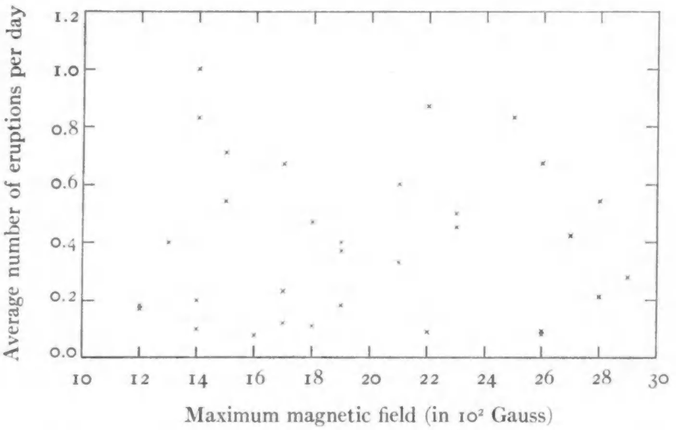

FIG. 5.—The average number of eruptions per day associated with spot groups having a maximum area between three and four hundred millionths of the sun's hemisphere is plotted against the maximum value of the magnetic field in the spot. It is clear that there is no close correlation.

TABLE 5

Type	α	β	βγ	γ	All Types
Number of eruptions of importance 3	7	24	18	8	57
Total number of eruptions	137	781	314	117	1349
$\frac{\text{Eruptions of importance 3}}{\text{Total number of eruptions}}$	5.1%	3.1%	5.7%	6.8%	4.2%

It seems probable that the fraction increases from type to type and that the α value is discordant, owing to insufficient data.

CONCLUSIONS

The probability, *P*, of an eruption occurring in the neighborhood of a spot group depends on the following factors:

a) It is proportional to the area *a*.

b) The factor of proportionality is 2.6 *k*: *k* is itself a function of the type of spot group, and its values are given in Table 2; while 2.6 is a factor applied to correct for the partial nature of the eruption observations.

c) It is a function $f(i)$ of the rate of increase of area, and this function is given in Figure 4.

d) It is not influenced by the maximum magnitude of the magnetic field.

e) There is no explicit influence of the age of the spot group, except a possible increase in activity in the final stages of decay.

The probability may thus be generally expressed as

$$P = 2.6\, k \cdot a \cdot f(i) \ ,$$

but in the final stages of decay, the probability may assume a higher value than is given by this expression.

Commonwealth Solar Observatory
Canberra
December 16, 1938

THE GALACTIC STRUCTURE IN TAURUS

II. THE SPACE DISTRIBUTION OF THE STARS

S. W. McCUSKEY

ABSTRACT

An analysis of general star counts to the 15 mag. for areas in Taurus selected for their uniformity of stellar surface distribution and apparent freedom from nebulosity has yielded the following picture of galactic structure for the longitude and latitude range $\lambda = 120°$ to $150°$, $\beta = 0°$ to $-30°$.

a) The characteristic feature of the run of space density with distance from the sun is a high negative gradient in all latitudes. No reasonable assumption of a uniform interstellar absorption will eliminate the large decrease in density within 600 parsecs of the sun. For the present analysis a value 0.5 mag. per kiloparsec has been used as the coefficient of absorption. The application of larger coefficients leads to improbably high densities at distances of 4 or 5 kiloparsecs. A local clustering of stars near the sun appears to be evident from the data. The presence of a high negative density gradient in other longitudes has, of course, been known for some time.

b) At high latitudes ($-20°$ to $-30°$) a high concentration of stars appears to be present in the immediate vicinity of the sun. This effect may be spurious, however, and due to a serious variation of the luminosity function for this range in latitude. A survey of the spectral distributions reveals a large excess of F stars in the vicinity.

c) A cross-section of the galaxy in these longitudes in a plane perpendicular to the galactic plane is shown in Figure 2. Contours indicate the curves of equal space density.

d) At a distance of 400 parsecs from the sun the decrease in density in a direction perpendicular to the galactic plane is more rapid than that in the neighborhood of the sun. The variation is exhibited in Figure 4.

For distances greater than 1000 parsecs the maximum space density does not occur in the adopted galactic plane (pole 12^h40^m, $+28°$) but some 50–200 parsecs from it. The effect may be interpreted, tentatively, as an indication of the asymmetric position of the sun relative to the galactic plane.

e) Star counts in eight of the most highly obscured regions have been analyzed to determine the approximate distance and absorbing power of the nebulous matter. The mean values for ϵ and r are 1.9 mag. and 142 parsecs, respectively.

f) To provide surface-distribution data in addition to that used in the present article, a table of log $N(m)$ for 31 supplementary regions in Taurus is appended.

Further discussion of the general Taurus-Orion region will be deferred until the colors and spectra for the brighter stars are available. At present the star counts are being extended to fainter magnitude limits in the unobscured areas.

The complexity of the galactic structural details in Taurus, as evidenced in the surface distribution of stars brighter than photographic magnitude 15, has already been shown in a previous communication,[1] bearing the same general title as above. Star counts, made from plates taken with the 4-inch Ross lens of the Harvard

---

[1] *Ap. J.*, **88**, 209, 1938. This paper and the present one form Part III of a series entitled "Investigations of Galactic Structure," published as a result of co-operative research between the Harvard College Observatory and astronomers elsewhere.

College Observatory and based as closely as possible on the International Scale of photographic magnitudes, have indicated that much of the irregularity of the Taurus region is due to an extensive near-by layer of absorbing material. Concentrations of this veil of obscuring matter have been found to absorb as much as 4 mag. in photographic light, while the average for the whole region is about 1.5 mag.

By an inspection of the plates it has been possible to choose 38 regions of 3.1 square degrees each, in which the overlying nebulosity apparently has little influence on the star counts. These areas have been combined in zones at intervals of 2°.5 in galactic latitude, the average range in longitude being 14°.4 for a zone. Mean values of log $N(m)$ as a function of m for these zones are tabulated in the paper mentioned above (hereafter called "I").

TABLE 1

AVERAGE MAXIMUM RESIDUALS, LOG N(ZONE) *minus* LOG N(AREA)

m	Average Max. Residual	P.E. of Counts	m	Average Max. Residual	P.E. of Counts
8.0	0.19	±0.08	12.0	0.06	±0.04
9.0	.12	.07	13.0	.07	.04
10.0	.07	.04	14.0	.07	.03
11.0	0.07	±0.04	15.0	0.07	±0.03

It has been assumed that the mean values of log N(m) for the various zones of latitude represent the background structure of the galaxy in this region. That no serious fluctuations occur among the areas of a given zone is shown in Table 1, in which the average maximum residual, log N(zone) *minus* log N(area), has been entered. For comparison, the probable errors in counting are also tabulated. On the average, the largest deviation from the mean of a zone is not significantly larger than the errors inherent in the counts. No dependence of these fluctuations upon galactic latitude was found.

It has been shown in I that the zone means of log $N(m)$ progress smoothly with galactic latitude. For analysis of space densities, therefore, either the mean values of log $N(m)$ taken from Table 4 of I or the values derived from the curves of Figure 2 (same paper) may be used.

The density function at $\beta = 0^\circ$.—An attempt to determine from general star counts the arrangement of the stars in space must necessarily involve a knowledge of, or an assumption concerning, the interstellar absorption for the region investigated. Whether the amount of this general absorption depends in a simple way upon the distance of the stars concerned is problematical. Heretofore investigators have assumed a constant coefficient of absorption, A; and in spite of the uncertainty in such an assumption, I have adopted a similar procedure here.

In the absence of extensive counts of external galaxies and of color excesses for the Taurus region, A has been determined by choosing the most reasonable of the space-density distributions computed under various assumptions of interstellar absorption. The variation of the absorbing medium with galactic longitude makes it inadvisable to use an average coefficient, such as that derived by Joy[2] from the galactic rotation effects in the radial velocities of Cepheid variables.

An analysis of the mean values of log $N(m)$, converted into log $A(m)$, for the apparently unobscured regions in the $\beta = 0^\circ$ zone in Taurus was made by trial and error, using the $(m, \log \pi)$ tables as discussed by Bok.[3] In the preliminary solution A was assumed to be zero. Column 2 of Table 2 gives the density function $D(r)$ which best represents the observed values of log $A(m)$. The average difference between observed and computed values of $A(m)$ was 3.9 per cent. The luminosity function for photographic magnitudes proposed by van Rhijn[4] has been used in the computation. The curves of Figure 1 indicate the closeness with which the observed log $A(m)$ are fitted by the computed values, for $\beta = 0^\circ$ as well as for the other zones of latitude to be discussed later. $D(r)$ is expressed throughout the analysis in terms of the density near the sun as unit.

Preliminary to a recomputation by trial and error for various assumptions as to the coefficient of absorption, I have used a formula, given by Seeliger and others, which provides a rapid means of converting the densities computed with $A = 0$ into the densities for other values of A. Columns 3, 4a, and 6 of Table 2 give the values of $D(r)$ computed in this way for $A = 0.3$, 0.5, and 1.0 mag. per kiloparsec.

---

[2] *Publ. A.A.S.*, **7**, 218, 1933.

[3] *The Distribution of the Stars in Space* ("Astrophysical Monographs"), p. 26, 1937.

[4] *Groningen Pub.*, No. 47, 1936.

An inspection of Table 2 shows the improbability of the assumed value $A = 1.0$ mag. per kiloparsec. The region of the sky in question lies near the anti-center of the galaxy; and, if the present dimensions of the system and the position of the sun given by dynamical considerations are adopted, a concentration of stars at 3000–5000 parsecs greater than that near the sun appears unlikely, although the presence of a spiral-arm effect is not to be considered impossible. On the other hand, however, too much stress cannot be put upon the accuracy of the densities at distances greater than 2500 parsecs.

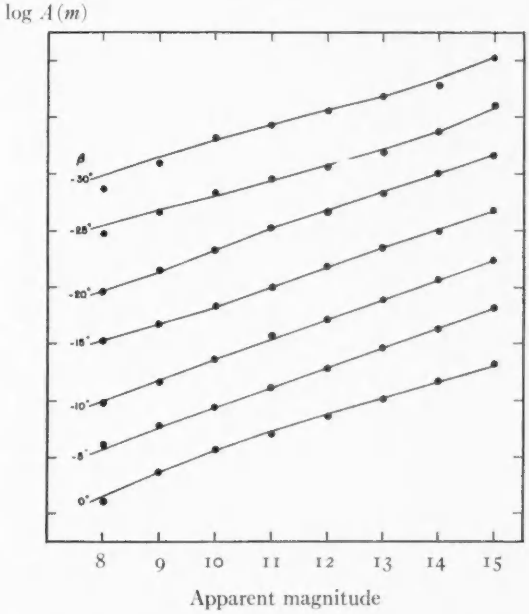

FIG. 1.—Observed and computed variations of log $A(m)$. The points are observed values; the curves are computed. Ordinates are values of log $A(m)$, the zero point of the scale being shifted for each curve. Abscissas are photographic magnitudes.

All of the functions of Table 2 agree in showing a region of relatively high density extending to distances of 400 or 500 parsecs from the sun, followed by a rapid decrease in density in the next 500 parsecs. The presence of this high negative gradient in several directions from the sun has been apparent in many previous investigations of galactic structure and forms a part of the evidence for the existence of a local cluster.

The reality of the space distribution of stars found here rests naturally upon the assumptions made concerning interstellar absorption. If, as an alternative to the foregoing analysis, the star density in the galactic plane were assumed to be the same at all distances as that near the sun, then the following distribution of absorption would be necessary in order that the observed data be reproduced:

TABLE 2

DENSITY FUNCTIONS IN THE GALACTIC PLANE

(1) r (PARSECS)	$D(r)$						
	(2) $A=0$	(3) $A=0.3$	(4) $A=0.5$		(5) $A=0.8$	(6) $A=1.0$	(7) van Rhijn
			(*a*)	(*b*)			
100	1.00	1.06	1.10	1.00	1.00	1.20	0.93
160	1.00	1.09	1.16	1.10	1.20	1.34	.87
250	1.00	1.14	1.25	1.10	1.50	1.55	.76
400	0.75	0.88	0.95	1.10	1.00	1.21	.68
630	0.35	0.40	0.46	0.46	0.45	0.49	.60
1000	0.10	0.14	0.22	0.22	0.25	0.29	.28
1600	0.05	0.09	0.12	0.12	0.10	0.31	.28
2500	0.03	0.08	0.18	0.05	0.20	0.68	0.55
4000	0.02	0.12	0.30	0.05	0.35	1.24	....
6300	0.15	0.13	0.42	0.10	0.50	1.80	....

r	$\leqslant 200$	316	500	800	1260	2000	$\geqslant 3000$ parsecs
Δm*	0.0	0.2	1.0	1.8	3.1	4.7	5.0 mag.

* Δm is the absorption suffered by the light of a star at distance r.

It may be inferred from these results and from the evidence of other investigators that the alternative to a local cluster of stars surrounding the sun is a local ring-shaped condensation of obscuring matter, whose effect is practically complete, at least in the direction of the galactic anti-center, for stars at distances exceeding 2500 parsecs. In this direction the condensation would be greatest at distances of 200–700 parsecs. That the sun is immersed in such an extensive dark nebula of the dimensions and shape indicated seems highly improbable.

The inherent difficulty and uncertainty in fixing the value of the interstellar absorption may be eliminated to a large degree by the use of data on the colors and spectral types of faint stars in the field to be analyzed. With this in view a program of color determinations for the stars in Taurus whose spectral types will be forthcoming in the *Henry Draper Extension* is now under way. The resulting color excesses, combined with the fairly well-known ratio of selective to general interstellar absorption, should fix more securely the values for absorption in the Taurus fields.

Pending the completion of these data and in view of the results presented in Table 2, it will be assumed that a satisfactory first approximation to the galactic structure in Taurus may be obtained by the use of a constant coefficient $A = 0.5$ mag. per kiloparsec for the general absorption. The half-thickness of the absorbing layer will be taken as 300 parsecs.

The similarity of the star-count data for relatively unobscured areas in Taurus to that in Perseus, where Shapley and Miss Jones[5] find a great many external galaxies at low galactic latitudes, indicates that the total absorption cannot be very large. More recent nebular counts to the eighteenth mag., made by Miss Jones, in regions surrounding some of the darkest obscurations in Taurus have shown a surprisingly large number of objects shining through several of the regions selected for the present analysis as being relatively clear. These results, kindly communicated by Dr. Shapley and Miss Mohr, confirm, at least qualitatively, the absence of appreciable absorption in the areas between the clouds.

Van Rhijn[6] has recently published an analysis of star counts for space density in the galactic plane which furnishes a comparison with the function $D(r)$ computed from the Taurus counts with $A = 1.0$. Van Rhijn's densities are for longitude 145°, which corresponds to the mean longitude, in the galactic plane, of the present investigation. The two analyses agree well for distances greater than 500 parsecs, as is shown in the last two columns of Table 2. For the smaller values of r, the differences are quite large.

---

[5] *Harvard Bull.*, No. 909, 1938.

[6] *Op. cit.*

Density functions at higher latitudes.—Using the adopted value for A, 0.5 mag. per kiloparsec, I have computed by trial and error the density functions at intervals of 5° in galactic latitude to the limit of the counted region at $\beta = -30°$. The resulting functions are given in Table 3. Figure 1 indicates the agreement between computed and observed values of log $A(m)$. Variations in the accepted luminosity function with height above the galactic plane, according to the work of Oort,[7] have been adopted for these computations.

TABLE 3

STELLAR SPACE DENSITY AS A FUNCTION OF GALACTIC LATITUDE

r (PARSECS)	$D(r)$						
	$\beta=0°$	$\beta=-5°$	$\beta=-10°$	$\beta=-15°$	$\beta=-20°$	$\beta=-25°$	$\beta=-30°$
40	1.00	1.00	1.00	1.00	1.00	1.00	1.00
63	1.00	1.00	1.00	1.00	1.00	2.50	3.00
100	1.00	1.00	1.00	1.00	1.00	2.50	2.50
160	1.10	1.10	0.75	1.10	1.10	2.00	1.50
250	1.10	0.80	0.60	0.80	0.80	0.50	0.50
400	1.10	0.45	0.40	0.50	0.50	0.10	0.10
630	0.46	0.35	0.30	0.20	0.20	0.05	0.05
1000	0.22	0.25	0.25	0.10	0.10	0.05	0.03
1600	0.12	0.20	0.15	0.05	0.05	0.05	0.03
2500	0.05	0.20	0.10	0.05	0.05	0.05	0.05
4000	0.05	0.20	0.05	0.05	0.05	0.05	0.05
6300	0.10	0.15	0.05	0.05	0.05	0.05	0.05

The principal features of the galactic structure in Taurus, evident from Table 3, are:

1. At every range in latitude the high negative density gradient is apparent, with the region at $\beta = -10°$ particularly conspicuous because of the abrupt and rapid decrease in $D(r)$ between 200 and 600 parsecs. An abrupt decrease in density occurs also in the galactic plane at approximately 500 parsecs.

2. There appears to be a high concentration of stars very near the sun in the latitude interval $-20°$ to $-30°$, an effect which is no doubt due to uncertainty in the luminosity function for this range in latitude and longitude. An inspection of the spectral distributions

---

[7] *B.A.N.*, **6**, 281, 1932.

of stars given in the *Yale Zone Catalogues*[8] for $\delta = +20^\circ$ to $+30^\circ$ shows that the number of F stars in a region at λ 133°, $\beta = -25^\circ$, is double; and at $\lambda = 125^\circ$, $\beta = -31^\circ$, it is three times the number of F stars at $\lambda = 133^\circ$, $\beta = -18^\circ$. The influence of this increase in stars with $M \sim 5$ in the range $m = 8$ to 10 may readily account for the high densities computed by use of the usual luminosity function. Too much stress cannot be laid on these high values of $D(r)$ because of the statistical uncertainty in dealing with the brightest stars in the small areas necessarily employed here.

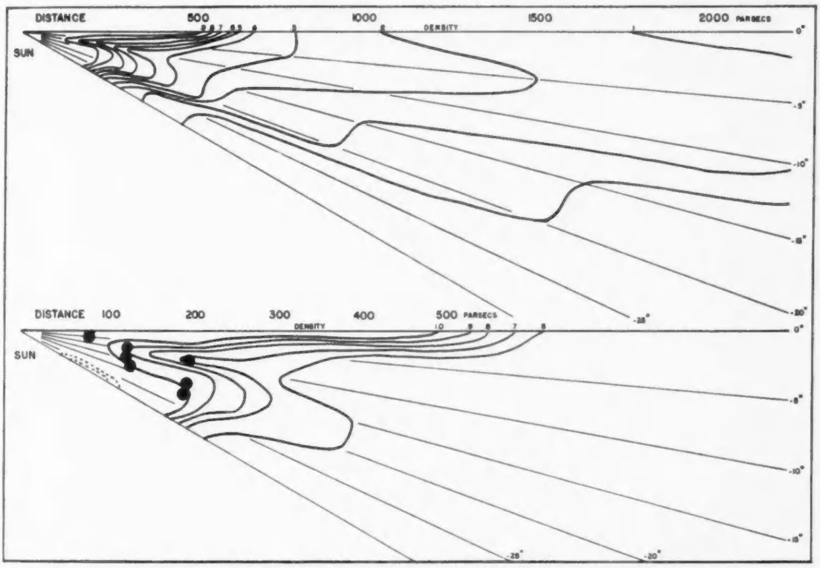

FIG. 2.—Stellar density distribution in Taurus (λ 138°) in a plane perpendicular to the galaxy. The curves are equidensity contours. The upper figure shows the entire region reliably covered by the counts; the lower figure shows the region near the sun, drawn on an enlarged scale. The points in the latter figure indicate the computed positions of the Taurus nebulosity at various latitudes.

3. At distances from the sun exceeding 1000 parsecs, the maximum star density appears near $\beta = -5^\circ$ rather than in the galactic plane.

Figure 2 shows a cross-sectional picture of the structure of the galaxy, in a plane perpendicular to the galactic plane and passing through the sun, for this anti-center region. Equidensity contours have been drawn for the larger region reliably covered by the counts, as well as for the local region surrounding the sun. The variations of $D(r)$ mentioned above are conspicuous, and the presence of a local cluster of stars with its plane of symmetry somewhat inclined to the galactic plane is suggested. It is interesting to note that the inclination found here for the irregularities in star density is nearly the same as that of Gould's belt of bright B stars.

---

[8] *Trans. Yale Univ. Obs.*, Vols. 9 and 10.

The dependence of the details pictured in Figure 2 upon the assumption concerning the behavior of the interstellar absorption should be stressed again. It may be shown, however, that no reasonable assumption of a constant coefficient, A, will remove the observed local cluster effect. Even the distribution of absorbing matter deduced in the preceding section on the basis of a uniform star density in the galactic plane does not remove the negative density gradient at $\beta = -20^\circ$. Using this absorption distribution, I find the following run of densities $D(r)$ for $\beta = -20^\circ$:

r	$\leqslant 160$	250	400	630	1000	1600	2500 parsecs
$D(r)$	1.0	0.8	0.5	0.5	0.8	1.0	1.0

The density decrease within 600 parsecs of the sun persists, and, in addition, a very improbable concentration of stars appears at heights exceeding 500 parsecs from the galactic plane.

A comparison of the general run of star densities for equal distances on either side of the galactic plane in the longitude range 120°–150° is furnished by Table 4. An area at λ 149°, $\beta + 6^\circ$, analyzed by Bok,[9] has been compared with the zone $\beta = -10^\circ$, as given in Table 3.[10]

While there is some evidence for a higher negative gradient at $+10^\circ$, the computations are so dependent upon the brighter stars that little significance can be attached to the difference between the two regions. No conclusion can be drawn for the values of $r > 2500$ parsecs, because of the uncertainty in the densities arising from counts to the 15 mag. only.

A recent investigation by Oort[11] has led to a picture of galactic structure considerably different from the one given here. Using Hubble's[12] nebular counts to determine the total absorption of photographic light in the neighborhood of Selected Areas, Oort has derived relative space densities which indicate that the sun is situated in a star void, the density rising in all galactic longitudes to values at least twice that near the sun.

---

[9] *Harvard Circ.*, No. 371, 1931.

[10] The value $+6^\circ$ on the co-ordinate system used by Bok is nearly $+10^\circ$ on the Harvard system used here.

[11] *B.A.N.*, **8**, 233, 1938.

Admittedly, the use of small sample areas, such as those furnished by the nebular data, does not lead to very certain values for the interstellar absorption. That the fluctuations in log N(neb.) do not always measure truly the presence of absorbing matter is shown in Table 5. Several of the areas included in the Taurus analysis fall near the points for which Hubble has given values of log N(neb.). For these areas a correlation between the fluctuations of nebular density and star density has been obtained. Differences in log $N(m)$ for the star-count data have been formed in the sense log N(zone) *minus* log N(area), and the resulting residuals have been averaged for group means of log N(neb.). The position of the areas in the sky is shown in Figure 3.

TABLE 4

DENSITIES ON OPPOSITE SIDES OF THE GALACTIC PLANE

r (Parsecs)	z (Parsecs)	$\beta = -10°$	$\beta = +10°$	r (Parsecs)	z (Parsecs)	$\beta = -10°$	$\beta = +10°$
100	17	1.00	1.00	1000	174	0.25	0.30
160	28	0.75	0.40	1600	278	.15	.30
250	44	0.60	0.40	2500	435	.10	.30
400	70	0.40	0.30	4000	697	.05	.20
630	110	0.30	0.30	6300	1096	0.05	0.20

The conspicuous lack of correlation between the differences in log N(neb.) and those in Δ log N(stars) should suffice to indicate the uncertainty in using the former for predictions of the total absorption.

If we ascribe the difference in log N(neb.) between rows 1 and 2 of Table 5 to absorption, it is apparent that the absorption must occur beyond the average distance of the fifteenth-magnitude stars. As the areas included are all at galactic latitudes greater than 15°, the absorbing layer would necessarily be high above the galactic plane, probably at a height in excess of 500 parsecs. Oort has already pointed out that the presence of considerable absorption at 500 parsecs would eliminate much of the irregularity of structure resulting from his analysis.

---

[12] *Ap. J.*, **79**, 8, 1934.

TABLE 5

CORRELATION OF LOG N(NEB.) WITH Δ LOG N(STARS)

AREAS	$\overline{\text{LOG } N\text{(NEB)}}$	Δ LOG N(STARS)			
		$m=12$	13	14	15
28, 29, 30, 31	1.83	−0.03	0.00	−0.01	0.00
14, 69	1.21	− .01	− .04	− .05	− .04
81, E	0.73	+0.25	+0.21	+0.17	+0.21

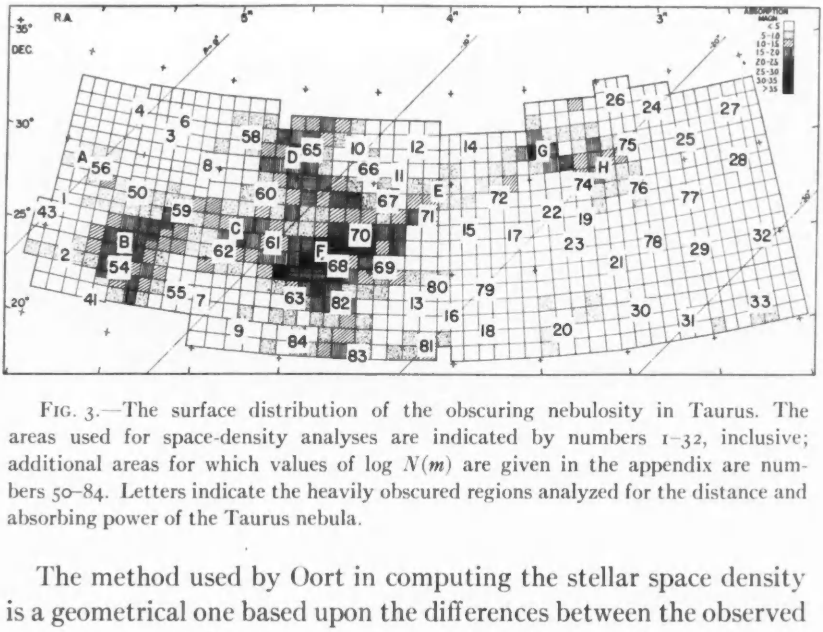
RA
5ʰ
4ʰ
3ʰ
DEC
+35°
30°
25°
20°
ABSORPTION MAGN
< 5
5-10
10-15
15-20
20-25
25-30
30-35
> 35
1
2
3
4
6
7
8
9
10
11
12
13
14
15
16
17
18
19
20
21
22
23
24
25
26
27
28
29
30
31
32
33
41
43
50
54
55
56
58
59
60
61
62
63
65
66
67
68
69
70
71
72
74
75
76
77
78
79
80
81
82
83
84
A
B
C
D
E
F
G
H

FIG. 3.—The surface distribution of the obscuring nebulosity in Taurus. The areas used for space-density analyses are indicated by numbers 1–32, inclusive; additional areas for which values of log $N(m)$ are given in the appendix are numbers 50–84. Letters indicate the heavily obscured regions analyzed for the distance and absorbing power of the Taurus nebula.

The method used by Oort in computing the stellar space density is a geometrical one based upon the differences between the observed star counts and the counts to be expected if the surfaces of equal density are parallel to the galactic plane. No knowledge of the luminosity function or of the distribution of the stars in distance is required. It is interesting, therefore, to compare the densities computed in the previous sections for the Taurus region with those computed for the same data by the Oort-Vashakidse method.

For that purpose I have taken the necessary information concerning the distribution of densities perpendicular to the galactic plane, as well as the values of log $A(m)$ for the galactic polar caps, from Oort's paper. Inasmuch as the details of the method are described fully in Oort's paper, only the results of the computation will be given here. Admittedly, the lack of data for $m > 15$ in the Taurus region and the inhomogeneity likely to arise from the use of different sources of observational material somewhat restrict the application of the geometrical method in the present instance. As a first approximation, however, the results may be considered satisfactory.

TABLE 6

COMPARISON OF OORT-VASHAKIDSE AND STANDARD METHODS

r (PARSECS)	$D(r)$									
	$\beta=-10°$		$\beta=-15°$		$\beta=-20°$		$\beta=-25°$		$\beta=-30°$	
	(A)	(B)	(A)	(B)	(A)	(B)	(A)	(B)	(A)	(B)
0......	1.00	1.00	1.00	1.00	1.00	1.00	1.00	1.00	1.00	1.00
250......	0.60	......	0.80	......	0.80	......	0.50	0.68	0.50	0.69
400......	0.40	......	0.50	0.42	0.50	0.54	0.10	0.40	0.10	0.40
630......	0.30	0.36	0.20	0.34	0.20	0.40	0.05	0.24	0.05	0.20
1000......	0.25	0.31	0.10	0.26	0.10	0.27	0.05	0.18	0.03	0.13
1600......	0.15	0.26	0.05	0.17	0.05	0.14	0.05	0.12	0.03	0.06

The comparison of space densities is exhibited in Table 6. For each latitude the columns headed "A" and "B" give, respectively, the densities obtained by the use of the standard luminosity function and those obtained by the geometrical method. The absorption has been assumed to be 0.5 mag. per kiloparsec in a layer 300 parsecs in half-thickness.

It is apparent that the densities computed by the geometrical method are consistently larger than those computed by using the luminosity function. At present I see no logical way of accounting for the observed differences. An examination of the data on the variations of density and the luminosity function with height above the galactic plane reveals no inconsistency in these quantities. The principal knowledge concerning the fluctuations of the luminosity function, added since the publication in the *Bulletin of the Astronomical Institutes of the Netherlands*, No. 238, of the function used here, implies that the slight revision of densities resulting would only enhance the observed discrepancy. Reconciliation of the differences in Table 6 by the adoption of a more rapid decrease of density with z would require an unreasonably large revision, as is shown by the last two columns of Table 8.

TABLE 7

EFFECT OF ABSORPTION ON DENSITIES COMPUTED GEOMETRICALLY

(Magnitudes per Kiloparsec)

r (PARSECS)	$D(r)$ AT $\beta = -20°$		
	$A=0$	$A=0.5$	$A=1.0$
386	0.49	0.55	0.60
506	.43	.47	.54
687	.32	.38	.46
925	.25	.30	.38
1250	.18	.21	.26
1678	0.11	0.13	0.17

The relative insensitivity of an analysis by the geometrical method to changes in the assumed uniform absorption coefficient is shown in Table 7. Densities have been computed for three values of the absorption at latitude $-20°$. A layer 300 parsecs in half-thickness has been assumed.

The results by the Oort-Vashakidse method of analysis for three values of the absorption coefficient are presented in Figure 4, which is a cross-sectional view of the galaxy perpendicular to its plane at λ 138°. Equidensity curves have been drawn for $D(z) = 0.5$, 0.3, 0.2, and 0.15. The sun is at the left-hand upper corner of each drawing. Ordinates are values of z, and abscissas are distances in the galactic plane. The dashed sections of the equidensity curves indicate that the data are too uncertain to be of value.

A comparison of this figure with Figure 2 shows the similarity of galactic structure obtained by the two methods. The presence of a local cluster effect at $\beta -20°$ is again substantiated. For $A = 1.0$ mag. per kiloparsec, the equidensity curves are quite similar to those published by Oort.

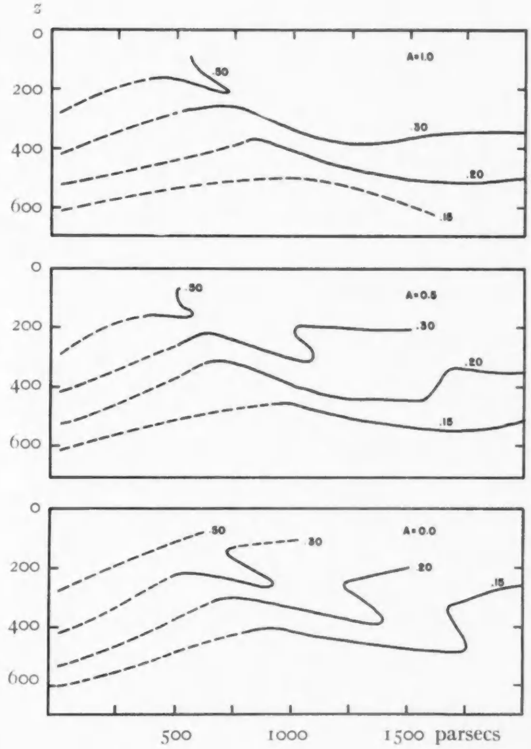

FIG. 4.—Density distributions computed by the Oort-Vashakidse method. Ordinates are values of z in parsecs; abscissas are distances in the galactic plane. Dashed curves indicate uncertain data. The sun is at the upper left in each figure. The curves are equidensity contours.

The variation of density perpendicular to the galactic plane.—The data in Table 3 and the cross-sectional view of the galaxy in Figure 2 both indicate the dependence of the star density upon z. Table 8, however, shows more directly the density decrease with distance from the galactic plane. The first column gives the height, z, in parsecs; the second, third, and fourth give the star densities in a direction perpendicular to the galactic plane at distances of 500, 1000, and 2000 parsecs from the sun in the direction of the galactic anti-center. The fifth column gives the density variation for the neighborhood of the sun for stars with $M \geqslant 4.5$, as deduced by Oort[13] and used by me in the geometrical method of analysis described in the previous section. In the sixth column I have included the density variation necessary to reconcile the geometrical method of analysis with the method which employs the standard luminosity function.

At distances from the sun > 1000 parsecs, the maximum density apparently occurs between 50 and 200 parsecs from the galactic plane, as is shown in Figure 2, rather than in the galactic plane. One may infer either that the adopted system of co-ordinates defining the galactic plane is in error by some 5° or that the sun is situated from 50 to 200 parsecs north of the galactic plane. The first contingency seems unlikely, because van Rhijn[14] has derived a correction to the reference system used here which would place the plane of symmetry approximately at $\beta = +4^\circ$ on the Harvard system. If the second alternative is correct, the distance of the sun from the galactic plane becomes two to three times the value derived from Cepheid variables and other highly luminous objects. It must be emphasized, however, that the evidence for this maximum is to be

TABLE 8

DENSITY VARIATION PERPENDICULAR TO THE GALACTIC PLANE

DISTANCE FROM SUN / z (PARSECS)	$D(z)$			AVERAGE $D(z)$	
	500 Parsecs	1000 Parsecs	2000 Parsecs	Oort	McC.
0	0.96	0.22	0.08	1.00	1.00
25	.58	.23	.11	0.98	0.85
50	.40	.24	.13	0.94	0.70
100	.36	.25	.17	0.88	0.47
200	.26	.20	.20	0.68	0.16
300	0.04	.12	.16	0.45	0.08
500	....	0.04	0.06	0.21	0.04

---

[13] *B.A.N.*, **6**, 249, 1932; **8**, 97, 1936.

[14] *Groningen Pub.*, **43**, 1929.

considered highly uncertain until counts for fainter stars are available.

Table 8 shows the density gradient obtained for the region within 500 parsecs of the sun to be considerably higher than the gradients obtained by Oort,[13] whose values agree well with those found by van Rhijn and Schwassmann.[15]

The dark nebula in Taurus.—Although the distance and absorbing power of a dark nebula, computed from general star counts, are uncertain because of the large dispersion in the luminosity function, an approximate position of the Taurus nebulosity may be obtained from the data at hand. It has been assumed that the same density law and the same value for the general interstellar absorption coefficient (A = 0.5 mag. per kiloparsec) hold for an obscured region as for the mean of the unobscured areas at the same latitude as the nebula. The density functions for the analyses have been taken, therefore, from Table 3. On the assumption of a thin absorbing screen placed at various distances, the best agreement between observed and computed log $A(m)$ in the obscured areas was obtained by trial and error.

TABLE 9

THE DARK NEBULA IN TAURUS

Region	Area (Sq. Deg.)	λ	β	Absorption (Mag.)	Distance (Parsecs)
A	4.8	147°	0°	1.1	80
B	6.2	148	−4	1.6	80
C	5.5	143	8	1.5	200
D	4.1	138	8	2.0	125
E	4.1	133	15	1.0	125
F	3.5	141	12	3.5	125
G	2.8	128	17	2.2	200
H	4.1	127	−20	2.3	200
Mean				1.9	142

Eight areas in Taurus, visibly affected by obscuration, have been analyzed in this way, the results being shown by Table 9. The positions of these regions in the sky have been indicated in Figure 3.

---

[15] *Zs. f. Ap.*, **10**, 161, 1935.

In Figure 5 the values of log $A(m)$ have been plotted as a function of m for both the obscured and the comparison regions. The computed variation of log $A(m)$ obtained on the assumptions of distance and absorbing power given in Table 9 is indicated by the lower curve in each figure. Vertical lines through the points represent the mean errors in log $A(m)$ due both to the natural uncertainty in counting and to errors in the magnitude scale.

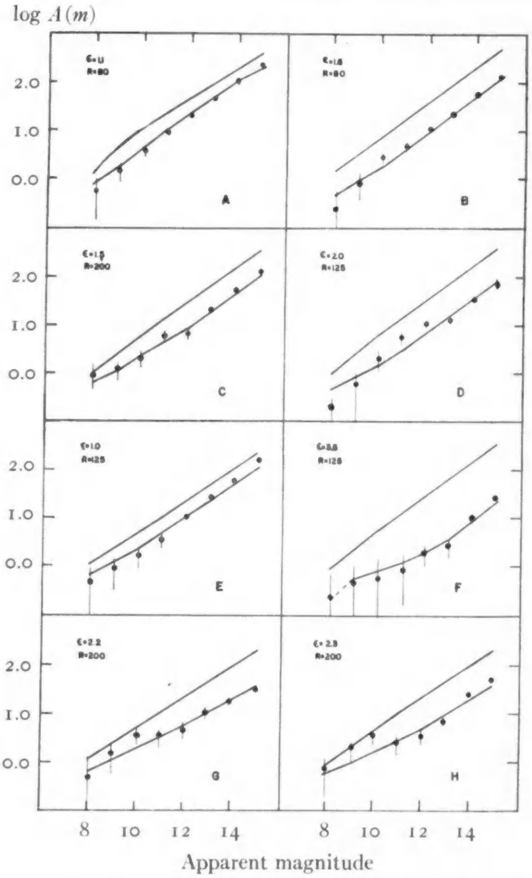

FIG. 5.—Wolf diagrams for eight regions in the Taurus cloud. The upper curve in each case represents the comparison region; the points and the lower curve are for the obscured area. Ordinates are values of log $A(m)$; abscissas are photographic magnitudes.

The distances deduced for the Taurus nebula at the eight points investigated agree as well as may be expected from the limitations of the method. Since the nebulous material is near by, the computation of its distance from small areas involves the least certain of the star-count data, viz., the brightest stars.

In the mean, the obscuration in Taurus appears to be due to an absorbing layer at a distance certainly less than 200 parsecs and absorbing about 1.9 mag. in concentrated portions. The average distance (142 parsecs) found here for the Taurus cloud agrees with the value of 145 parsecs recently listed by Greenstein,[16] who finds 1.1 mag. absorption averaged over a much larger area of the sky than that covered by the present analysis.

The distances computed for the eight areas in the Taurus cloud have been plotted on the distribution diagram, Figure 2. Although there is some suggestion that the absorbing layer is inclined to the galactic plane, the data are too meager to warrant any conclusion to this effect. When the data on colors and spectra for faint stars are available for this region of the sky, a much more precise discussion of the Taurus nebula can be made.

The picture of galactic structure presented in the preceding pages is admittedly tentative as far as the details are concerned. There seems to be little doubt, however, of a distinct local cluster effect when the analysis is based upon star counts in regions relatively free of localized obscuration. A dearth of sufficiently detailed data on the numbers of stars fainter than $m = 15.0$ precludes carrying the analysis farther at present.

To complete the present study and to put it on a sound basis, spectra, colors, and counts to fainter limits are necessary. These data are now being obtained. With the help, also, of counts of extragalactic nebulae, a much better determination of the absorption function can be made. Further discussion of this section of the galaxy will be deferred until the observational material is complete.

A second investigation along the lines described in this paper is planned for the Orion region, in the longitude range adjacent to that covered here.

Appendix.—At the suggestion of Professor van Rhijn, I am including in Table 10 the values of log $N(m)$ for 31 supplementary areas in Taurus. $N(m)$ is, as usual, the number of stars brighter than magnitude m. These regions, 3.1 square degrees each, have not been selected for their freedom from apparent obscuration. They represent average samples for the Taurus region of the galaxy. Figure 3 indicates the positions in the sky.

---

[16] *Harvard Ann.*, **105**, 360, 1937.

TABLE 10

VALUES OF LOG $N(m)$ FOR 31 SUPPLEMENTARY REGIONS IN TAURUS

AREA	λ	β	m							
			8	9	10	11	12	13	14	15
56......	146°8	+ 0.1	9.69	0.20	0.70	1.20	1.58	1.80	2.10	2.56
50......	147.2	− 2.7	9.74	0.16	.56	0.97	1.27	1.66	2.07	2.50
58......	139.2	5.1	9.82	0.05	.45	0.84	1.24	1.65	2.05	2.46
59......	145.6	5.0	9.47*	9.86*	.24	0.63	1.02	1.42	1.83	2.10
54......	149.6	5.0	9.80	0.24	.70	0.97	1.20	1.51	1.84	2.17
65......	137.5	8.0	9.69	0.02	.37	0.70	1.03	1.28	1.60	1.97
60......	141.3	8.0	......	9.00*	.10	0.82	1.27	1.66	2.05	2.43
62......	144.5	7.8	0.07	0.25	.50	0.78	1.10	1.46	1.89	2.33
55......	148.5	7.9	9.71	0.16	.56	0.94	1.33	1.72	2.13	2.50
66......	135.5	10.0	9.60	0.35	.71	1.01	1.34	1.66	2.05	2.48
61......	142.0	10.0	9.52	9.89	.23	0.60	0.96	1.32	1.77	2.20
67......	136.2	12.8	......	9.80	.60	1.01	1.37	1.70	2.02	2.38
70......	139.0	12.9	9.70	0.05	.24	0.47	0.80	1.19	1.57	1.91
68......	140.8	12.9	9.02*	9.70	.28	0.46	0.63	0.85	1.18	1.51
63......	143.6	13.0	0.10	0.37	.60	0.88	1.13	1.40	1.81	2.20
71......	135.2	15.0	9.60	0.04	.40	0.75	1.09	1.42	1.77	2.10
69......	138.5	15.0	9.52	9.97	.36	0.70	1.02	1.34	1.66	1.98
82......	142.0	15.0	9.52	9.86	.21	0.57	0.91	1.21	1.50	2.00
84......	144.8	15.0	0.11	0.50	.80	1.09	1.40	1.70	2.00	2.32
72......	131.5	17.7	9.32	0.00	.54	0.98	1.35	1.63	1.88	2.35
80......	137.5	17.5	9.28	0.02	.59	0.96	1.30	1.64	2.00	2.33
83......	143.5	17.6	9.97	0.21	.49	0.75	1.00	1.27	1.53	1.80
75......	125.6	20.2	0.00	0.62	.86	1.08	1.30	1.50	1.77	2.20
74......	128.2	20.0	9.90	0.26	.55	0.82	1.12	1.40	1.71	2.01
79......	136.5	20.0	9.79	0.36	.70	1.04	1.38	1.70	2.03	2.38
81......	140.0	20.2	0.00	0.31	.64	0.97	1.30	1.60	1.94	2.27
27......	118.2	21.5	9.70	0.10	.50	0.88	1.20	1.51	1.96	2.36
76......	126.0	22.5	9.70	0.16	.48	0.78	1.08	1.38	1.62	2.15
77......	124.2	25.0	9.70	0.04	.40	0.75	1.05	1.42	1.80	2.40
78......	127.7	25.2	9.75	0.13	.52	0.91	1.26	1.51	1.75	2.40
33......	126.2	−32.5	......	9.47	0.10	0.71	1.20	1.50	1.65	2.18

* Extrapolated.

WARNER AND SWASEY OBSERVATORY
CASE SCHOOL OF APPLIED SCIENCE
February 1, 1939

PHYSICAL PROCESSES IN GASEOUS NEBULAE

VI. THE EQUATIONS OF RADIATIVE TRANSFER

LAWRENCE H. ALLER, JAMES G. BAKER,[1] AND DONALD H. MENZEL

ABSTRACT

The general equations of transfer for bound-bound, bound-free, and free-free transitions for a hydrogenic nebula are derived from the usual macroscopic equations by the identification of the emissivity and absorptivity functions with those given in Paper I of this series. The integration of these equations is reserved for another paper.

In the previous papers[2] we have considered the problem of the decrement of the Balmer series and have shown the decrement to be very sensitive to the method of excitation. Thus far we have distinguished three cases: A, B, and C. Cases A and B are based on a model of a nebula in which the nuclear star radiates no energy in the Lyman lines. Case A is for a nebula transparent in the lines, so that all the Lyman-line radiation, produced in the nebula as a result of cyclic processes, is allowed to escape from the nebula. In case B none of the Lyman-line radiation, except Lyman α, escapes. This is the extreme case considered by Zanstra. The third model, C, is for a relatively transparent nebula (as in case A) but with a nuclear star radiating like a black body in the region of the Lyman lines. The additional stellar line radiation absorbed by the nebula alters the decrement markedly, raising the intensity of $H\alpha$ relative to $H\beta$.

In Table 1 we summarize the theoretical Balmer decrements for various values of the electron temperatures according to the three cases. The tabulated value is the intensity of $H\alpha$ referred to $H\beta$ as unity. The observational data for the planetary nebulae agree best, as we have shown, with the results of case B.

The surface brightness of a nebula that follows either case A or case C will be low. Such nebulae will, accordingly, be difficult to observe spectroscopically. Greenstein and Henyey[3] have observed, in certain faint extended nebulae, what appears to be a high Balmer decrement. Greenstein kindly warns us, by letter, that the observation is still open to question because of the possible blending of $H\alpha$ with the nebular lines of *N* II. Whatever may be the explanation of this phenomenon, a high Balmer decrement leads to no theoretical difficulty, since it may be explained in terms of case C.

---

[1] Society of Fellows, Harvard University.

[2] Paper II in *Ap. J.*, **86**, 70, 1937; Paper III in *ibid.*, **88**, 52, 1938; Paper V in *ibid.*, **88**, 422, 1938.

[3] *Ap. J.*, **87**, 79, 1938.

The great theoretical differences in decrement according to various models show that a more exact treatment of the nebular radiation field is to be desired. In the present paper we lay the basis for a more thorough analysis of the transfer problem.

TABLE 1

T_e (K)	A	B	C
5,000	1.86	2.43	12.5
10,000	1.92	2.50	6.0
20,000	1.98	2.59	4.0
40,000	2.07	2.71	3.3
80,000	2.17	2.83	3.0

In the notation of paper I we may write down the equations of transfer almost at once. We consider the nebulous envelope to be stratified in parallel planes, since Milne has shown that the problem of the spherical shell can be reduced to a plane problem as far as radiative transfer is concerned. We choose an x-axis with co-ordinates increasing outward. Let a beam of energy of specific intensity $I\,(x, \theta)$, confined within a solid angle $d\omega$ making an angle θ with the positive direction of x, fall on a slab of 1 square centimeter in cross-section and of thickness dx. The total amount of energy removed from the beam by a transition from state n' to n will be

$$\frac{1}{4\pi}\,E_{n'n}\,d\omega\,dx\,\sec\theta\ ,$$

where we have integrated $I\,(x, \theta)$ with respect to the frequency over the line. The energy returned to the beam by the emissions in $d\omega$ is

$$\frac{1}{4\pi}\,E_{nn'}\,d\omega\,dx\,\sec\theta\ .$$

The induced emissions, treated as negative absorptions, are included in the term $E_{n'n}$. To derive the transfer equations we must consider the emission and absorption in the frequency range $d\nu$. The two preceding expressions may be multiplied by a function $\varphi(\nu - \nu_{nn'}) \equiv \varphi_\nu$, which represents the profile of the absorption or emission coefficient. We must have

$$\int_0^\infty \varphi(\nu - \nu_{nn'}) d\nu = 1 \, . \tag{1}$$

We note, also, that

$$a_{n'n}(\nu) = \frac{\pi \epsilon^2}{mc} f \varphi_\nu \, . \tag{2}$$

Should the spectral distribution of the emitted quantum not be equal to that of the absorbed, we must introduce different expressions for φ_ν for the two processes.

The equation of transfer for the lines now becomes

$$\cos\theta \frac{dI_\nu}{dx} = -\frac{1}{4\pi} [E_{n'n} - E_{nn'}] \varphi_\nu \, . \tag{3}$$

The equivalent form

$$\cos\theta \frac{dI_\nu}{dx} = -\frac{1}{4\pi} [F_{n'n} - F_{nn'}] h\nu \, \varphi_\nu \, , \tag{4}$$

which refers to the number of transitions, is sometimes useful.

In an analogous manner the transfer equation for the bound-free transitions for a particular ν may be written

$$\cos\theta \frac{dI_\nu}{dx} = -\frac{1}{4\pi} \sum_{n'} [E_{n'\kappa} - E_{\kappa n'}] \, . \tag{5}$$

The summation over n' is due to the fact that radiation of a given frequency may arise by capture on any one of a number of discrete levels from various elements $d\kappa$ of the continuum, such that

$$\nu = RZ^2 \left(\frac{1}{n'^2} + \frac{1}{\kappa^2} \right) .$$

Since $E_{1\kappa} = F_{1\kappa} h\nu$, we obtain the equivalent form

$$\cos\theta \, \frac{dI_\nu}{dx} = -\frac{1}{4\pi} \sum_{n'} [F_{n'\kappa} - F_{\kappa n'}] h\nu \, . \tag{6}$$

Similarly, the equation of transfer for the case of free-free transitions becomes

$$\cos\theta \, \frac{dI_\nu}{dx} = -\frac{1}{4\pi} \int_0^\infty [E_{\kappa'\kappa} - E_{\kappa\kappa'}] d\nu_{\kappa'} = -\frac{1}{4\pi} \int_0^\infty [F_{\kappa'\kappa} - F_{\kappa\kappa'}] h\nu d\nu_{\kappa'} \, . \tag{7}$$

The integration in (7) is carried out subject to the condition

$$\nu = RZ^2 \left(\frac{1}{\kappa^2} - \frac{1}{\kappa'^2} \right) , \tag{8}$$

where ν is held constant.

Although we have represented the transfer in terms of three separate equations, one for each process, we shall have, in general, all three types of processes acting at any given frequency, and the right-hand side of the transfer equation will include all three terms. Frequently, of course, only one will predominate. We should further note that, when neighboring lines of a series overlap, as always occurs near a series limit, the right-hand side of equations (3) and (4) should include a summation over the significant values of n.

We now consider the transformation of these equations with the aid of expressions developed in earlier papers for the emissivity and absorptivity terms. We first discuss the equation of transfer for the bound-bound processes.

Recalling I-4, I-5, and I-9, and making use of (3) or (4), we obtain

$$\left. \begin{aligned} \cos\theta \, \frac{dI_\nu}{dx} = -\frac{N_i N_\epsilon}{4\pi\sigma} \frac{\mathrm{K} Z^4}{T_\epsilon^{3/2}} \frac{g}{n'^3} e^{X_{n'}} \Big\{ [b_{n'} - b_n e^{-h\nu/kT_\epsilon}] I_\nu & \\ - b_n \sigma e^{-h\nu/kT_\epsilon} \Big\} \frac{2hRZ^2}{n^3} \varphi_\nu \, , & \end{aligned} \right\} \tag{9}$$

where $\sigma = 2h\nu^3/c^2$. In the foregoing form the equation of transfer is useful for problems in which the variation of absorption coefficient with wave length is of prime importance.[4]

---

[4] E.g., this form may be convenient for a discussion of absorption-line profiles in stellar atmospheres.

For the problem at hand, considerable simplification may be effected without too great a sacrifice of accuracy if, at least in the earlier approximations, we assume an average absorption coefficient over the line. Let $\Delta\nu_{nn'}$ be the effective half-width of the absorption coefficient. Accordingly, we may define a mean φ_ν such that

$$\int_0^\infty \varphi_\nu \, d\nu = \overline{\varphi}_\nu \, \Delta\nu = 1 \,, \qquad \text{or} \qquad \overline{\varphi}_\nu = \frac{1}{\Delta\nu} \,. \tag{10}$$

Equation (9) now becomes

$$\left.\begin{aligned} \cos\theta \, \frac{dI_\nu}{dx} = -\frac{N_i N_\epsilon}{4\pi\sigma} \frac{\mathrm{K}Z^4}{T_\epsilon^{3/2}} \frac{g}{n'^3} e^{X_{n'}} \Big\{ & [b_{n'} - b_n e^{-h\nu/kT_\epsilon}] I_\nu \\ & - b_n \sigma e^{-h\nu/kT_\epsilon} \Big\} \frac{2hRZ^2}{n^3} \frac{1}{\Delta\nu_{nn'}} \,. \end{aligned}\right\} \tag{11}$$

It is interesting to note that the frequency difference, $\Delta\nu'$, between two successive members of a given series, is

$$\Delta\nu' = RZ^2 \left[\frac{1}{n^2} - \frac{1}{(n+1)^2} \right] \sim \frac{2RZ^2}{n^3} \,. \tag{12}$$

Hence, if the line broadening is such that successive lines just overlap,

$$\Delta\nu_{nn'} \sim \Delta\nu' \,, \tag{13}$$

and the factor

$$\frac{2RZ^2}{n^3} \frac{1}{\Delta\nu_{nn'}} \sim 1 \,. \tag{14}$$

Near the series limit, where $b_n \rightarrow 1$, we see that (9) must run continuously into the analogous equation for the bound-free transitions, which is easily found to be

$$\cos\theta \, \frac{dI_\nu}{dx} = -\frac{N_i N_\epsilon}{4\pi\sigma} \frac{\mathrm{K}Z^4}{T_\epsilon^{3/2}} \sum_{n'_{\min}}^{\infty} \frac{g}{n'^3} e^{X_{n'}} \{ [b_{n'} - e^{-h\nu/kT_\epsilon}] I_\nu - \sigma e^{-h\nu/kT_\epsilon} \} \,. \tag{15}$$

The summation of (16) must obviously be extended over only those values of n' whose series limits lie to the red of the frequency in question. The quantity $n'_{\min}$ is thus seen to be the smallest value of n' that will satisfy the relation

$$\frac{RZ^2}{n'^2} \leq \nu \, . \tag{16}$$

For free-free transitions the equation becomes

$$\cos\theta \, \frac{dI_\nu}{dx} = -\frac{N_i N_\epsilon}{4\pi\sigma} \frac{\mathrm{K} Z^4}{T_\epsilon^{3/2}} \frac{kT_\epsilon}{2hRZ^2} \, \bar{g} \, \{[1 - e^{-h\nu/kT_\epsilon}] I_\nu - 1\} \, . \tag{17}$$

Note that, since we are dealing here entirely with the continuum (assumed to be in thermodynamic equilibrium), the *b*-factors do not enter. The present transfer equations differ from those given by Milne,[5] Ambarzumian,[6] Chandrasekhar,[7] etc., in the specific character of the absorption coefficients. The number of discrete states has not been limited to two, three, or four, as is commonly done. These equations are quite general and involve no assumptions concerning the dilution of the radiation. They are equally applicable to stellar atmospheres or gaseous nebulae,[8] although in the former case a solution involves great complexities. The ratios of the successive values of the b_n's will determine whether a line appears in absorption or emission. Fluorescent cycles and interlocking effects are all taken into account by the equations of transfer used in conjunction with those of radiative and of statistical equilibrium. The latter can be generalized to include the effects of collisional excitation and deexcitation of the stationary states.

The solution of the transfer equations for the lines even in the nebular problem is very difficult, as one must consider the interlocking between the continuum and the discrete states. For the Lyman continuum the equation of transfer can be solved in a straightforward manner by means of successive approximations. The solution of the transfer equations for the free-free transitions is very simple.

---

[5] *Zs. f. Ap.*, **1**, 98, 1930.

[6] *M.N.*, **93**, 50, 1932.

[7] *Zs. f. Ap.*, **9**, 266, 1935.

[8] D. H. Menzel, *Pop. Astr.*, **47**, 6, 1939.

We shall see that we can set up and solve the transfer equation for the Lyman continuum quite independently of any knowledge of the population of the discrete levels (except the first). For each point in the nebula the solution will be characterized by a value of the dilution factor of the Lyman continuum radiation, the value of b_1, and the electron temperature T_ϵ. When the transfer problem for the lines is considered, we shall see that an intimate knowledge of T_ϵ, and therefore of both the dilution factor and b_1, is required, because the population of the higher states depends largely on the electron captures. Before we can attack the problem of radiation transfer for the lines, we must solve it for the Lyman continuum. In the next paper of the series we shall discuss the transfer of radiation in the Lyman continuum.

HARVARD UNIVERSITY
December 19, 1938

THE TEMPERATURES OF SECONDARY COMPONENTS IN ECLIPSING BINARY SYSTEMS

ZDENĚK KOPAL

ABSTRACT

The temperatures of the secondaries in eclipsing systems have been studied on the basis of their spectra and surface intensities. The main results are: (1) The temperatures of the secondaries are normal dwarf temperatures, agreeing very well with Kuiper's recent temperature scale. (2) The discrepancy between the ionization and surface temperatures in systems displaying partial eclipses can, qualitatively at least, be explained by the ionizing effect of the diluted radiation of the primary. (3) There appears to be no relationship between the difference in spectral type and the separation of the components or their mass-ratio. (4) The black-body radiation law would seem to be fulfilled conclusively even for B-type stars.

As is well known, the temperatures of the secondaries in eclipsing binary systems can be arrived at in two independent ways: from their spectra (ionization temperatures), and, provided the temperature of the primary is known, from the ratios of their surface brightnesses (effective temperatures). Both methods should, in general, lead to very similar results; yet it is a familiar fact that this is frequently not the case, the discrepancies in many systems widely exceeding the limits of observational error. The aim of the present paper is to discuss the discrepancies on the basis of the whole material available at present, in order to throw light on the possible cause.

Before entering upon a discussion of our material, some remarks on the accuracy of the underlying observational data are appropriate. The reliability of spectroscopic results has been the subject of several recent investigations.[1] If both components are very unequal in luminosity, the spectra of the secondaries cannot be determined unless the eclipses happen to be total. If the eclipses are partial and the luminosities of the components are comparable, the spectra necessarily overlap, and it may be difficult to distinguish their character unquestionably. One of the features of such systems is the frequent similarity of both spectra. It has been suggested[2] that this similarity may be an effect of the radiation of the primary. It seems unlikely that the heating effect of the incident radiation is sufficient to equalize the surface temperatures of both components.[3] Its ionizing effect in the outer atmospheric layers might, however, be dominant; we shall discuss this possibility in some detail.

---

[1] Cf. Eddington, *M.N.*, **86**, 325, 1926; or Wyse, *Lick Obs. Bull.*, No. 464, 1935.

[2] Eddington, *op. cit.*

The observed values of the ratios of the surface intensities may also be subjected to some uncertainties. They presume a knowledge of the reflection and ellipticity constants, as it is clear that the ratios must be formed from the rectified intensities in both minima. The loss of light in the secondary minimum is frequently very slight and hardly observable. In such cases its depth has sometimes been assumed so as to fit the other and better observed characteristics of the light-curves. We may, then, have to deal with "uniform" and "darkened" ratios of surface brightnesses, differing sometimes widely.

The ratio of the surface brightnesses of the two components determines the temperature of the secondary only if the temperature of the primary is known and if a definite law of radiation, such as that of a black body, is adopted. Any deviation of either star from black-body radiation may be a source of error. Another uncertainty may arise from the effect of darkening—and in close binaries the actual state of affairs is complicated still more by the fact that we are dealing with two different kinds of darkening, corresponding to the original and the reflected radiation of either star. The disturbing effect of the darkening must, however, not be overestimated. It would be really troublesome if the eclipsed fraction were only a small part of the disk and if the ratio of the radii were very different from unity. But if the eclipses are total or nearly total—and such systems will form the essential part of our material—its effect is minor; the resulting effective temperature corresponds in this case to the mean optical depth averaged over the whole eclipsed portion of the disk.

The material which forms the basis of the present investigation is shown in Tables 1 and 2. Apart from a few additions, it contains most of the spectroscopic material recently compiled by Wyse.[4] The stars RU Cancri, RX Geminorum, and AD and AW Herculis had to be omitted because of the lack of reliable photometric data; the system TT Hydrae was excluded because the existing solution obviously does not check with the visibility of both spectra. The elements of TT Hydrae should be redetermined.

---

[3] Cf. Milne, *M.N.*, **87**, 45, 1926.

[4] *Op. cit.*

Table 1 contains the systems where the more massive and smaller primary is totally eclipsed in the deep minimum by its less luminous mate; in such systems the spectrum of the secondary could be determined unquestionably. Successive columns give the designation, the spectrum of the primary and secondary, respectively, and the observed ratio of surface brightnesses (in systems displaying reflection, the ratio of the faint sides). If the depth of the secondary minimum has not been reliably determined from the observations and the photometric solution is not unique, both limiting values of J_1/J_2 are given, the first corresponding to the "uniform" and the second to a completely "darkened" solution. The fifth column gives the

TABLE 1

Designation	Sp_1	Sp_2	J_1/J_2	$\log T_{2\mathrm{eff}}$	Authority
SY And.....	A0	K1	33, 24	3.70, 3.72	Shapley, *Princeton Contr.*, No. 3
TW And....	dF0	G6	10.5	3.68	Dugan, *Princeton Contr.*, No. 14
WW And...	A5	F3	3.7, 3.1	3.80, 3.82	Wyse, *Lick Bull.*, No. 464
RS Ari......	F9	G5	2.27	3.79	Lange, *A.N.*, **228**, 71
S Cnc.......	A0	G5	16.5	3.75	Fetlaar, *B.A.N.*, No. 108
RZ Cnc.....	K0	K4	*4.26**	3.62	†Hertzsprung, *B.A.N.*, No. 146
RS CVn....	F4	dG8	25	3.61	Sitterly, *Princeton Contr.*, No. 11
TW Cas....	B9	A0	1.1, 1.4	4.05, 4.02	McDiarmid, *Princeton Contr.*, No. 7
SX Cas.....	A6	G6	6.8	3.74	Dugan, *Princeton Contr.*, No. 13
U Cep......	A0	G8	18.4	3.74	*Ibid.*, No. 5
UZ Cyg.....	A3	K1	29.0, 18.5	3.68, 3.71	Shapley, *op. cit.*
TW Dra....	A6	K2	16.8	3.68	McDiarmid, *op. cit.*
RY Gem....	A2	K2	80, 26	3.69, 3.63	Wyse, *op. cit.*
RX Her.....	A0	A0	1.0	4.03	Shapley, *op. cit.*
RT Lac.....	G9	K1	1.4	4.62	Fowler, *Ap. J.*, **52**, 257
AR Lac.....	K0	G5	*0.34*	3.77	†Schneller and Plaut, *A.N.*, **245**, 387
UX Mon....	A5	dG1	3.52	3.81	Lause, *A.N.*, **260**, 289
RZ Oph.....	G0	gK5	28, 12	3.53, 3.57	Shapley, *op. cit.*
RY Per.....	B6	dF8	12, 10	3.84, 3.86	Fetlaar, *op. cit.*
U Sge.......	B9	gG2	13.3	3.71	*Ibid.*
RW UMa...	dF9	dG9	5.31	3.71	*Ibid.*

* The italicized values of the ratios of surface intensities refer to the photographic light-curves, the rest to the visual ones.

† Solution carried out on the basis of photographic light-curve.

effective temperatures of secondaries calculated by the use of the formulae

$$\frac{J_1}{J_2} = \frac{e^{c_2/\lambda T_2} - 1}{e^{c_2/\lambda T_1} - 1} \tag{1}$$

and

$$T_{\text{eff}}^4 = 2T^4 , \tag{2}$$

where $c_2 = 1.432$ cm grad, $\lambda_{\text{vis}} = 5290$ A, $\lambda_{\text{pg}} = 4250$ A,[5] and the effective temperatures of the primaries are taken according to their spectra from Kuiper's recent effective temperature scale.[6] The possible scatter of individual temperatures and the fact that a considerable range of wave lengths may be "effective" in both the visual and photographic light, together with the possibility of deviations from black-body radiation, impose a limit upon the accuracy of the temperatures computed in this way.

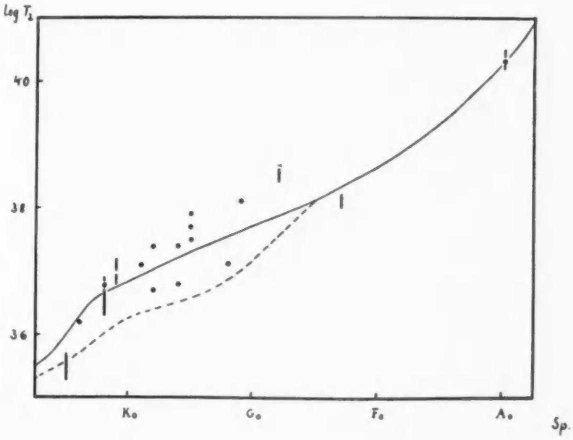

FIG. 1

If we plot the temperatures of the secondaries against their spectra, we obtain the results shown in Figure 1. The full line represents Kuiper's temperature scale for main-sequence stars; the dotted line, the giant branch. A glance at the diagram shows that the secondaries fall, on the average, close to the main-sequence stars, although they are abnormal in many respects. The majority of them are subgiants with radii much resembling the radii of giants; their masses, on the other hand, are normal dwarf masses, and their densities, consequently, are exceedingly low. The present results do, however, show that Kuiper's scale, in the low temperature range at least, is sound.

---

[5] Cf. Unsöld, *Physik der Sternatmosphären*, p. 53, Berlin, 1938.

[6] *Ap. J.*, **88**, 429, 1938.

TABLE 2

Designation	Sp_1	Sp_2 (Obs.)	J_1/J_2	$\log T_{2\mathrm{eff}}$	$Sp_2\,(c)$	$\log w_H$	$\log w_{ca}$	$\log w_0$	Authority
S Ant......	A8	A8	1.2	3.88	F0	1.27	0.622	0.767	Joy, *Ap. J.*, **64,** 287
σ Aql......	B8	B8	*1.34**	4.05	B9	0.695	0.420	1.26	§Wylie, *Ap. J.*, **56,** 232
TT Aur....	B3	B3	1.56	4.18	B5	1.16	0.596	0.975	Joy and Sitterly, *Ap. J.*, **73,** 77
WW Aur...	A7	A7	1.17	3.90	A7.5	0.163	0.077	1.80	Dugan, *Princeton Contr.*, No. 10
AR Aur....	A0	A0	1.21	4.00	A2	0.606	0.302	1.99	Nassau, *A.J.*, **45,** 135
β Aur......	A0	A0	*1.00*	4.03	A0	0.00	0.00	1.60	§Stebbins, *Ap. J.*, **33,** 395
SS Cam....	gG1	dF5	0.20, 0.21	3.83	F4	*	*	*	McDiarmid, *Princeton Contr.*, No. 7
SV Cam...	dG3†	dG5†	5.27	3.65	K2	4.06	1.81	0.81	Pierce, *Princeton Contr.*, No. 18
RW Cap...	A3	A4	3.7	3.83	F3	3.58	1.69	1.33	Shapley, *Princeton Contr.*, No. 3
TV Cas....	B9	A0	13.3, 14.1	3.78	G0	6.79	3.30	1.05	McDiarmid, *op. cit.*
XX Cas....	B4	B6	1.9	4.11	B7	1.74	0.864	0.936	Pierce, *op. cit.*
U CrB.....	B3	B3	13.2	3.89	A8	6.68	3.28	2.07	Dugan, *unpublished*‡
Y Cyg.....	O9.5	O9.5	1.00	4.45	O9.5	0.00	0.00	1.58	Dugan, *Princeton Contr.*, No. 12
GO Cyg....	B9	A0	*2, 1, 2.3*	3.97	A3	1.80	0.868	0.857	‖Liau, *Lyon Publ.*, **1,** 13
YY Gem...	dM1	dM1	1.5	3.53	M1.5	0.616	0.279	1.41	Joy and Sanford, *Ap. J.*, **64,** 250
Z Her......	F2	F2	4.7, 4.5	3.75	G3	3.07	1.44	1.94	Shapley, *op. cit.*
TX Her....	A2	A2	1.5	3.94	A5	1.43	0.528	1.60	Balanowsky, *Pulkovo Bull.*, No. 96
u Her......	B3	B3	2.18	4.13	B7	1.88	0.960	1.08	Dufay, *Lyon Bull.*, **12,** 155
SW Lac....	G3	G3	1.13	3.74	G4	0.499	0.231	0.812	Nijland, *A.N.*, **248,** 81
U Oph.....	B5	B5	1.2	4.16	B6	0.429	0.214	1.27	Shapley, *op. cit.*
AG Per....	B3	B3	*1.28*	4.22	B4	0.627	0.318	1.16	§Huffer, *Washburn Publ.*, **15,** 198
V Pup.....	B1	B3	1.3, 1.2	4.31	B2	0.463	0.241	0.754	Shapley, *op. cit.*
V356 Sgr...	B9	A1	*1.3*	4.03	A0	0.558	0.270	0.980	‖Voûte, *Lembang Ann.*, **5,** 2
W UMa....	F8	F8	*1.0*	3.79	F8	0.00	0.00	0.843	‖Schilt, *B.A.N.*, No. 83
Z Vul......	B3	B3	4.7	4.01	A1	4.06	2.00	1.18	Shapley, *op. cit.*

* The italicized values of the ratios of surface intensities refer to the photographic (or photoelectric) light-curves, the rest to the visual curves.

† Cf. Pierce, *Princeton Contr.*, No. 18, foot of p. 8.

‡ Quoted according to Wyse, *Lick Obs. Bull.*, No. 464.

§ Solution carried out on the basis of a photoelectric light-curve.

‖ Solution carried out on the basis of a photographic light-curve.

The two-spectra systems displaying partial eclipses have been compiled in Table 2. Successive columns give the designation, the observed spectra, the photometric ratios of the surface intensities, and the corresponding effective temperatures of the secondaries. The spectra of the less luminous secondaries have, as a rule, been observed at the time of the greatest separations of their lines, i.e., at the quadratures; but at the same time the advancing side of the secondary is fully exposed to the radiation of the primary which, however diluted, may yet control the ionization in the outer layers of the secondary's atmosphere. A glance at the corresponding columns of Tables 1 and 2 shows a very significant fact in this connection, namely, that while the spectra of the components in systems displaying total eclipses are usually very different, the spectra of the components in partially eclipsing systems are strikingly similar. Frequent comment of observers that "the spectrum of the secondary is exactly similar to that of the primary but that the lines are of vanishing intensity," even if the actual luminosities of the components are nearly equal, suggests still more that the "lines of vanishing intensity" are not properly the lines of the secondary but those excited by the incident radiation.

Let us follow this possibility in more detail and fix our attention upon the components of a binary with the temperatures T_1, T_2. Suppose that $T_1 > T_2$; the problem is to find a distance at which the ionizing effect of the diluted radiation of the primary is equal to that of the radiation of the secondary at the periphery of its atmosphere, i.e., to find a distance at which the diluted radiation of the primary is capable of exerting control upon the ionization. The degree of ionization at any point along the ray is given with sufficient accuracy for our purposes by the equation

$$\frac{N''N_e}{N'} = 10^{15.86 - \frac{5040I}{T} + \frac{u_{r+1}}{u_r}} \cdot T^{3/2} \cdot w \,, \tag{3}$$

where N'' is the number of ions per unit volume;
N' is the number of neutral atoms per unit volume;
N_e is the number of free electrons per unit volume;
T is the surface temperature;
I is the ionization potential;
u_r is the statistical weight of the corresponding rth state; and
w is the dilution factor.

Setting, as usual,

$$N'' = xN$$

$$N' = (I - x)N \ ,$$

where N is the sum of the ions and atoms, we find that our condition $x_1 = x_2$ is fulfilled at the distance where

$$w = 10^{5040 I \left(\frac{1}{T_1} - \frac{1}{T_2}\right)} \left(\frac{T_2}{T_1}\right)^{3/2} . \tag{4}$$

The sixth column of Table 2 gives the spectral classes corresponding to the computed effective temperatures of the secondaries, and the two succeeding columns contain the dilution factors computed with the aid of equation (4) for hydrogen ($I = 13.53\ eV$) and calcium ($I = 6.09\ eV$); the ninth column gives the dilution factors w_0 deduced from the observed separations of the components; the last column contains the references for the visual orbits.

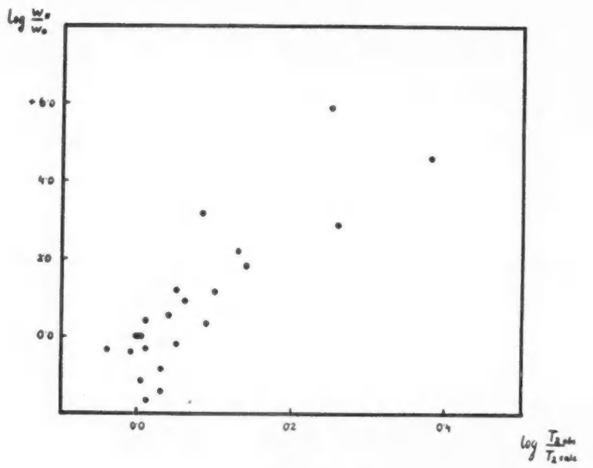

FIG. 2

The significance of these results can be shown most conveniently in the form of a diagram. In Figure 2 the ratios of the temperatures of the secondary components corresponding to their observed and computed spectra are plotted against the ratios w_H/w_0, both in the logarithmic scale. A glance shows that the relation between these quantities in the sense expected does exist. The ionizing effect offers, thus, a reasonable qualitative explanation for most of the discrepancies between the observed and the computed spectral types of the secondaries.

Mention should also be made that, with the spectral material from Table 1 and the computed true spectra from Table 2, the relation between the difference in the spectra of the two components and their separation or mass-ratio, found by several investigators, disappears altogether. Such a relationship seems to have arisen from the selection of the material, and chiefly from the use of fallacious spectral types for systems displaying partial eclipses.

Wyse's very careful study of twenty-five systems indicates that eclipsing binaries, on the whole, appear to have perfectly normal spectra. Exception is noted only in the unexpected tendency of a few secondaries to display bright hydrogen lines. The secondary components of RY Geminorum, TT Hydrae, and RZ Ophiuchi show $H\beta$ clearly in emission, and in the secondary spectra of WW Andromedae and RX Geminorum the Balmer lines are progressively weaker toward the red, indicating that $H\alpha$ is probably bright. Wyse considers the possibility that we are dealing here with the flash-spectra. If so, it is clear from equation (4) that, with N_e of the order of 10^{11} (Menzel and Cillié[7]), the ionization will almost exclusively have been governed by the diluted radiation of their high-temperature primaries. The duration of the flash-spectrum could, however, under no circumstances have exceeded a few minutes, and it seems doubtful whether its lines would have been intense enough to impress the plate. The occurrence of bright lines might more probably be accounted for by fluorescent emission in the atmospheres of these late-type subgiants, the continuous absorption coefficient of which is effectively zero. The fact that $H\alpha$ exhibits a stronger tendency to appear in emission than $H\beta$, and so on, would be exactly in agreement with expectation.[8] A further quantitative study of these conspicuous emission lines is desirable.

The ratios of the surface intensities, if observed in two detached spectral regions, at least, offer an interesting possibility of checking how closely the radiation of real stars of different temperatures comes to black-body radiation. In Table 3 are listed all the systems for which both the visual and photographic orbits are reliably known. The second and third columns give the observed ratios of the surface intensities in visual and photographic light, respectively, and in the fourth column the ratios of the two preceding columns are given. The fifth column contains the same theoretical ratios computed with the aid of Planck's formula for the visual and photographic effective wave lengths and the temperatures of the respective components. If the observations had been absolutely accurate and the black-body law followed exactly, the corresponding values of the fourth and fifth columns would be equal. They are, in fact, unequal; but the disagreement may be entirely due to observational errors. The mean value of the ratio $\frac{O}{C}$ is 0.93 ± 0.13.

---

[7] *Harvard Circ.*, No. 410, 1935.

[8] Cf. Woolley, *M.N.*, **94**, 641, 1934; Pannekoek, *M.N.*, **95**, 725, 1935.

TABLE 3

Designation	J_1/J_2 vis	J_1/J_2 pg	$\left(\frac{J_1/J_2 \text{ pg}}{J_1/J_2 \text{ vis}}\right)_{\text{obs}}$	$\left(\frac{J_1/J_2 \text{ pg}}{J_1/J_2 \text{ vis}}\right)_{\text{calc}}$	$\frac{O}{C}$	Authority*
TW And. . .	10.5	17.7	1.69	1.65	1.03	M. Shapley, *Ap. J.*, **56,** 439
RS CVn. . . .	25	35	1.41	1.59	0.89	Sitterly, *Princeton Contr.*, No. 11
TW Dra. . . .	16.8	19.9	1.18	1.90	0.62	Baker, *Laws Bull.*, No. 33
RX Her. . . .	1.0	1.12	1.12	1.00	1.12	*Ibid.*, No. 25
TX Her. . . .	1.5	1.8	1.20	1.14	1.05	*Ibid.*, No. 31
SW Lac. . . .	1.13	1.25	1.11	1.11	1.00	Schilt, *B.A.N.*, No. 68
UX Mon. . .	3.52	11.0	3.12	1.84	2.35	M. Shapley, *Harvard Bull.*, No. 854
Z Vul.	4.7	5.1	1.08	1.30	0.83	Baker, *op. cit.*, No. 26

* The sources given in the last column refer to the photographic orbits.

There are three systems where the observations have been carried out in several wave lengths and which, consequently, enable us to extend the check in more detail as shown on opposite page.

If we assume that the effective temperature of the primary is for U Cephei (A0) $T_{1\text{eff}} = 10{,}000°$, for u Herculis (B3) $T_{1\text{eff}} = 18{,}600°$, and for U Sagittae (B9) $T_{1\text{eff}} = 11{,}500°$, the effective temperatures of the secondaries resulting for each wave length are as given above. Their mean values are: for U Cephei, $T_{2\text{eff}} = 5{,}200°$, which corresponds, according to Kuiper, to the spectral class dG7 (observed spectrum is dG8); for u Herculis, $T_{2\text{eff}} = 13{,}600°$, corresponding to spectral class B7; and for U Sagittae, $T_{2\text{eff}} = 5{,}100°$, spectrum = gG1 (Joy observed gG2). But the significant fact is that for all these stars the resulting temperatures seem to be remarkably constant, i.e., the observed ratios of the surface intensities can very accurately be represented as those of two black-body radiators of constant temperatures, coinciding with the temperatures of both components, in a very wide spectral range. This suggests that even for early B-type stars the departures from black-body radiation, if any, are probably small.[9]

λ_{eff}	J_1/J_2^*	log $T_{2\mathrm{eff}}$	Authority
	U Cephei		
6165 A......	12.5	3.722	Rosenberg, *Ap. J.*, **83**, 67, 1936
5290........	18.4	3.723	Dugan, *Princeton Contr.*, No. 5, 1920
4015........	55.3	3.711	Rosenberg, *op. cit.*
	u Herculis		
5200........	2.18	4.126	Dufay, *Lyon Bull.*, **12**, 155, 1930
4830........	1.87	4.168	Krat, *Zs. f. Ap.*, **11**, 71, 1936
4370........	2.41	4.129	*Ibid.*
4250........	2.48	4.126	Baker, *Laws Bull.*, No. 28
3940........	2.56	4.130	Krat, *op. cit.*
3815........	2.78	4.133	*Ibid.*
	U Sagittae		
6100........	10.0	3.70	Walter, *Zs. f. Ap.*, **16**, 167, 1938
5290........	13.3	3.71	Fetlaar, *B.A.N.*, No. 108, 1927
4300........	16.3	3.73	Walter, *op. cit.*

In conclusion, the writer is deeply indebted to Professor Henry Norris Russell for his stimulating suggestions, to which the present paper owes a great deal. It is also his pleasure to express to Dr. Harlow Shapley his appreciation for the privilege of working at the Harvard Observatory, where the foregoing study was carried out.

Harvard College Observatory
February 1939

---

[9] This seems, however, at variance with current views—recently strengthened by the discrepancies between color and effective temperatures for early spectral types—that these stars deviate widely from black-body radiation.

PHOTOMETRY OF THE SOLAR GRANULES

PHILIP C. KEENAN

ABSTRACT

Photometric measures of the solar photograph of July 10, 1937, were reduced with the aid of a correction for the spreading of the image, derived from the profiles of the finest markings visible. The largest distinct granules have a corrected diameter of 1″.4 and are 15 per cent brighter than the background matter visible between them. The data for the average bright granules recognizable under favorable observing conditions are much less certain, but the most probable values for their dimensions are 1″.0 to 1″.2 and for the ratio of granular to background intensity, between 1.15 and 1.20.

In view of the importance of establishing at least the order of magnitude of the brightness of the granules, which are the characteristic unit structures of the solar surface, and the difficulty of securing photographs under sufficiently steady atmospheric conditions to bring out this fine detail, it seems worth while to make available now the measures of the best plate thus far obtained at the Yerkes Observatory, taken on July 10, 1937. A reproduction of a portion of this plate, as well as counts of granules and micrometric measures of their apparent dimensions, has already been published.[1]

The plate, of Eastman Type Va-G, was calibrated by exposures through a tube sensitometer lighted by a tungsten bulb providing illumination with its maximum emission not far from 5500 A, the effective wave length of the solar photograph. The measurements were carried out on a recording photoelectric microphotometer of Beals's design. In this instrument a 15× magnified image of the plate is projected upon a screen containing a variable rectangular aperture which defines the area being measured at any moment. For the solar measurements the aperture had a width in the direction of motion corresponding to 0″.14 on the sun's disk, and a height of about 0″.9.

When tracings are made in the usual manner, by taking runs more or less at random across the disk, the brightness at the centers of the granules can be found only by correcting statistically for the fact that the defining aperture may pass across any part of the granules lying in its path and in many cases will miss their centers entirely. In the present work this difficulty was avoided by taking advantage of the ease and precision with which the plate image could be adjusted with respect to the slit on the screen. Each granule chosen for measurement was placed centrally with respect to the aperture and recorded on a separate run. This procedure had the added advantage that only distinct granules on those portions of the disk where the definition was sharpest were measured.

---

[1] *Ap. J.*, **88**, 360, 1938.

In order to reduce the observed mean intensity ratio, J_G/J_B, of the center of the granule to the background, to the true ratio on the basis of the usual assumption that the intensity due to any point is distributed according to the exponential function $S(r) = (a/\pi)e^{-ar}$, where r is the distance from the given point and a is the "spreading constant" which measures the combined effect of atmospheric scintillation and instrumental resolving power, it is necessary to determine a for the moment of observation. The procedure introduced by Wanders in connection with his sunspot observations,[2] and followed by Plaskett[3] and by ten Bruggencate, Grotrian, and von der Pahlen[4] in their photometry of the sun's surface, is to take microphotometer tracings perpendicular to the sun's limb. If it is considered that the real limb is, for all practical purposes, perfectly sharp and that the distribution of intensity near the edge of the sun's disk can be represented satisfactorily by a linear formula or by a cosine formula, the observed profile of the limb provides a determination of the spreading constant. However, this method proved inadequate for the present study because the blurring was confined to such a small distance (about 2″) that slight errors in the estimation of the position of the true limb on the plate, which was necessarily somewhat underexposed in this part, and the uncertainty in our knowledge of the law of darkening for the last 0.1 per cent of the radius of the disk prevented a satisfactory determination of a. The value of 0.75 estimated in this way had to be discarded as much too low, since it was inconsistent with the observation of surface detail as small as 1″ in diameter (see Fig. 1).

The value finally adopted for the spreading constant was obtained by assuming that the observed profiles of the smallest isolated granules which were well defined on the plate were produced entirely by this factor. This neglect of the finite size of the small granules naturally led to an overestimate of the amount of spreading (a minimum value for a); but the result was probably of the right order of magnitude, for there is no reason to suppose that finer detail would not be brought out by still better conditions of observation. Of course, the corrections from the smallest granules could be safely applied only to those large enough to be well above the limit of resolution, but in any case the reduced intensities would be expected to be significant for these objects alone.

---

[2] *Zs. f. Ap.*, **8**, 108, 1934.

[3] *M.N.*, **96**, 402, 1936.

[4] *Zs. f. Ap.*, **16**, 51, 1938.

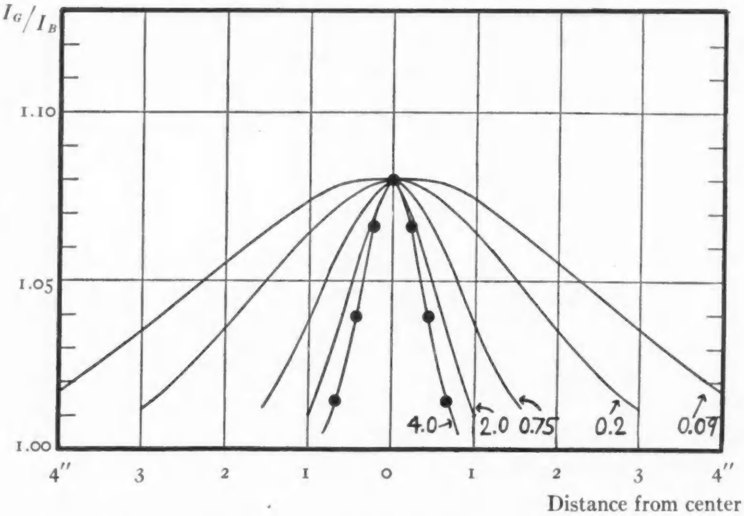

FIG. 1.—Comparison of observed mean profile for ten small granules (filled circles) with profiles computed for true diameter of 0″.1 and the indicated values of the spreading constant.

In Figure 1 the plotted points represent the mean observed profile from 10 of the smallest granules which showed a reasonably strong central intensity. The continuous curves are the profiles computed by the application of the spreading function for the indicated values of a to a flat-topped granule of diameter 0″.1. The adopted intensity for the flat-topped granule varies with a and was computed in each case to produce the observed central intensity of 1.080. The predicted profiles were built up by dividing the area around each point into radial zones $0\rlap{.}''1$ in thickness, estimating graphically on polar co-ordinate paper the relative contributions of granule and background to each zone, and summing the contributions from all zones, weighted according to the spreading function. This is essentially the method of calculation followed by ten Bruggencate *et al.*[5]

It is at once evident from inspection of the figure that a definite lower limit for a ($\sim$4.0) is set by the observations. The size chosen for the assumed true granules was so small that each curve represents quite closely the spreading to which infinitely fine detail would be subjected for the indicated values of a. Thus, the curves allow one to estimate the minimum diameters that could be measured even for a point source of illumination photographed under the corresponding conditions of observation.

Since the larger granules are now known rarely to exceed $2''$ in diameter, Figure 1 suggests that individual granules would not be expected to be shown on plates for which a is less than about 0.5 to 1.0. A test of this conclusion was made by running tracings across the edge of the moon's disk on a photograph of the partial solar eclipse of February 3, 1935, when the definition was good enough to show the granules over parts of the sun's surface but was evidently not very much above the limit necessary for resolution. The moon served in this case as a convenient knife-edge permitting the average value of a for several points along the rim to be estimated as about 0.8, in agreement with expectation.

For the plate under investigation a spreading factor of 4.0 was adopted and applied to the observed profiles of 13 of the largest granules which from their symmetry appeared to be individual objects and not irregular groupings of smaller ones. In the absence of evidence to the contrary, the true granule was again assumed to be flat-topped, so that the problem was to fit the observed mean profile (Fig. 2) by choosing cylindrical granules of various diameters with the central intensities necessary to produce the observed value of 1.13 and by calculating the profiles as modified by the spreading function.

Figure 2 shows that a good fit is obtained for a diameter of $1\rlap{.}''4$, corresponding to a true brightness ratio (granule to background) of 1.15. The greatest source of error lies in the assignment of the true diameter. From the consistency of the individual observed profiles the uncertainty in the abscissas of the points plotted in Figure 2 can scarcely exceed 0.1, corresponding to a minimum possible diameter of 1″.0 and a maximum central intensity of 1.24.

---

[5] *Op. cit.*, p. 104.

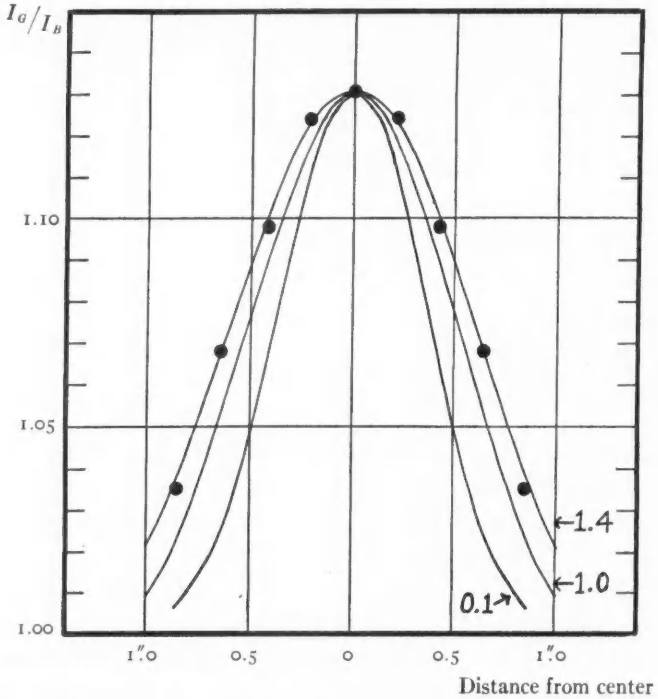

FIG. 2.—Profiles computed for $a = 4.0$ and flat-topped granules having the true diameters indicated for each curve. The filled circles represent the mean profile observed for thirteen large granules.

For statistical studies it is more important to have the mean intensity ratio for all of the bright granules greater than about 1″ in apparent diameter—the same objects for which counts were published in the previous paper.[1] However, their profiles were not sufficiently larger than those of the smallest granules to allow a direct determination of their true diameters, and the uncertainty must remain considerable. Measures of 42 granules gave $(J_G/J_B)_{\text{obs}}$

= 1.103 with a dispersion of only ±0.0196. In Table 1 the corresponding true intensity ratio for $a = 4.0$ is given as a function of the assumed diameter.

As measured on the tracings, their mean diameter at about one-third maximum height was 1″.62 with a dispersion of ±0.40, while the same dimension for the 13 large granules studied separately was 1″.74. The ratio of apparent diameters is presumably less than that of the actual sizes, so that it is reasonable to assume a mean diameter of 1″.0–1″.2 and to adopt 1.15 as the most probable intensity ratio for these granules.

TABLE 1

Assumed Diameter	I_G/I_B true
1″.4	1.12
1.2	1.13
1.0	1.16
0.8	1.22
0.6	1.34

The good agreement between the diameters measured on the tracings and the previously published micrometer measures indicates that a density of about one-third the maximum was taken as the edge of the image in making settings with the measuring engine. Since the true mean diameter appears to be nearer 1″.2 than the value of 1″.4 adopted as a first approximation in the earlier paper,[1] an improved estimate of the area covered by the granules can now be made. On the scale of 1″ to 735 km the average large granule has a diameter of about 880 km and a surface area of 609,000 km². From the counts on this plate their total number on the sun was estimated at 2,580,000, whence it follows that the granules occupy about 26 per cent of the surface area of the sun.

It is interesting to see what effect the presence of the granules will have on the sun's spectral-energy-curve. As a first approximation we consider the radiation as the sum of the emissions of two sources at different black-body temperatures, the granules and the cooler, but more extensive, background area. The hotter granules will contribute relatively more to the radiation at short wave lengths than in the long-wave region. The intensity ratio of 1.15 at 5500 A corresponds to a temperature difference of about 200°; but in order to estimate the maximum possible effect, let us work with the ratio 1.3 ($\Delta T = 400°$), corresponding to the smallest assumed diameters listed in Table 1, and give to them the liberal allowance of 20 per cent of the total surface. At 5500 A the radiation temperature represented by Mulders' spectral-energy-curve[6] is close to 6265°. The temperature of the granules would then be 6580° and that of the background 6180°. The resultant radiation due to these sources will then be represented by

$$\bar{I}_\lambda = 0.2 I_\lambda(6580°) + 0.8 I_\lambda(6180°) .$$

The ratio $R = \bar{I}_\lambda / I_\lambda(6265°)$ represents the gain in intensity at each wave length due to the existence of this temperature difference and is shown in Table 2 for a few ultraviolet wave lengths, where the effect begins to be appreciable.

TABLE 2

λ	R
3000 A	1.008
900	1.24
400	4.32
200	47.5

Even at very short wave lengths the gain resulting from the observed difference in temperature is small in comparison to the large ultraviolet excess, amounting to at least 10^4 at 900 A and corresponding to a temperature difference of the order of 5000°, which has been suggested several times to account for such phenomena as the presence in the chromospheric spectrum of emission lines of high excitation potential.[7]

Finally, it should be pointed out that the computations of the spreading corrections show that we have obtained just sufficiently good definition to derive significant data, and even a slight improvement in observing conditions should reveal much more concerning the fine structure of the sun's surface. The corollary is that one good plate is more useful than any number of fair ones.

YERKES OBSERVATORY
February 1939

---

[6] *Zs. f. Ap.*, **11**, 132, 1935. See also Unsöld, *Physik der Sternatmosphären*, p. 39, 1938.

[7] Cf. Menzel, *Harvard Circ.*, No. 410, pp. 33–37, 1936; Unsöld, *op. cit.*, pp. 425–426 and Fig. 137.

A SURVEY OF THE DURABILITY OF ALUMINIZED MIRRORS IN ASTRONOMICAL USE

ROBLEY C. WILLIAMS

ABSTRACT

A survey has been made of the durability of mirror coatings of aluminum and chromium-aluminum used by astronomical observatories in the United States and Canada. Some general remarks are given concerning the deterioration of the coatings and their care and expected life. It is concluded that the most probable useful life of a coating of either of the films is from two and one-half to upward of five years, depending upon the excellence of the coating, its care, and the degree to which it is subjected to condensed moisture and dirt particles.

Although films of aluminum or chromium-aluminum have been used for coating astronomical mirrors since 1932, until now no systematic inquiry has been made concerning the durability of the films when used under actual observing conditions. Inasmuch as the expense of coating a large mirror by the evaporation process is considerably greater than that of coating it by chemical silvering, the natural question of the performance and durability of the coating is of paramount importance. To be sure, for astronomical research in which the ultraviolet region of the spectrum is investigated, an aluminum coating is indispensable; but even in consideration of durability and convenience alone, it is felt by many that aluminum is sufficiently superior to silver to justify its higher cost.

In the autumn of 1938 the writer undertook to obtain from as many astronomical institutions as possible on this continent full information regarding the life and performance of aluminized mirrors. A questionnaire was sent to twenty-two observatories and planetaria, and reports were received from sixteen of them. Information was obtained from those using the two leading types of film—aluminum and chromium-aluminum—although no distinction between the types was asked for in the inquiries. Installations used for solar work and stellar work are included in the report, as well as cases where the chief use of the mirror is for instructional purposes. Although the answers to the inquiries were received over an interval of two months, it is believed that the mean date of December 1, 1938, represents the reports with sufficient accuracy. The most important information received on the reports concerning mirrors whose coatings are now in use is contained in Table 1. The first three columns are self-explanatory. The fourth column lists the time that the mirror, with its present coating, has been in use, both with respect to the number of months since the mirror was coated and the number of hours that the mirror has been actively in use. The fifth column attempts to describe briefly the cleaning methods used with this film, while the sixth column is a condensed statement of the general atmospheric conditions which might cause deterioration of the film. The seventh column lists the signs of deterioration of the present coating, but these evidences are somewhat indefinite because permanent deterioration cannot always be distinguished from temporary dirt, which can be cleaned off. The eighth column gives an estimate of the efficiency of the coating at present compared with its efficiency when new. The entries in this column, too, are somewhat uncertain, since such estimates are difficult and are strongly influenced by the amount of dust and dirt collected on the mirror surface. The last column contains statements of the life of previous coatings of either of the types of aluminum films.

Complete justice cannot be done to the description of the durability of the mirror coatings of each institution in a table of this brevity, and it is believed that some general remarks based upon the reports as a whole will be useful. The most striking fact gathered from the reports is that the life of the coating is strongly dependent upon the atmospheric conditions under which the mirror is used. Aluminum appears to be relatively vulnerable to the effects of moisture, particularly in those cases where condensation is sufficient to dissolve part of the chemically active deposits of dirt which collect upon all mirrors. When this occurs, the aluminum is dissolved in many small areas, and the mirror takes on a "freckled" appearance. The dissolving effect of the condensations is particularly troublesome at those locations where the mirror is generally covered with a layer of ash from smokestacks. Dry dust and sand appear to harm a mirror coating only in that their removal is liable to mark the aluminum film with many minute scratches.

TABLE 1

REPORT ON ALUMINIZED MIRRORS

Observatory	Size of Mirror (Inches)	Use	Time in Use	How Cleaned	Atmospheric Conditions	Signs of Deterioration	Percentage of Efficiency Compared with New Coating	Life of Previous Coating
Allegheny	18	Solar	+2 yr. 100 hr.	Never	Smoke, fumes	Few scratches	95	Never recoated
	12	Solar	+2 yr. 100 hr.	Never	Smoke, fumes	None	95	Same
Cook	28	Stellar	18 mo. 1000 hr.	Alphasol every 6 mo.	Fog, fumes, railroad smoke, gas-heater fumes	Small pinholes, some bloom	60	Same
	26	Solar	31 mo. 500 hr.	Alphasol every 2 wk.	Same	Very small pinholes	80	Same
	11	Stellar	28 mo. 2000 hr.	Alphasol every 3 mo.	Same	Bloom	60	600 hr.
	6	Solar	5 mo. 120 hr.	Same	Same	None	90	600 hr.
	4	Solar	5 mo. 120 hr.	Same	Same	None	90	600 hr.
Dunlap	19	Stellar	5 mo. 700 hr.	Never	Slight conds.*	None	100	38 mo.
	19	Stellar	42 mo. 100 hr.	Water	Slight conds.	Some stain and bloom	75–60(?)	Never recoated
	20	Stellar	42 mo. 150 hr.	Dusted	Slight conds.	Slight bloom	75	Same
Dominion Astrophysical	19	Stellar	9 mo.	Never	Good	None	100	
	19	Stellar	9 mo.	Never	Good	None	100	

* Condensations or "sweats."

TABLE 1—*Continued*

Observatory	Size of Mirror (Inches)	Use	Time in Use	How Cleaned	Atmospheric Conditions	Signs of Deterioration	Percentage of Efficiency Compared with New Coating	Life of Previous Coating
Griffith	13	Solar	5 mo. 1300 hr.	Soap and water	Salt air, dust, and wind	None	70	34 mo. 8000 hr.
	13	Solar	12 mo. 1900 hr.	Soap and water	Same	None	70	34 mo. 8000 hr.
	13	Solar	12 mo. 1900 hr.	Soap and water	Same	None	70	34 mo. 8000 hr.
	13	Solar	12 mo. 1900 hr.	Soap and water	Same	None	80	34 mo. 8000 hr.
	13	Solar	12 mo. 1900 hr.	Soap and water	Same	None	80	34 mo. 8000 hr.
	13	Solar	12 mo. 1900 hr.	Soap and water	Same	None	80	34 mo. 8000 hr.
	17	Solar	11 mo. 1800 hr.	Soap and water	Same	None	90	35 mo. 8200 hr.
Harvard College	10	Stellar	About 12 mo.; 300–500 hr.	Never	Frequent conds.	Pinholes, areas pulled off, thin spots	60	Never recoated
	24	Stellar	About 12 mo.; 300–500 hr.	Brushed every 3–4 mo.	Frequent conds.	Same	90	Same
	20	Stellar	About 12 mo.; 300–500 hr.	Never	Frequent conds.	Same	90	Same
Kirkwood	8	Stellar	26 mo.	Dusted	Heavy conds.	None	90	Same
	24	Stellar	14 mo.	10% HNO_3 once	Heavy conds.	Freckled with fine brown spots	50(?)	Same
	12	Stellar	14 mo.	Same	Heavy conds.	Same	50(?)	Same

TABLE 1—*Continued*

Observatory	Size of Mirror (Inches)	Use	Time in Use	How Cleaned	Atmospheric Conditions	Signs of Deterioration	Percentage of Efficiency Compared with New Coating	Life of Previous Coating
Lick	36	Stellar	5 mo.	Dusted each month. Alphasol every 6 mo. Strong HNO_3 every year	Some dust, tree pollen	None	100	54 mo.
Lowell	15	Stellar	50 mo.	Dusted	Excellent	Very little	90	Never recoated
McMath-Hulbert	18	Solar	700 hr.	Never	Dust and conds.	None	80	800–1000 hr.
	9½	Solar	700 hr.	Never	Dust and conds.	None	80	800–1000 hr.
	22	Solar	700 hr.	Alphasol once	Dust and conds.	Peeled in small spots	80	800–1000 hr.
	12	Solar	300 hr.	Never	Dust and conds.	None	80+	800–1000 hr.
	16	Solar	300 hr.	Never	Dust and conds.	None	80+	800–1000 hr.
Michigan	37½	Stellar	14 mo. 1200 hr.	50% HNO_3 every 6 mo.	Frequent conds., severe fumes, smoke and ash	Numerous pinholes, coating becoming ing thin	85	12 mo. 1000 hr.
	10½	Stellar	14 mo. 1200 hr.	Same	Same	Some pinholes	85+	12 mo. 1000 hr.
	15	Stellar. Student observatory	33 mo. 750 hr.	Never	Conds., some dust	None	90	Never recoated
	Many small	Spectrohelioscopic	33 mo. 100 hr.	Never	Same	None	90	Same

TABLE 1—*Continued*

Observatory	Size of Mirror (Inches)	Use	Time in Use	How Cleaned	Atmospheric Conditions	Signs of Deterioration	Percentage of Efficiency Compared with New Coating	Life of Previous Coating
Mt. Wilson....	100	Stellar	45 mo. 7500 hr.	Alphasol every 18 mo.	Infrequent dust storms and conds., tree pollen	Small numerous pinholes	97	Never re-coated
	60	Stellar	11 mo. 2000 hr.	Alphasol every 12 mo.	Same	Same	97	34 mo. 4450 hr.
	29	Stellar	16 mo. 3500 hr.	Alphasol every 24 mo.	Same	Same	97	44 mo. 8700 hr.
	19	Solar	11 mo. 1100 hr.	Alphasol every 12 mo.	Same	Same	97	17 mo. 2900 hr. 34 mo. 2200 hr.
	22	Stellar	11 mo. 2100 hr.	Same	Same	Bloom, scratches from removing cover		32 mo. 6500 hr.
Naval.........	7	Eclipse 6/8/37	Few hours	Soap and water once	Moist sea air, fine coral dust, high wind	Corroded slightly in spots	90–95	Never re-coated
Steward.......	9×13	Stellar	40 mo.	Dusted every 2 mo. Alphasol every 6 mo.	Much alkaline dust	Pinholes appear larger by transmitted light than when new	100	Same
	8×14	Stellar	40 mo.	Never	Same	Same	100	Same
	10	Stellar	40 mo.	Never	Same	Same	100	Same
	10	Stellar	40 mo.	Never	Same	Same	100	Same

TABLE 1—*Continued*

Observatory	Size of Mirror (Inches)	Use	Time in Use	How Cleaned	Atmospheric Conditions	Signs of Deterioration	Percentage of Efficiency Compared with New Coating	Life of Previous Coating
Vassar	6	Stellar	48 mo. 10 hr.	Soap and water	Coal smoke and ashes	Numerous pinholes, bloom, slight discoloration around pinholes	85	Never recoated
	$5\frac{1}{2}$	Stellar	48 mo. 80–100 hr.	Alcohol 3 times	Same	Pinholes	85–90	Same
	$4\frac{1}{2}$	Stellar	48 mo. 80–100 hr.	Alcohol 3 times	Same	Pinholes	85–90	Same
	3	Stellar	48 mo. 80–100 hr.	Alcohol 3 times	Same	Pinholes	85–90	Same
Yerkes	24	Stellar	60 hr.	Dusted, soap and water every 3–4 mo.	Occasional conds., dust in summer	None	Almost new	36 mo. 1500 hr. 12 mo. 400 hr.
	5×6	Stellar	400 hr.	Same	Same	Unequally semitransparent	80	36 mo. 1500 hr.
Mt. Locke (McDonald)	10×36	Nebular spectrographic	500 hr.	Same	Some dust in early spring	Surface bloom, discoloration, pinholes	Almost new	12 mo. 500 hr.
	24	Same	500 hr.	Same	Same	Same	Almost new	12 mo. 500 hr.

The most commonly observed deterioration is that caused by pinholes, particularly when the mirror is observed by transmitted light, although the exaggerated appearance of extremely small pinholes, when observed against the dark background of the generally opaque mirror, is coming to be universally recognized as largely a visual effect. The loss of light by transmission through the minute holes is, in most cases, utterly negligible, but there is some feeling that they are serious as starting-points for more extended deterioration. The most serious evidences of deterioration are those of bodily removal of the film over measurably large areas and a general decrease in the opacity of the film to the point where there is appreciable loss of light by transmission. There are only two cases reported where the film has lost reflectivity through a type of staining or discoloration which apparently cannot be removed safely. Apparently, aluminum surfaces do not deteriorate solely as a result of age, if they are kept well protected, but deteriorate rather from the accumulation of dirt and moisture coming from use.

When the surface dust on the mirror is dry and not imbedded in the film, it can be safely removed by careful dusting with a brush or chamois duster. It is reported from the McMath-Hulbert Observatory that daily dusting of the mirrors with a clean, dry air-blast at 15–40 pounds pressure greatly increases the useful life of the coatings. The frequent dusting prevents any accumulation of dirt which might later be dissolved by condensation of moisture to form a chemically active solution. When the surface dirt on the mirror is found to be slightly adherent, it can be removed with mild soap and water or with pure alcohol. When the dirt has had the time and occasion to become strongly adhered to the film, the solvents generally used are Alphasol (a neutral detergent) or concentrated nitric acid. Both of these fairly severe treatments are followed by liberal rinsing with water, and occasionally alcohol is subsequently used to promote rapid drying.

Mirrors are frequently recoated before the useful life of one coating is at an end, for at least two reasons. In those installations—particularly in tower telescopes—where scattered light is troublesome, the mirrors are frequently recoated in order to maintain a surface free of scratches. In other observatories, where the aluminizing equipment is conveniently near, it is found that recoating is only a little more laborious than thorough cleaning. However, as might be expected, the most general cause of recoating is that the old coating either appears to be badly deteriorated or else gives evidence of its state by greatly lowered photographic efficiency.

Some contrasting examples of the useful life of mirror coatings are these: At the Oak Ridge Station of the Harvard College Observatory a 10-inch finder mirror has been in use about 500 hours, over a period of 12 months, and its efficiency is estimated at 60 per cent of that of a new coating. At the Kirkwood Observatory the 24-inch mirror has been in occasional use for 15 months, and its efficiency is estimated at less than 50 per cent. On the other hand, an 8-inch mirror at the same observatory, in use for 27 months, appears as good as new. At the Lick Observatory the first coating of the 36-inch mirror was in use for 54 months before its efficiency in the violet and ultraviolet dropped to around 60 per cent. At Mount Wilson Observatory the coating on the 100-inch mirror is 45 months old, while its efficiency is estimated at 97 per cent. At the Griffith Observatory the length of life obtained from all mirror coatings is approximately 8000 hours of use.

At the Observatory of the University of Michigan the proximity of the smokestacks of the university heating-plant results in nightly deposits of soot and ash upon the mirror surface. This, combined with the frequent condensations of the Great Lakes climate, has a severely deteriorating action upon the aluminum. The coating on the $37\frac{1}{2}$-inch primary was last applied in October, 1937, and at the present time (March 1, 1939) there is notable evidence of deterioration. This is confined chiefly to the area immediately surrounding the central hole, and much of it is shadowed by the 11-inch secondary mirror. It is computed that with this instrument the coating could be entirely removed over a central disk 24 inches in diameter, and the average reflectivity would be reduced by only 33 per cent. Fortunately, with reflectors in closed tubes the deterioration appears to be greatest near the central hole, where the air currents are the greatest and there are no side walls to collect the dirt. The $37\frac{1}{2}$-inch mirror is cleaned about semiannually with concentrated nitric acid, followed with distilled water and alcohol.

Ordinary cleansers, such as alcohol or soap and water, will not affect in the slightest the deposition of greasy ash that is deposited upon the mirror. The secondary of the $37\frac{1}{2}$-inch reflector becomes coated with the usual grime of a soft-coal-burning town, but there is little bodily deposit of particles upon it. It is cleaned with nitric acid; and although it has remained uncovered night and day, it shows practically no deterioration.

The increase in reflectivity of the coating on the $37\frac{1}{2}$-inch mirror brought about by a thorough cleaning is rather striking. Before the last cleaning of the mirror the reflectivity was measured as 45 per cent; while after the cleaning, the measured reflectivity was about 80 per cent. This enormous range in reflectivity, owing to surface conditions, demonstrates the difficulty of determining the efficiency of a clean mirror when the estimation is made with one covered with a deposit of dirt.

It is clear from the preceding discussion that the useful life of aluminum coatings can be increased by eliminating the simultaneous occurrence of the two principal deteriorating agents: deposits of chemically active material and condensations of moisture. If, in any particular installation, means can be adopted for either keeping the mirror constantly dry or keeping it constantly free of deposited dirt, the life of the mirror coating will be greatly prolonged. Either one of the deteriorating agents, acting alone, apparently will not cause rapid and severe removal of portions of the aluminum film.

One of the questions asked on the inquiries was the frequency with which silvering had formerly been done. The general answer was twice yearly, except for observatories in especially smoky surroundings or those in particularly clean and dry surroundings. The range of frequency of silvering was from one month to one year. The bi-yearly interval is closely connected with the dependence of chemical silvering upon the prevailing temperature. Many observatories reporting bi-yearly silvering stated that three to four silverings a year were really needed. No observatory reported that it had discontinued aluminum in favor of silver, although one statement concerning discontinuance was: "Not yet."

The material in the reports provides a basis for the estimation of the expected life of an aluminum or chromium-aluminum coating.

The life of a mirror coating, of course, depends upon the minimum efficiency allowable in the spectral region used. It appears from the reports that a mirror combination is considered too inefficient to be used when its reflectivity has dropped to approximately 65 per cent of its original value, although in some instances, as mentioned above, the increase of scattered light becomes serious before the reflectivity of the mirror has dropped more than a few per cent. Another factor influencing the length of time that the coating on the primary can be used is the ease with which the secondary mirrors can frequently be recoated. If the secondary mirror is constantly maintained in a nearly new condition, the reflectivity of the primary can drop to 65 per cent of its original value (90 per cent) before the combination as a whole is only 65 per cent efficient, compared with two new coatings. This allows the absolute reflectivity of the primary to drop to about 58 per cent. If both primary and secondary have to be recoated together, the 65 per cent figure will be reached when each minor has dropped to 80 per cent of its original efficiency, or to an absolute reflectivity of 72 per cent.

The deterioration of the aluminum film depends upon the local climatic and atmospheric conditions, the care used in cleaning the mirror, and the original excellence of the coating. The effect of the atmospheric conditions is probably the greatest and has already been discussed. Care in cleaning consists chiefly in refraining from rubbing the mirror when its surface is covered with gritty material, in rinsing off thoroughly the cleaning agents, and in careful rubbing during the final drying. Unfortunately, the original excellence of the coating cannot be determined with certainty until the coating is several days old. The coating is soft when it first comes from the vacuum chamber; and unless it has been surface-hardened by washing, great care should be taken to keep it free of dust and grit for the first few weeks of its life. If "bloom" appears on the mirror within a short time, and if it cannot be removed with cleaning or *light* rubbing, the evidence is good that the surface was not adequately cleaned before the film was deposited. A long life cannot be anticipated for such a mirror.

If we assume that the reflectivity of the primary can be allowed to drop to about 65 per cent of its original value, and if we assume that the original coating was good and its subsequent care also good, then the expected life can be set at about two years as the lower limit and upward of five years as an upper limit. These limits are imposed by the deteriorating influence of moisture and dirt, and the lowest limits apply to climates similar to those at Bloomington, Pittsburgh, and Ann Arbor. The most probable life of a primary mirror in these climates is about two and one-half to three years if great care is taken in cleaning the aluminum surface. The aluminizing process, as applied to astronomical mirrors, is not yet old enough to predict the extreme upper length of life of a mirror at places like Flagstaff, Mount Locke, and Mount Palomar. A mirror life of five years appears regularly to be expected at those institutions favored by a dry and clean atmosphere.

It is a pleasure to express my appreciation of the generous and pleasant co-operation extended by the many observatories included in this survey.

OBSERVATORY OF THE
UNIVERSITY OF MICHIGAN
March 1939

A STUDY OF THE EQUIVALENT WIDTHS OF HELIUM LINES IN EARLY-TYPE STARS

LEO GOLDBERG

ABSTRACT

The theoretical strengths of the *He* I lines in the diffuse 2p−nd series have been employed, together with E. G. Williams' measures of equivalent widths, to construct curves of growth for the helium lines in fifty-seven O- and B-type stars. Comparisons of these curves with a theoretical curve for helium atoms at a temperature of 20,000° permits a determination of the quantities V and Δ. V is defined by the relation

$$\log v' = \log v_0 + V ,$$

where v_0 is the most probable kinetic velocity of helium atoms at a temperature of 20,000°, and $\log v'$ measures the height of the flat portion of the curve of growth. V then represents the combined changes in $\log v_0$ engendered by differences in temperature, turbulence, and/or Stark effect. The form of the curve of growth is relatively insensitive to temperature. A plot of V against spectral class shows no correlation for dwarf and intermediate stars, but there is a rapid increase in V toward the earlier spectral subdivisions for the supergiants. If the value of V is a measure of the Stark broadening in the dwarf and intermediate stars and of turbulence in the supergiants, the results indicate that turbulence depends rather strongly on the temperature, which in turn suggests that radiation pressure may be one of the forces responsible for turbulence in stellar atmospheres.

Several curves of growth have been constructed from the somewhat meager observations of the equivalent widths of *O* II and *N* II lines in the B stars. They agree with the helium curves in indicating large turbulent velocities in the supergiant atmospheres.

The quantity

$$\Delta = \log X_0 - \log X_0' ,$$

where X_0 is the optical depth at the center of an absorption line and X_0' is its theoretical strength, is employed to calculate $\log N$, the number of two-quantum helium atoms per square centimeter above the photosphere in the O and B stars. Log N shows a decided maximum at about class B4. The apparently anomalous weakening of the singlet lines, as compared with the triplet lines, of helium among the B spectral subdivisions on either side of class B4, which has been attributed by Struve to departures from thermodynamic equilibrium, is found to result quite naturally from the decrease in $\log N$ on either side of class B4 and from the properties of the curve of growth.

It is shown that, when the positions of these lines on the curve of growth are taken into account, the relative intensities of the forbidden line λ 4470 and the permitted line λ 4472 in γ Pegasi lead to a value of 10^3–10^4 volts/cm for the average mol-electric field in this star. The value agrees with Struve's estimate of the field strength from studies of the hydrogen lines and is in accord with an electron pressure of the order of 10^{-4} atmospheres.

The application of curves of growth to the study of absorption lines in solar and stellar spectra has already met with considerable success in the realm of complex metallic atoms. The theory of these curves was first developed by Minnaert and Slob,[1] who discussed the manner in which the equivalent width of an absorption line varies as a function of the so-called "number" of absorbing atoms. Menzel[2] later provided the theoretical justification for Allen's[3] empirical discovery that W/λ, rather than W, is correlated with the number of absorbing atoms.

Thus far, no attempt has been made to construct curves of growth for helium in early-type stars. The reasons have been twofold: first, there have been, until recently, no extensive measures of equivalent widths of helium absorption lines; and second, laboratory or theoretical data on the transition probabilities have been lacking. Both these needs have now been met, at least in part. E. G. Williams[4] has published the total absorptions of thirteen lines of *He* I from λ 3820 to λ 4922, in the spectra of some eighty O- and B-type stars. These measures, together with the transition probabilities computed by Hylleraas[5] and by Goldberg,[6] open up the possibility of constructing empirical curves of growth for helium lines.

The form of the curve of growth for helium in early-type stars is complicated by a number of factors. The work of Struve and Elvey[7] has indicated that turbulence plays an important role in the formation of absorption lines in giant stars. In addition, there is the possibility that emission from the rarefied outer portions of supergiant atmospheres is complicating the line formation. Investigations by Struve and others[8] have conclusively shown that Stark effect and collisions are active influences in the atmospheres of early-type dwarf and intermediate stars.

As a preliminary it will be useful to determine a theoretical curve of growth for helium lines in early-type stars. In deriving such a curve, we shall first assume that only Doppler broadening and radiation damping are instrumental in the line broadening. Menzel[9] has shown that the functional form of the curve of growth for a line may be written as

---

[1] *Proc. Amsterdam Acad.*, **34**, Part 1, 542, 1931.

[2] *Ap. J.*, **84**, 462, 1936.

[3] *Mem. Comm. Solar Obs.*, **1**, No. 5, 1934.

[4] *Ap. J.*, **83**, 279, 1936.

[5] *Zs. f. Ap.*, **106**, 395, 1937.

[6] *Ap. J.*, in press.

[7] *Ap. J.*, **79**, 409, 1934.

[8] Struve, *Ap. J.*, **70**, 15, 1929; **69**, 173, 1929; Elvey, *Ap. J.*, **70**, 141, 1929.

$$\frac{W}{\lambda} = F(X_0) , \tag{1}$$

where F is some function and

$$X_0 = \frac{N_a}{b(T)} \cdot e^{-\chi_{J'}/kT} \frac{1}{3\sqrt{\pi R}} \cdot \frac{\pi\epsilon^2}{mc} \cdot \frac{c}{v_0} \cdot S . \tag{2}$$

Here X_0 is defined as the optical depth $N\alpha_{\nu_0}$ at the center of the absorption line, N_a is the total number of atoms of a particular element in a given stage of ionization per square centimeter above the stellar photosphere, $b(T)$ is the partition function, $\chi_{J'}$ is the lower excitation potential of the line, R is Rydberg's constant in sec^{-1}, v_0 is the most probable kinetic velocity of the atoms under consideration, and S is the so-called "strength" of the line in atomic units.

When X_0 is very small,

$$\frac{W}{\lambda} \sim \sqrt{\pi}\, \frac{v_0}{c} X_0 ; \tag{3}$$

and when X_0 is very large,

$$\frac{W}{\lambda} \sim \frac{\pi^{1/4}}{2} \left(\frac{v_0}{c}\right)^{1/2} \left(X_0 \frac{\Gamma}{\nu}\right)^{1/2} , \tag{4}$$

where Γ is the damping constant for the transition and ν is the frequency in sec^{-1}. The damping constant for a line is the sum of the reciprocal mean lifetimes of the two levels involved. Values of Γ for pure radiation damping have been computed for the helium lines.[10]

At intermediate values of X_0,

$$\frac{W}{\lambda} \sim 2\, \frac{v_0}{c} \left(\frac{\log X_0}{0.434}\right)^{1/2} . \tag{5}$$

---

[9] *Op. cit.*; cf., also, *Pop. Ast.*, **47**, 66, 1939.

[10] Goldberg, *op. cit.*

For small and intermediate values of X_0, one curve suffices for all the lines of a given element. For large values of X_0, however, each line has its own particular curve, since no two lines have exactly the same value of Γ/ν. The variations of Γ/ν among the helium lines are, nevertheless, relatively small within each multiplicity group (singlets or triplets). Consequently, average values may be adopted: 3.0×10^{-6} for the singlets and 3.0×10^{-8} for the triplets. The large disparity between these two values is understandably due to the fact that, in so far as radiation is concerned, the lowest triplet level is metastable.[11]

The velocity parameter, v_0, is given by

$$v_0 = 1.289 \cdot 10^4 \sqrt{\frac{T_0}{\mu}} \text{ cm/sec}^{-1} , \tag{6}$$

where T_0 is the temperature and μ the atomic weight. For helium, $\mu = 4$; and with $T_0 = 20{,}000°$, (3), (5), and (4) become, logarithmically,

$$\log \frac{W}{\lambda} = \log X_0 - 4.27 ; \tag{7}$$

$$\log \frac{W}{\lambda} = \tfrac{1}{2} \log (\log X_0) - 4.04 ; \tag{8}$$

$$\log \frac{W}{\lambda} = \tfrac{1}{2} \log X_0 + \tfrac{1}{2} \log \frac{\Gamma}{\nu} - 2.44 . \tag{9}$$

If we plot $\log W/\lambda$ against $\log X_0$ from equations (7), (8), and (9), we may obtain the complete curve of growth by asymptotically joining (8) to (7) and (9). The resulting curve is shown in Figure 1, for the two values of Γ/ν corresponding to the singlet and triplet lines of helium. The extent of the flat portion, as compared with that of a metallic curve of growth, is of interest. The singlet radiation-damping constant for helium is of the same order of magnitude as that for the metals, but the low atomic weight of helium leads to a large value of v_0, and consequently acts to broaden the Doppler cores of the lines. The small value of the triplet damping constant creates a situation whereby a thousand-fold increase in the number of absorbing atoms serves merely to double the total absorption. This point is significant in connection with Struve's[12] suggestion that the combination of diluted radiation and the metastability of the lowest triplet level of helium tends to promote an overpopulation of the triplet levels in the atmospheres of supergiant O and B stars. We shall presently return to a consideration of this problem.

---

[11] In a private communication Dr. G. H. Shortley points out that the probability of a transition from 1s2s ^1S or ^3S to 1s^2 ^1S is zero for electric dipole, electric quadrupole, and magnetic dipole radiation. Consequently, in the absence of external influences, the mean lives of the 2s levels are infinite.

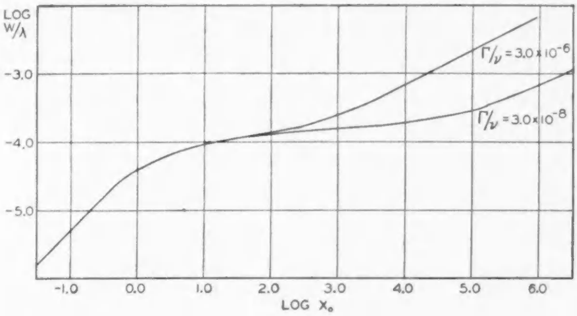

FIG. 1.—Curve of growth for helium atoms for $T_0 = 20{,}000°$

The question now arises as to how the theoretical curve of Figure 1 is likely to differ from the true curve of growth for the helium lines in an early-type star. The theoretical curve for a temperature of 20,000° will unquestionably be altered by interatomic collisions, Stark effect, turbulence, and also by the temperature dispersion among the early-type stars. The curve of growth is relatively insensitive to temperature, since v_0 is inversely proportional to the square root of the temperature. For an increase in T_0 from 20,000° to 30,000°, or for a decrease to 13,000°, the Doppler and intermediate portions of the curve will be raised or lowered by only 0.1 in log W/λ, and the damping portion will be shifted vertically by half that amount. It is necessary to point out that the X_0 scale will also be shifted by 0.1 in log X_0, because X_0 is proportional to c/v_0.

There is evidence[7] that large turbulence effects are present in the atmospheres of supergiant stars. Turbulence acts to alter the curve of growth in exactly the same manner as does an enhancement of the temperature—by an increase in the velocity parameter v_0 and a consequent upward shift of the curve of growth.

---

[12] *Ap. J.*, **82**, 252, 1935.

It is unlikely that collisions and Stark broadening play a very significant role in the formation of lines in supergiant atmospheres, although these effects should be of considerable importance in the dwarf and intermediate stars. Some recent calculations by Struve[13] indicate that the collisional damping constant for the diffuse series lines of *He* I may be many times larger than the classical value. Such an increase in the damping constant would, of course, raise the damping portion of the curve in Figure 1 by an amount that presumably depends upon the electron pressure. Menzel[14] has pointed out that the Stark width of a line may be considered as a "core" in the same sense as a Doppler core. In the process of the growth of an absorption line there will always be a range of X_0 over which $\log W/\lambda \propto \log X_0$, and one over which $\log W/\lambda \propto \frac{1}{2} \log X_0$, irrespective of whether Stark broadening is more important than Doppler broadening for weak lines. If Stark broadening does predominate over Doppler broadening, the value of $\log W/\lambda$ at which the curve of growth begins to flatten out is governed by the width of the "Stark core." Now these widths are known to increase with serial number in the diffuse series; and, strictly speaking, the various lines may not be combined on the same curve, except when X_0 is very small or very large. If, however, we assume an average broadening for all the lines of a series, the combination may be attempted. To the extent that this approximation holds, Stark broadening will alter the curve of growth in the same manner as will turbulence or an increase in the temperature, namely, by an increase in the effective value of v_0.

There is one further question that merits consideration in connection with the influence of Stark effect on the curve of growth. This question pertains to the degree in which the forbidden components of the helium lines affect the zero-field transition probabilities of the permitted lines. There is little doubt but that, in electric fields, the forbidden components are strengthened at the expense of the permitted lines. Ordinarily, however, the forbidden components are not observed separately in the spectra of early-type stars. The observed total absorption is the sum of the individual components of the line, both permitted and forbidden. I am indebted to Dr. G. H. Shortley for informing me that the sum of the strengths of the permitted and forbidden components of a line, such as 2p – 5p, 5d, 5f, 5g, in an electric field is the same as the strength of the permitted line 2p – 5d in a zero-field.

---

[13] *Observatory*, **61**, 53, 1938.

[14] *Private discussion.*

We now proceed to the derivation of empirical curves of growth from Williams' measures of equivalent widths and from the theoretical strengths of the helium lines. Williams' list of helium lines includes nine diffuse series lines, the triplets at $\lambda\lambda$ 4472, 4026, and 3820 and the singlets at $\lambda\lambda$ 4922, 4388, 4144, 4009, 3927, and 3872. Of the four remaining lines, three are sharp-series members, for which accurate transition probabilities are not available, while the one subordinate-series line, λ 3965, lies within the wing of $H\epsilon$ and is therefore unsuitable for quantitative study.[15] Accordingly, only diffuse-series members will be employed in constructing empirical curves of growth.

The optical depth at the center of the absorption line, X_0, is given by (2). It is likely that the general opacity is variable with wave length; N_a, in consequence, will exhibit a reciprocal variation. If most of the opacity in high-temperature stars is produced by the ionization of hydrogen—a not unlikely hypothesis—the opacity should vary nearly as λ^3. Such an opacity variation may be represented by writing

$$N_a = N_a' \left(\frac{\lambda'}{\lambda}\right)^3 , \tag{10}$$

where N_a' is the value of N_a at some standard wave length λ'. For convenience we choose $\lambda' = 5000$ A. If we substitute (10) in (2) and insert the values of the constants, we obtain

$$X_0 = 3.510 \cdot 10^{-12} \frac{N_a'}{b(T)} \left(\frac{\lambda'}{\lambda}\right)^3 e^{-\chi_{J'}/kT} \sqrt{\frac{\mu}{T_0}}\, S . \tag{11}$$

---

[15] Cf. Williams, *op. cit.*, p. 316.

Logarithmically, with $\mu = 4$,

$$\log X_0 = -11.16 + \log \frac{N'_a}{b(T)} - \frac{5040}{T}\chi_{J'} - \tfrac{1}{2}\log T_0 + \log X'_0 \,, \qquad (12)$$

where

$$\log X'_0 = \log S + 3\log \lambda' - 3\log \lambda \,. \qquad (13)$$

In the diffuse series the difference between the excitation potentials of $2\ ^3P^o$ and $2\ ^1P^o$ is sufficiently small (0.26 of a volt) that it may be disregarded in (12). For the diffuse series, then, $\log X'_0$ differs from $\log X_0$ only by an additive constant. Accordingly, if we plot $\log W/\lambda$ against $\log X'_0$, we shall obtain empirical curves of growth for these lines. A comparison of these curves with that shown in Figure 1 for $T_0 = 20{,}000°$ should provide useful information regarding the behavior of helium lines in the B stars. The diffuse series lines employed in the analysis are conveniently listed in Table 1. The columns are self-explanatory. The tabulated values of $\log X'_0$ were derived from the theoretical strengths computed by the writer.[6] A preliminary plot of $\log W/\lambda$ against $\log X'_0$ for the lines shown in Table 1 brought forth the interesting information that all of these lines fall either on the steep Doppler portion or on the intermediate portion of the curve of growth. In no star was there any evidence that damping had begun to predominate in the line broadening. This result greatly facilitates the comparison between the

TABLE 1

VALUES OF LOG X'_0 FOR DIFFUSE SERIES OF *He* I

Line	λ	$\log X'_0$
$2\ ^3P^o-4\ ^3D$	4472	+1.38
$5\ ^3D$	4026	+1.05
$6\ ^3D$	3820	+0.81
$2\ ^1P^o-4\ ^1D$	4922	+0.79
$5\ ^1D$	4388	+0.45
$6\ ^1D$	4144	+0.15
$7\ ^1D$	4009	−0.03
$8\ ^1D$	3927	−0.22
$9\ ^1D$	3872	−0.40

observed curves and the curve of Figure 1, as may be demonstrated from the following considerations.

The effects of temperature dispersion, turbulence, and Stark broadening on the Doppler and intermediate branches of the curve of growth may be accounted for, on the average, by introducing, in (3) and (5), an effective value of the velocity parameter, which we denote by v'. The expression

$$\log v' = \log v_0 + V \tag{14}$$

serves to define the quantity V. If v_0 is the most probable kinetic velocity of helium atoms at a temperature of 20,000°, V represents the change in $\log v_0$ that is engendered by the combined effects of a temperature other than $T_0 = 20{,}000°$, turbulence, and Stark broadening. For any star, $\log W/\lambda$ will be given by

$$\log \frac{W}{\lambda} = \log X_0 + \tfrac{1}{2} \log \pi - \log c + \log v_0 + V \tag{15}$$

in the Doppler portion of the curve of growth, and by

$$\log \frac{W}{\lambda} = \log (\log X_0)^{1/2} + \log 2 + \tfrac{1}{2} \log \frac{1}{0.434} - \log c + \log v_0 + V \tag{16}$$

in the intermediate region. Since X_0 is inversely proportional to v_0, (12) becomes

$$\log X_0 = -11.16 + \log \frac{N'_a}{b(T)} - \frac{5040}{T} \chi_{J'} - \tfrac{1}{2} \log T_0 - V + \log X'_0 . \tag{17}$$

We may now compare Figure 1 with the observed curves. It may be seen from (16) and (17) that a vertical adjustment of the theoretical curve with respect to an observed curve will yield a value of V and that a horizontal adjustment gives the quantity

$$\Delta = \log X_0 - \log X'_0 . \tag{18}$$

The results for twelve O and B stars are shown in Figures 2 (giants), 3 (intermediates), and 4 (dwarfs). The classifications and luminosity groupings are taken from Williams. The crosses and dots represent the triplet and singlet lines, respectively, of the *He* I diffuse series. The curve passing through the plotted points in each diagram is the

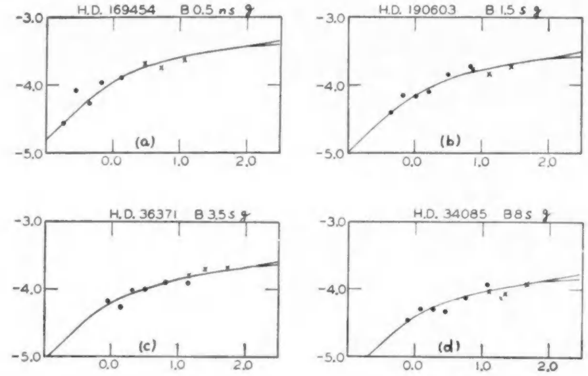

FIG. 2.—Curves of growth for supergiant stars. Ordinates are log W/λ; abscissae, log X_0.

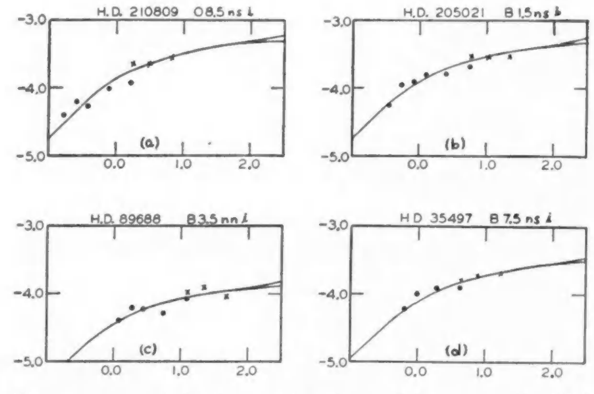

FIG. 3.—Curves of growth for intermediate stars. Ordinates are log W/λ; abscissae, log X_0.

theoretical one of Figure 1, after a suitable adjustment of the scale of ordinates. Curves similar to these were constructed for 57 stars, and values of V and Δ were derived from comparisons with Figure 1.

The quantity Δ provides a means for determining the number of atoms in the 2 $^1P^0$ and 2 $^3P^0$ levels of helium. By (17) and (18), with $T_0 = 20{,}000^\circ$,

$$\Delta = -13.31 + \log \frac{N'_a}{b(T)} - \frac{5040}{T} \chi_{J'} - V \,. \tag{19}$$

The numbers of helium atoms in the 2 $^1P^0$ and 2 $^3P^0$ levels are given

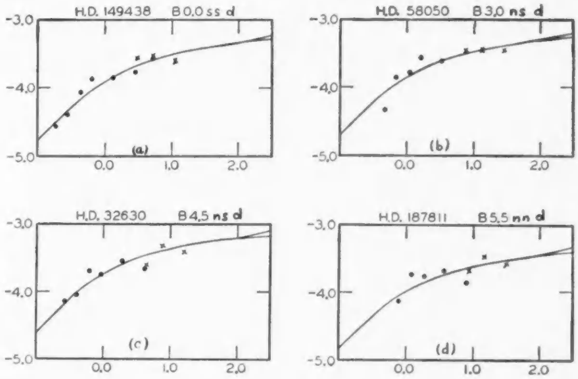

FIG. 4.—Curves of growth for dwarf stars. Ordinates are log W/λ; abscissae, log X_0

in terms of the total number of helium atoms by the Boltzmann formula:

$$\log N = \log \bar{\omega}_{J'} + \log \frac{N'_a}{b(T)} - \frac{5040}{T} \chi_{J'} \,, \tag{20}$$

where

$$\bar{\omega}_{J'} = (2S + 1)(2L + 1) \tag{21}$$

is the statistical weight of the lower term. Hence, by (19), (20), and (21)

$$\log N = \log (2S + 1)(2L + 1) + 13.31 + \Delta + V \,. \tag{22}$$

The Δ's and the V's for the various stars are known from the observed curves of growth. Equation (22), therefore, leads to a determination of the number of helium atoms per square centimeter above the photosphere at λ 5000 in the 2 $^1P^0$ or the 2 $^3P^0$ levels. The values of V, Δ, and log N for 57 stars are given in Table 2. The first

TABLE 2

HD	Sp.	Lum.	V	Δ	log $N(2\ ^1P^0)$	log $N(2\ ^3P^0)$
886	B2.5ss	i	+0.57	+0.03	14.39	14.87
4180	B5.0nn	i	+ .30	−0.13	13.96	14.44
11415	B4.5ns	i	+ .20	+0.74	14.73	15.21
13854	B1.0s	g	+ .30	+0.10	14.19	14.67
14134	B1.5s	g	+ .22	+0.42	14.43	14.91
21291	B6.5s	g	− .17	+0.04	13.66	14.14
22928	B7.5nn	i	+ .16	+0.20	14.15	14.63
24398	B1.0s	g	+ .49	−0.22	14.06	14.54
24912	O8.0n	i	+ .68	−1.22	13.25	13.73
28446b	B0.0n	d	+ .45	−0.26	13.98	14.46
28446f	B0.5ss	d	+ .45	+0.03	14.27	14.75
30614	O9.0ns	g	+ .50	−0.50	13.79	14.27
32630	B4.5ns	d	+ .64	−0.16	14.27	14.75
34085	B8s	g	.00	+0.30	14.09	14.57
35497	B7.5ns	i	+ .32	−0.17	13.94	14.42
36371	B3.5s	g	+ .20	+0.36	14.35	14.83
36861	O7.5n	i	+ .43	−0.57	13.65	14.13
36862	B0.5ns	d	+ .51	−0.17	14.13	14.61
37128	B0.0s	g	+ .30	−0.41	13.68	14.16
38771	B0.5ns	g	+ .48	−0.33	13.94	14.42
39698	B3.0ns	i	+ .37	+0.58	14.74	15.22
40111	B0.5ns	i	+ .47	+0.20	14.46	14.94
41117	B1.5s	g	+ .16	+0.23	14.18	14.66
44743	B1.0s	i	+ .32	+0.26	14.37	14.85
58050	B3.0ns	d	+ .57	+0.08	14.44	14.92
74280	B5.0n	i	+ .21	+0.69	14.69	15.17
89688	B3.5nn	i	+ .48	+0.30	14.57	15.05
91316	B1.0s	g	+ .33	+0.11	14.23	14.71
100600b	B4.5n	i	+ .70	−0.39	14.10	14.58
120315	B5.0nn	d	+ .38	+0.50	14.67	15.15
149438	B0.0ss	d	+ .52	−0.33	13.98	14.46
149757	B0	i	+ .53	−0.54	13.78	14.26
149881	B0.5ns	i	+ .43	−0.09	14.13	14.61
160762	B3.5ss	i	+ .56	0.00	14.35	14.83
164353	B3.5s	g	+ .03	+0.66	14.48	14.96
169454	B1.0s	g	+ .31	−0.26	13.84	14.32
187811	B5.5nn	d	+ .40	+0.12	14.31	14.79
190603	B1.5s	g	+ .24	+0.06	14.09	14.57
191201	O9.5ns	i	+ .33	0.00	14.12	14.60
192422	B0.0ns	i	+ .38	−0.11	14.06	14.54
194279	B1.5ss	g	+ .59	−0.48	13.90	14.38
195592	O9.0ns	i	+ .70	−0.74	13.75	14.23
198478	B3.0s	g	+ .26	+0.11	14.16	14.64
200120	B4.5nn	i	+ .48	−0.23	14.04	14.52
204172	B0.5ns	i	+ .45	−0.45	13.79	14.27
205021	B1.5ns	i	+ .52	−0.05	14.26	14.74
206165	B2.5s	g	+ .20	+0.63	14.62	15.10
208185	B3.5ss	i	+ .72	−0.04	14.47	14.95
208947	B3.5ns	i	+ .60	0.00	14.39	14.87
210809	O8.5ns	i	+ .53	−0.57	13.75	14.23
212455	B4.0s	g	+ .27	+0.10	14.16	14.64
212571	B1.5nn	i	+ .46	−0.50	13.75	14.23
213420	B3.5ns	i	+ .44	+0.30	14.53	15.01
214680	O8.5ss	i	+ .39	−0.38	13.80	14.28
224151	B1.0ns	i	+0.23	+0.14	14.16	14.64

column gives the Henry Draper number of the star, the second and third columns contain Williams' spectral classification and luminosity grouping, while the last three columns give, in order, the values of V, Δ, and log $N(2\ {}^1P^0)$.

Figure 5 shows the distribution of the V's according to spectral subdivision. The crosses represent giants, the dots intermediates, and the circles dwarfs. In the latter two groups there is no apparent correlation of V with spectral class, but the giants show a conspicuous increase of V with increasing temperature. Now V is a measure of the combined changes produced in the curve of growth for $T_0 = 20{,}000^\circ$ by a change in temperature and by the presence of Stark effect and/or turbulence broadening. As has been stated earlier, the curve of growth is insensitive to temperature. The dispersion around $V = 0$, arising from a temperature dispersion around $T_0 = 20{,}000^\circ$, is probably no more than 0.20, while the uncertainty involved in determining V by fitting a theoretical curve to an observed one should be of the order of 0.1. With but one exception, all the values of V are positive, which indicates that the temperature dispersion is not the dominating factor in determining V. I should like to suggest that in the low-luminosity groups the value of V is a measure of the average Stark broadening in the diffuse series, while in the giants V measures the degree of turbulence in the stellar atmosphere. The pronounced increase of V with temperature for the giants suggests that the amount of turbulence is strongly dependent on the temperature and that radiation pressure may be partly responsible for the phenomenon.

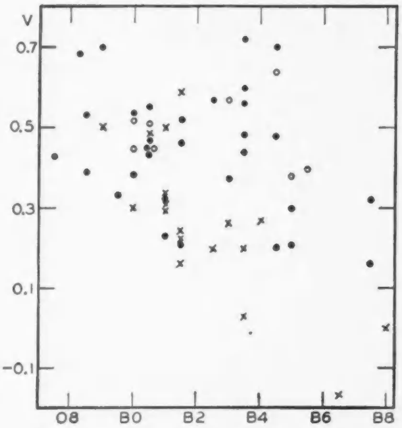

FIG. 5.—Variation of V with spectral subdivision. Crosses represent supergiants; circles, dwarfs; dots, intermediates.

It is interesting to compute the actual turbulent velocities which correspond to the values of V for the supergiants. If v' is the effective value of the velocity parameter as derived from the empirical curve of growth, v_0 is the thermal velocity of the helium atoms, and v_t is the turbulent velocity, then

$$v'^2 = v_0^2 + v_t^2 \,, \tag{23}$$

or

$$\log v_t = \tfrac{1}{2} \log (v'^2 - v_0^2) \,. \tag{24}$$

The values of log v_t were computed from equation (24) with an assumed temperature variation of from 30,000° at O9 to 13,000° at B8. The results are shown in Table 3, where the turbulent velocities are given in kilometers per second, and in Figure 6. The velocities are of the same order of magnitude as those found by Struve and Elvey[16] for the supergiant stars 17 Leporis, ϵ Aurigae, and α Persei.

TABLE 3

MOST PROBABLE TURBULENT VELOCITIES IN KILOMETERS PER SECOND OF *He* I ATOMS IN SUPERGIANT ATMOSPHERES

HD	Sp.	v_t	HD	Sp.	v_t
13854	B1.0s	16	41117	B1.5s	10
14134	B1.5s	12	91316	B1.0s	17
21291	B6.5s	− 5	164353	B3.5s	4
24398	B1.0s	27	169454	B1.0s	16
30614	O9.0ns	27	190603	B1.5s	13
34085	B8.s	5	194279	B1.5ss	35
36371	B3.5s	11	198478	B3.0s	14
37128	B0.0s	15	206165	B2.5s	12
38771	B0.5ns	26	212455	B4.0s	14

The variation of turbulent velocities with spectral subdivision is significant from the standpoint of the variation of the diffuse triplet intensities with spectral subdivision. Williams found that the mean equivalent width of the three diffuse triplets in the giant stars increases from about B9 to about B4 and then remains constant from B4 to O9. For the dwarfs and intermediate stars the mean diffuse triplet intensity reaches a maximum at B4 and then decreases rapidly toward the earlier spectral subdivisions. Consider two stars with the same value of the temperature but with different turbulent velocities. Since the diffuse triplets are on the horizontal portion of the curve of growth, it is obvious that the equivalent widths of the triplets will be greater in the star with the greater turbulent velocity. The turbulence appears to increase with the temperature for the giants. Hence, the expected decrease in triplet intensity for these stars from B4 to O9, because of the decrease in number of the absorbing atoms, is counterbalanced by a corresponding increase in the turbulent velocity.

---

[16] *Ap. J.*, **79**, 345, 1934.

The possibility that the giant B stars have turbulent atmospheres has already been inferred by Struve[17] from the peculiar behavior of several *O* II lines. Struve found that all the stronger *O* II lines are strengthened in the giants, whereas the faint lines are equally intense in the giants and the dwarfs. Essentially the same effect was noted by Williams[18] in the behavior of the *N* II lines. The most obvious way of proving whether or not these lines are broadened by turbulence in giant stars is to construct curves of growth from the measured equivalent widths. Williams[18] has published such measures for several multiplets of *O* II and *N* II. Naturally, one would like to construct curves for both giants and dwarfs, in order to test whether turbulence is present in the former and absent in the latter. Unfortunately, the lines are weak in the dwarfs, and consequently the uncertainty in the measures is too great to define curves of growth for so relatively few lines. The situation is more favorable

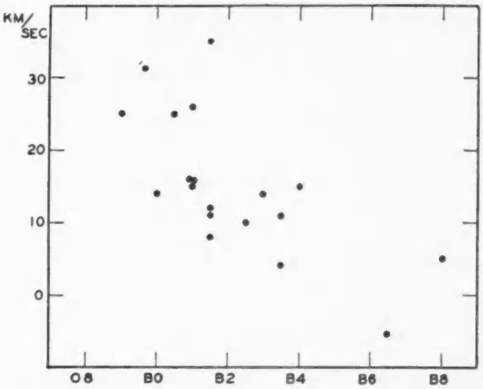

FIG. 6.—Turbulent velocities of helium atoms in supergiant B stars

in the giants, however; and the curves of growth should give a positive answer, at least, to the question whether turbulence is present or absent in these stars. The multiplets available for the analysis, including four of *O* II and one of *N* II, are shown in Table 4. For a given line, X'_0 is its theoretical strength in terms of a constant for the transition array to which the line belongs. All the tabulated lines of *O* II belong to the same transition array, $2p^23s - 2p^23p$. Both quartet multiplets of *O* II have identical lower excitation potentials, as have the two doublets. Accordingly, in constructing

---

[17] *Ap. J.*, **78**, 73, 1933

[18] *Op. cit.*

TABLE 4

O II AND *N* II LINES

Multiplet	λ	log X'_0	Multiplet	λ	log X'_0
	O II			*O* II	
$y^4P-e^4D^o$	4676	+0.25	$z^2P-e^2P^o$	3983	−0.17
	4662	+ .33		3973	+ .53
	4650	+ .90		3954	+ .13
	4641	+ .62		3945	−0.17
$z^2P-e^2D^o$	4417	+ .52			
	4415	+ .78		*N* II	
$y^4P-e^4P^o$	4367	+ .26			
	4326	− .47	$3s^3P^o-3p^3P$	4631	+0.57
	4320	+ .26		4614	− .13
	4317	+0.22		4607	.00
				4601	+0.09

a curve of growth, log W/λ was plotted against log X'_0 separately for each pair of *O* II multiplets and for the single multiplet of *N* II, and the three diagrams were then combined by the usual procedure of horizontal shifting. The resulting curves are shown in Figure 7 for eight supergiant B stars. The procedure in estimating the degree of turbulence from the plotted curves was the same as that followed for the helium lines. A theoretical curve for oxygen at $T_0 = 20{,}000^\circ$ was constructed, and a comparison between this curve and the empirical curves yielded a value of *V* for each star. These values, together with the corresponding turbulent velocities, are shown in Table 5. On the whole, the values of v_t are considerably larger than those derived from the helium lines. It must be emphasized, however, that the procedure of deriving a curve of growth from only a few multiplets is a highly uncertain one and that the actual numerical values in Table 5 are not to be taken too seriously. The procedure should certainly give the correct order of magnitude of the turbulent velocities, however, and the results may be regarded as verifying both the

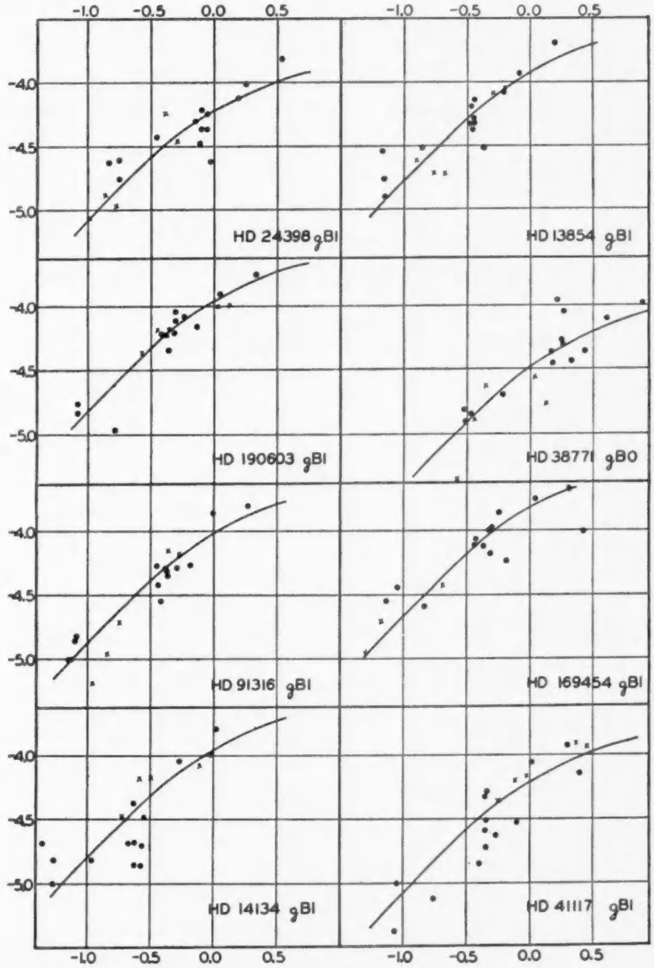

FIG. 7.—Curves of growth for O II and N II in eight supergiants. Crosses represent N II; dots, O II. Ordinates are log W/λ; abscissae, log X_0.

turbulent velocities derived from the helium lines and Struve's conclusions with respect to the *O* II lines. It is also possible that the larger turbulent velocities deduced from the high-level ionized lines may be an indication of differential turbulence of the kind suspected by Menzel[19] in the Cepheids.

THE HELIUM ANOMALY

About ten years ago Struve[20] pointed out that the relative intensities of the helium lines λ 4388, a singlet, and λ 4472, a triplet, varied markedly from star to star. Later Struve[21] compiled a more extensive array of observations, including line-intensity estimates for 116 stars of classes O and B. For each of these stars Struve made estimates of the relative intensities of three pairs of singlets and triplets. He summarizes his conclusions as follows:

TABLE 5

MOST PROBABLE TURBULENT VELOCITIES IN KILOMETERS PER SECOND OF *O* II AND *N* II ATOMS IN SUPERGIANT ATMOSPHERES

HD	Sp.	v_t	HD	Sp.	v_t
13854	B1.0s	27	41117	B1.5s	11
14134	B1.5s	25	91316	B1.0s	21
24398	B1.0s	11	169454	B1.0s	35
38771	B0.5ns	5	190603	B1.5s	26

1. At spectral classes B2, B3, and B4, or near the temperature at which all the helium lines are most intense, the singlet lines are nearly as intense as the triplets.

2. At spectral classes B0 and O, a marked fading of the singlets occurs as compared with the triplets. The diminution of singlet intensity appears to be more pronounced in the giants than in the dwarfs.

3. At the low-temperature end of the B sequence, in classes B7, B8, and B9, a similar weakening of the singlets takes place, but the change is not as marked as in the earlier types. There is no appreciable difference between giants and dwarfs in the latter subdivisions.

---

[19] *Pub. A.A.S.*, **6**, 370, 1930.

[20] *Nature*, **122**, 994, 1928.

[21] *Ap. J.*, **74**, 225, 1931; Russell, Mrs. Gaposchkin, and Menzel, *Ap. J.*, **81**, 114, 1935.

These conclusions are, in the main, verified by the measures made by Williams,[22] who finds that the ratio (Mean equivalent width of λ4388, λ4144)/(Mean equivalent width of λλ4472, 4026, 3820) varies from about 0.6 in class B4 to 0.3 in class O8. There is, however, little evidence from Williams' measures that the singlet lines are generally weaker in the dwarfs than in the giants, although this result may be ascribed to differences between Struve's and Williams' luminosity groupings. As Struve points out, the difference between the lower excitation potentials of the singlet and triplet members of a series is quite small—about three-tenths of a volt. Consequently, the relative numbers of atoms in any atmosphere approaching the conditions of thermodynamic equilibrium and capable of absorbing the singlet and triplet lines of a series should be essentially independent of the temperature.

Struve has provided two possible explanations for the relative strengthening of triplet lines in giant stars. The first[23] hypothesis, involving turbulence in the atmospheres of supergiants, supposed that the triplets of *He* I were near the horizontal portion of the curve of growth. Consequently, turbulence, which raises the flat portion of the curve, would strengthen the triplets and leave the intensities of the weaker singlets unchanged. This first explanation was later abandoned by Struve[24] in favor of a hypothesis involving departures from thermodynamic equilibrium in the supergiant atmospheres. The combination of two factors—(*a*) the diluted stellar radiation in the atmospheres of supergiant stars, and (*b*) the metastability of the lowest triplet level of helium, $2\ ^3S$—will tend to overpopulate all the triplet levels. Struve interprets the weakening of the singlet lines in the giants as evidence for large departures from thermodynamic equilibrium.

The material collected in Table 2 affords the means for a quantitative study of the nature of the *He* I anomaly. An inspection of Figures 2, 3, and 4 shows that the ratio of singlet to triplet equivalent width may vary considerably from one spectral class to another because of the properties of the curve of growth. At about class B3, where the helium lines are most intense, the triplets are well up on the flat portion of the curve (Figs. 2, *c*, and 3, *c*) while

[22] *Op. cit.*

[23] *Ap. J.*, **78**, 86, 1933.

[24] *Ibid.*, **82**, 252, 1935.

the singlets have just passed the steep portion. In class B0 (Figs. 2, *a*, and 4, *a*) the triplets are still on the intermediate portion of the curve, but the singlets have moved down on the Doppler branch. A similar situation exists in the later spectral classes (Figs. 3, *d*, and 4, *d*). There are a number of exceptions to this general behavior of the helium lines, and one of them has been purposely included in Figure 2, *d*. HD 34085, β Orionis, is classified as B8s by Williams, but for this star the positions of the helium lines on the curve of growth suggest a temperature corresponding more nearly to class B4. It is easily seen, from a comparison of the curve of growth of a star of class B3 with one of class B0, that the triplets are less weakened than are the singlets. The same effect should obtain in the later B spectral subdivisions. The singlets become weaker with respect to the triplets in the early and late B subdivisions, even though the relative numbers of atoms absorbing the singlets and triplets remain unchanged from one star to another. The weakening of the singlets takes place as a consequence of the decrease in the absolute numbers of atoms absorbing both the singlets and triplets on either side of the maximum at B3. Because of the properties of the curve of growth, the decrease in equivalent width is much more rapid for the singlets than for the triplets.

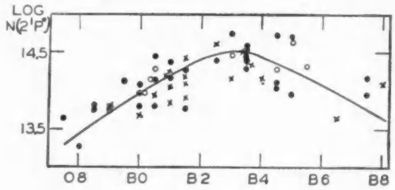

FIG. 8.—Variation of log N_2 ($^1P^0$) with spectral subdivision.

We may illustrate the nature of the variation in the singlet-triplet ratio of equivalent widths by the following procedure. If we plot log $N(2\,^1P^0)$ as ordinate against spectral class as abscissa, we obtain the curve shown in Figure 8. The crosses, dots, and circles refer, as before, to giants, intermediates, and dwarfs, respectively. From the mean curve drawn through the points, we derive the average values of log $N(2\,^1P^0)$ shown below:

Sp.	log $N(2\,^1P^0)$	Sp.	log $N(2\,^1P^0)$
O8	13.50	B4	14.34
B0	13.97	B6	14.00
B2	14.40	B8	13.66

The corresponding values of log $N(2\ {}^3P^0)$ may, of course, be computed by adding the logarithm of 3, 0.48, to the tabulated values. If we assume an average value of V for the B stars, we can calculate average values of log X_0 for the members of the diffuse series, and hence derive average values of W for these lines, for each spectral subdivision, from a mean curve of growth. We may then compute the ratio

$$\frac{\text{Mean } W(4144,\ 4388)}{\text{Mean } W(3820,\ 4026,\ 4472)}$$

for each subdivision and compare the variation in this ratio with the observed variation. We choose an average value of V of 0.40. From equations (18) and (22), setting $V = 0.40$, we have

$$\log X_0 = \log X_0' + \log N - \log (2S + 1)(2L + 1) - 13.71\ . \qquad (25)$$

Table 6 contains the average values of log X_0 computed for a number of spectral subdivisions from (25), and the corresponding values of W derived from the mean curve of growth. The resulting values of mean diffuse-singlet divided by mean diffuse-triplet equivalent width for the various spectral subdivisions are shown in Table 7, where they may be compared with the values read from Williams' smoothed curve. The agreement is excellent except for classes B6 and B8. The divergence there is probably due to the fact that a value of $V = 0.1$ would have been more nearly appropriate for the late spectral classes (see Fig. 5).

TABLE 6

λ	O8		B0		B2		B4		B6		B8	
	log X_0	W	log X_0	W	log X_0	W	log X_0	W	log X_0	W	log X_0	W
4472	+0.50	+0.74	+0.97	+1.02	+1.40	+1.23	+1.43	+1.20	+1.06	+1.05	+0.70	+0.85
4026	+ .17	.49	.64	0.74	1.07	0.98	1.10	1.00	0.73	0.80	.37	.60
3820	−0.07	+0.34	+0.40	+0.58	+0.83	+0.80	+0.86	+0.80	+0.49	+0.60	+0.13	+0.44
Mean W	......	+0.52	......	+0.78	......	+1.00	......	+1.00	......	+0.82	......	+0.63
4388	−0.43	+0.20	+0.04	+0.46	+0.47	+0.69	+0.50	+0.71	+0.13	+0.50	−0.23	+0.30
4144	−0.73	+0.10	−0.26	+0.29	+0.17	+0.50	+0.20	+0.53	−0.17	+0.32	−0.53	+0.16
Mean W	......	+0.15	......	+0.37	......	+0.59	......	+0.62	......	+0.41	......	+0.23

It seems reasonable to conclude, therefore, that the variation with spectral subdivision in the ratio of singlet to triplet equivalent width among the stars of class B is exactly what would be expected from the simple theory of line formation, and that the variation does not constitute an anomaly.

There is one interesting point in connection with Struve's suggestion that the relative weakening of the singlet lines in supergiants is brought about by departures from thermodynamic equilibrium and a consequent overpopulation of atoms in the triplet levels of helium. The curves shown in Figures 2, 3, and 4 have been plotted on the assumption that the relative populations of the 2 $^3P^o$ and 2 $^1P^o$ levels are governed by Boltzmann's law. If we now assume, in accordance with Struve's suggestion, that the 2 $^3P^o$ level is overpopulated, as compared with a Boltzmann distribution, then the triplet points must be shifted to the right, in the direction of an increased number of absorbing atoms, by an amount depending upon the degree of overpopulation. But because of the small value of the damping constant for the triplet lines and because of the occurrence of the triplets on the flat portion of the curve of growth, the population of the 2 $^3P^o$ level would have to be increased by an enormous factor (at least 100) before any appreciable increase in the total absorption could be detected, provided, of course, that radiation damping is the predominant damping mechanism in the giants. It is possible that the triplet levels of helium do possess abnormal populations, but such abnormalities can hardly be detected from the available observational material. Good measures of the faint diffuse triplets 3705 and 3634 and of the leading D3 line are necessary before the question can be definitely settled.[25]

TABLE 7

Variation of ratio: $\dfrac{\text{Mean } W(4144, 4388)}{\text{Mean } W(3820, 4026, 4472)}$

	O8	B0	B2	B4	B6	B8
Calculated	0.29	0.47	0.59	0.62	0.50	0.37
Observed	0.30	0.48	0.59	0.63	0.62	0.55

---

[25] These conclusions do not affect the explanation proposed by Struve and Wurm (*Ap. J.*, **88,** 84, 1938) of the *He* I anomaly in the outer shells of B stars.

THE FORBIDDEN HELIUM LINE λ 4470

The influence of the curve of growth upon the observed relative intensities of helium lines may now be discussed with relation to a question raised by Foster and Douglas[26] concerning Struve's identification of a line at λ 4470 with the $2\ ^3P^\circ - 4\ ^3F^\circ$ forbidden transition in neutral helium. The identification of λ 4470 with the helium line has been well established in all but one respect. The relative intensity of λ 4470, as compared with the permitted triplet at λ 4472 (0.2 in γ Pegasi), has seemed large in the light of laboratory expectations. Struve[27] found, from studies of hydrogen lines in early-type stars, that the observed line broadening requires an average mol-electric field strength of 10^3–10^4 volts per centimeter. J. M. Dewey[28] has shown, from laboratory measures, that the relative intensities of λ 4470 and λ 4472 depend upon the square of the electric-field strength in the following way:

$$\frac{I\ (4470)}{I\ (4472)} = 6.6 \times 10^{-10} F^2\ . \tag{26}$$

For γ Pegasi the intensity ratio is about 0.2; and Struve found, on substituting this value in (26), that F turned out to be 17,000 volts/cm. This value is much higher than that evidenced by the hydrogen lines. Struve recognized, of course, that the laboratory measures were made with emission lines and that the absorption lines would probably not follow the relation (26), because of the non-linearity of the curve of growth.

The relative intensities of λ 4470 and λ 4472 in emission are simply proportional to the theoretical strengths of the lines, and (26) may therefore be written

$$\frac{S(4\mathrm{f} - 2\mathrm{p})}{S(4\mathrm{d} - 2\mathrm{p})} = 6.6 \times 10^{-10} F^2\ . \tag{27}$$

We may now compute approximate values of the relative strengths of these lines in the spectrum of γ Pegasi and derive a value of F from (28). Log W/λ for λ 4472 in γ Pegasi is -3.57. Struve's estimate of 0.2 for the relative intensities of λ 4470 and λ 4472 gives a value for log W/λ of -4.27 for λ 4470. The value of V derived for γ Pegasi (HD 886) was 0.57; but since the Stark widths increase with serial number, the value $V = 0.4$ is probably more appropriate for λ 4472. If we employ a curve of growth with this value of V, we find that the difference in log X_0 for these lines is about 1.8. Since both λ 4470 and λ 4472 arise from the same lower level,

---

[26] *Phys. Rev.*, **44**, 325, 1923.

[27] *Ap. J.*, **69**, 173, 1929.

[28] *Phys. Rev.*, **28**, 1108, 1926.

$$\frac{X_0(2\mathrm{p} - 4\mathrm{f})}{X_0(2\mathrm{p} - 4\mathrm{d})} = \frac{S(2\mathrm{p} - 4\mathrm{f})}{S(2\mathrm{p} - 4\mathrm{d})} \sim \frac{1}{60} . \tag{28}$$

Thus, although the observed ratio of absorption intensity λ 4470/λ 4472 is 0.2, the required relative number of absorbing atoms is 1/60. This ratio gives for F:

$$F \sim 5 \times 10^3 \text{ volts/cm} .$$

It is probably that (28) will not apply accurately in a fluctuating electric field, but the rough calculation given above suffices to show that a mol-electric field of $10^3 - 10^4$ volts/cm is not inconsistent with the observed intensity of λ 4470 in the spectrum of γ Pegasi. It should be emphasized that the foregoing value refers to the average intramolecular electric field and obviously has no macroscopic significance. As Struve[29] has shown, such field strengths are concordant with stellar reversing-layer electron pressures of the order of 10^{-4} atmospheres.

In conclusion, it is a pleasure to record my appreciation to Dr. Menzel for many stimulating conferences on the problems discussed in this paper. Dr. Struve was kind enough to read the manuscript before publication and to offer many helpful comments.

HARVARD OBSERVATORY
February 1939

---

[29] *Ap. J.*, **70**, 90, 1929.

THE SPECTRA OF TWO REFLECTION NEBULAE*

J. L. GREENSTEIN[1] AND L. G. HENYEY

ABSTRACT

Spectra of the Orion nebula and of the Pleiades nebula have been obtained with the nebular spectrograph at the McDonald Observatory. The Orion nebula has a strong continuous reflection spectrum superposed over the bright-line spectrum. Spectrophotometric determinations of color show that these nebulae are slightly bluer than their illuminating stars. An interpretation of these results is given on the basis of our theoretical discussion of the colors of nebulae. Estimates of the albedo of the scattering and absorbing particles are obtained.

The nebular spectrograph at the McDonald Observatory has been used to determine the energy distribution of the scattered radiation in two reflection nebulae: the Pleiades and the Orion nebula, NGC 1976. The limit of accuracy in the spectrophotometry of nebulae is set by the great strength of the diffuse continuous spectrum of the Zodiacal Light and of the Galaxy. Two different types of nebulae are represented in these cases. In the Pleiades we know that the illuminating star, Merope, is in front of substantially all the nebulous material, while in the Orion nebula the Trapezium stars are behind or inside the nebulous mass.

Five plates of the Orion nebula were taken with exposures of 45 minutes, at distances from $3'$ to $8'$ south of the Trapezium. The slit is about one degree long in right ascension. The subsidiary slit of the spectrograph was set off several degrees in declination, to determine the strength of the sky background as a function of wave length. Spectra of the stars ι Ori and 42 Ori were obtained before and after the exposures on the nebula. Standardization was provided by a wedge spectrograph with exposures of 30 minutes. All plates exposed on one night were developed together, with a standard technique. Seven plates of the nebula near Merope were obtained similarly with exposures of 150 minutes. The slit was centered $3'$ south of the star in the region of the fainter nebulosities. (The brighter portion, near the star, cannot be observed with this instrument.) Plate XXIX contains an enlargement of the spectra of the Orion nebula 5′ south of θ_1 Ori, the Merope nebula, and a microphotometer tracing of the spectrum of the Orion nebula.

---

* *Contributions from the McDonald Observatory, University of Texas*, No. 11.

[1] National Research Fellow.

Microphotometer tracings of the various exposures were measured to determine the magnitude of Nebula *plus* Sky at fifteen wave lengths, from 6450 to 3390 A. Characteristic curves were obtained at five different wave lengths, from 6400 to 4100 A. The subsidiary slit yields the magnitude of the sky background at the corresponding wave lengths. After correction for the sky background we obtain the magnitudes of the nebula. Stellar spectra, traced with the same slit widths, require no correction for background intensity because of the shorter exposures required. The differential zenith distance corrections are small and are based on the Mount Wilson values. The surface photometry of the spectra is of moderate accuracy, but great uncertainty is introduced in the case of the Pleiades by the sky background. Since the nebula is very blue, compared to the sky, the uncertainty of the background correction is most serious in the red region, where it is large compared to normal photometric errors.

The continuous spectrum of the Orion nebula is quite bright, and the uncertainty introduced by the background is small. The difference between the nebula and the sky ranges from 0.4 to 2.0 mag. The microphotometer tracing reproduced shows that some uncertainty occurs in the tracing of the continuous spectrum of the nebula in the neighborhood of the emission lines $H\alpha$, $N1$, $N2$, and $H\beta$ and in the region of the continuous emission beyond the Balmer series limit. The mean observed difference in magnitude, Δm, with arbitrary zero point, between the Orion nebula and the star ι Ori, is given in Table 1. ι Ori is a star of type O8sk, with a photoelectric color index[2] of -0.23 mag. It is one of the least reddened O stars and has been used because of the difficulty of obtaining spectra of the brightest Trapezium star, θ_1 Ori, free from interference of the nebulosity. The color excess of the Trapezium stars is $+0.21$ mag. on the photoelectric scale. The gradient of the nebula with respect to ι Ori is $+0.21 \pm 0.03$, by a least-squares solution omitting points 1, 6, 12, 13, 14, and 15. Only an indirect comparison with the Trapezium is possible. The reduction of one exposure yields a

---

[2] Stebbins and Huffer, *Pub. Washburn Obs.*, **15**, No. 5, 1934.

PLATE XXIX

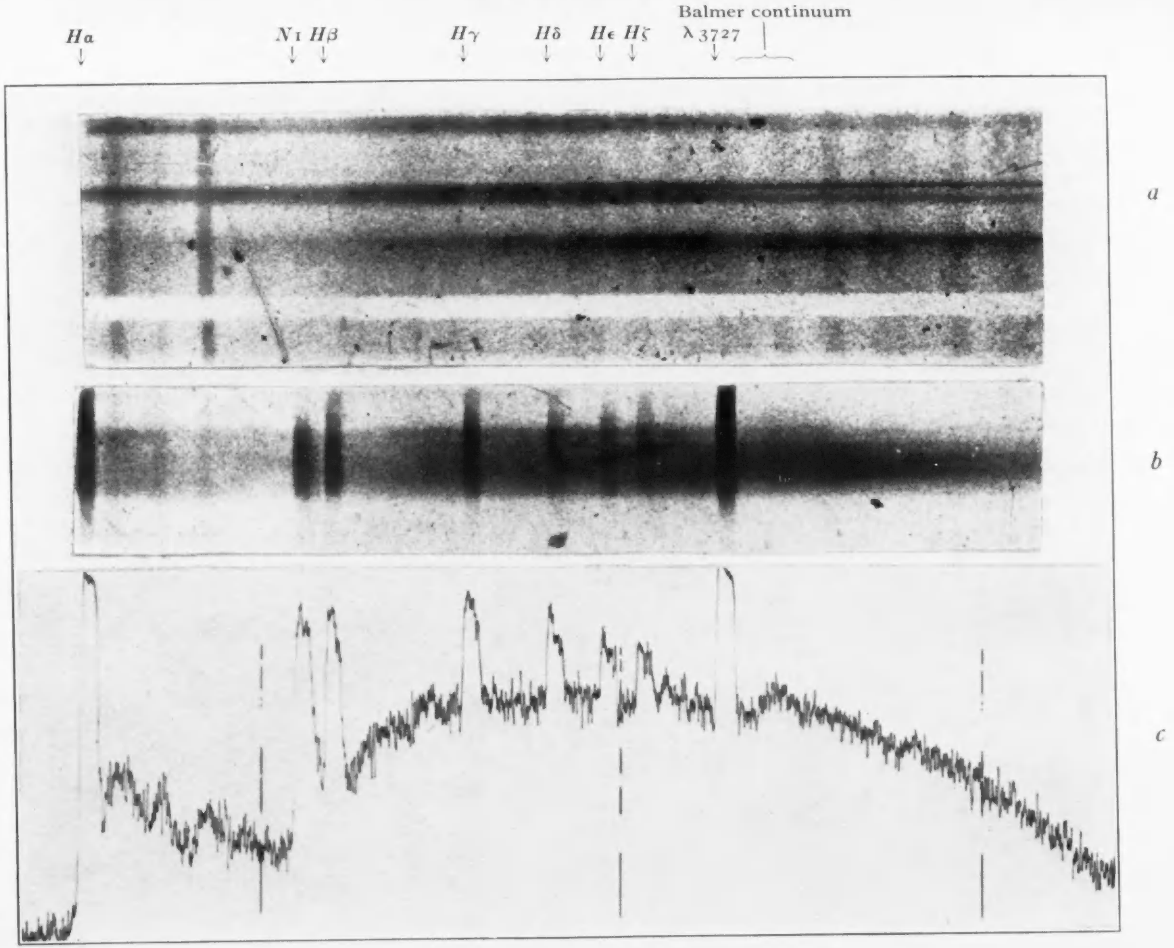

(*a*) Reflection Spectrum, Nebula near Merope; (*b*) Emission and Reflection Spectrum of the Orion Nebula; (*c*) Tracing of Spectrum of the Orion Nebula

Note Balmer emission continuum to the violet of λ 3737

UNIV. OF MICH.

gradient of +0.56 for the Trapezium relative to ι Ori. If we use a calibration of the photoelectric color differences in terms of the relative gradients,[3] the difference of gradient becomes +0.67. The nebula may be taken as −0.4 bluer in gradient than θ_1 Ori. If we use all twelve points, omitting only the region of the Balmer continuous emission, the difference in gradient is −0.5. The actual uncertainty may be estimated to be of the order of ±0.1. On the international scale of color index the nebula is −0.25 ± 0.05 mag. bluer than θ_1 Ori. The relative gradient of the nebula and ι Ori is nearly linear; hence we may further say that the intensity of the light scattered by the particles in the nebula varies roughly as λ^{-1}. Rayleigh scattering is excluded by the absence of a strong curvature.

TABLE 1

RELATIVE MAGNITUDES OF NEBULA AND STAR

Point	λ	Δm Orion–ι Ori	Δm Pleiades–Merope	Remarks
1	6450 A	−0.17	+0.16	$H\alpha$
2	6060	− .04	+ .12	
3	5710	− .01	+ .02	
4	5410	− .03	− .14	
5	5130	+ .04	− .25	
6	4880	− .12	− .22	$H\beta$, N_1, N_2
7	4650	+ .05	+ .20	
8	4440	− .01	+ .04	
9	4260	+ .04	+ .02	
10	4080	+ .11	+ .05	
11	3920	+ .12	− .02	
12	3770	.00	− .08	
13	3640	− .28	− .47:	Balmer cont.
14	3510	− .25	−0.55:	Balmer cont.
15	3390	−0.28	....	Balmer cont.

An interpretation of these results is possible on the basis of the theory of the colors of nebulae developed by us previously.[4] The illuminating star, dominantly the brightest star of the Trapezium group, is reddened. Therefore, the material in the nebula is capable of selective scattering or absorption. The radial optical thickness of the nebula is given approximately by the total absorption suffered

[3] Greenstein, *Ap. J.*, **87**, 151, 1938.

[4] Henyey and Greenstein, *Ap. J.*, **88**, 580, 1938.

by the Trapezium stars. The latter may be estimated as about seven times[3, 5] the photoelectric reddening, that is, more than 1.5 mag. The nebula is observed to be slightly redder than an unreddened O8 star, its color being roughly the same as that of the original radiation of the illuminating star. We have, therefore, the case of a spurious bluing, with the star inside the nebulosity. The observed color of a nebula relative to its illuminating star depends upon the variation of the extinction coefficient of the material and also upon geometrical factors.

If J is the intensity of the nebula compared to the star, τ_1 the optical thickness, and κ the extinction coefficient, then the measured color,

$$d \log J = \frac{\partial \log J}{\partial \log \tau_1} \cdot d \log \kappa \, .$$

From this equation we can estimate the "color factor," $\partial \log J / \partial \log \tau_1$, if we know the variation of κ with wave length. We shall adopt the relation, $\kappa \propto \lambda^{-1}$, in which case $d \log \kappa$ is -0.25 mag. between the effective wave lengths defining the international scale. For the Orion nebula we obtain a color difference of -0.25, which yields a color factor of the order of 1 ± 0.05. Consulting Figure 2 or Figure 5 of our theoretical discussion,[4] we may conclude that the present results are consistent with an albedo of $\frac{2}{3}$ for the nebular particles. If the extinction coefficient varies more slowly than λ^{-1}, the albedo will be higher. Much more rapid variation than λ^{-1} can be excluded by the nearly linear gradient.

The intensities of the emission lines have also been measured on these plates and will be discussed separately. It may be of interest to consider here the relative brightness of the continuous spectrum to the emission lines. This ratio varies with wave length and has been evaluated for the photographic magnitude range, roughly from 4900 to 3600 A. The total intensity of the lines in this region was obtained, as well as the total intensity in the continuous spectrum, both corrected for the sky background. There is an excellent correlation between the intensity of the reflected radiation and that produced by atomic processes, over a fivefold range of surface bright-

---

[5] Oort, *B.A.N.*, No. 308, 1938.

ness. The continuous spectrum is −0.21 ± 0.04 mag. brighter than the emission lines.

The results of the comparison of the nebula south of Merope with that star, given in Table 1, are quite disappointing, as far as photometric accuracy is concerned. The origin of the large accidental error lies in the excessive faintness of the nebula, which never attains the intrinsic brightness of the sky and is usually 1 mag. fainter. For such an object the effect of photometric errors is multiplied by a large factor in the application of the background correction; pre-exposure effects are also possible. In the region of the dip in the sensitivity-curve of the Agfa Super Pan Press film used (points 4, 5, and 6) serious discordances occur. The inclusion of the discordant points gives almost zero weight for the slope of the relative energy-curve. The region of the Balmer continuous absorption is also uncertain. If we omit these points, a least-squares solution yields a difference in gradient between nebula and star of −0.22. The uncertainty lies between ±0.1 and ±0.2. We adopt the difference of color index on the international scale as −0.1 ± 0.07 mag. No trace of emission lines has been found in these spectra of the Pleiades nebula.

The spectrophotometric color of the faint nebula near Merope may profitably be supplemented with a direct color determination made at the Yerkes Observatory with the Fabry photometer. Three points in the brighter regions of the nebula, at a mean distance of 8′ from Merope, were observed, and the surface brightness determined. A point 2° off the nebulosity established the sky brightness, and stars of the North Polar Sequence gave the calibration. These determinations were made on both the photographic and the photovisual scales (Eastman Ortho Press plate and No. 15 filter). The intrinsic surface brightness of the nebula is about 3.8 mag. per square degree photographically, and 4.2 mag., photovisually. The mean color index of the nebula is −0.5 ± 0.15 mag. The photoelectric color index of Merope is −0.12 mag., which indicates that it is − 0.04 mag. bluer than the mean unreddened A0 stars. We adopt the color index of Merope as −0.15 ± 0.1 mag. The nebula is then −0.35 ±0.18 mag. bluer than the star. Values of the color difference between star and nebula have been obtained by Struve, Elvey, and

Keenan,[6] who find −0.3 ± 0.2 mag. spectroscopically, and −0.2 ± 0.1 mag. photoelectrically. Collins[7] has obtained −0.49 mag., which, after correction for the color of the sky,[8] yields −0.27 mag. We adopt the weighted mean value of −0.19 ± 0.06 mag.

The photoelectric color excess of Merope, a B7n star, is given as −0.02 ± 0.02 mag., which indicates no significant reddening by the nebular material. In this case we should interpret our results on the basis of a model in which the star is in front of the body of obscuring material. We lack a direct estimate of the optical thickness of the Merope nebula, but we may tentatively adopt a value of 1.5 mag. photographic absorption, estimated by Watson.[9] If we again assume that the intrinsic extinction coefficient varies as λ^{-1}, the observed difference in color corresponds to a color factor of 0.76 ± 0.24. Figure 1 of our previous discussion[4] shows the predicted color factor for a symmetrical phase function. The albedo derived on the basis of these curves lies between 0.8 and 1.0, a very high value.

McDonald Observatory
and
Yerkes Observatory
March 1939

---

[6] *Ap. J.*, **77**, 274, 1933.

[7] *Ap. J.*, **86**, 529, 1937.

[8] Greenstein, *Ap. J.*, **87**, 581, 1938.

[9] Unpublished.

STUDIES OF DIFFUSE NEBULAE*

J. L. GREENSTEIN[1] AND L. G. HENYEY

ABSTRACT

Emission-line intensities have been measured in the spectrum of the Orion nebula. The Balmer decrement agrees with the predicted values for an electron temperature near 5000°. The excessive strength found for *Hα* may arise from blending with the lines of [*N* II]. Measures of the continuous emission beyond the Balmer limit yield an electron temperature near 5000°. It is found that the lines of high excitation are concentrated at the center of the nebula. The intensity of the continuous reflection spectrum in various parts of the nebula is observed to be closely correlated with the intensity of the emission lines.

Photometry of nine diffuse nebulae yields a slightly steeper Balmer decrement, while the faint nebulae near γ Cygni display excessively strong *Hα*. A résumé is given of the spectra of other objects observed with the nebular spectrographs.

Spectrophotometry of the emission lines in diffuse nebulae may yield information concerning the mode of excitation and the electron temperature in these objects. We present here the results of such a study of the nebulae, made with the nebular spectrographs at the Yerkes and McDonald observatories. The general photometric technique is the same as in previous investigations employing these instruments.[2] The McDonald spectrograph has been used to determine the relative line intensities in the outer portions of the Orion nebula, NGC 1976, from 3′ to 15′ distant from the exciting star, θ_1 Ori. There were available seven exposures on the nebula, as well as two on the star ι Ori (O8), four on 42 Ori (B2), and eight on 23 Tauri (B7). The measured magnitudes from microphotometer tracings of the stars were averaged to yield magnitudes along the spectrum of a mean star. If we adopt the zero point of the color-temperature scale as A0 = 14,000°, the reduction of the photoelectric color indices of the stars involved[3] yields a color temperature of 17,000° for the mean star. The relative magnitude of the emission line compared to the mean star was corrected for background, zenith distance, dispersion, and the black-body energy factors. A correction for the Balmer line and continuous absorption was applied, on the assumption that the continuous absorption is zero at the spectral type of ι Ori (O8).

---

* *Contributions from the McDonald Observatory, University of Texas*, No. 11.

[1] National Research Fellow.

[2] Greenstein, *Ap. J.*, **88**, 605, 1938.

[3] Stebbins and Huffer, *Pub. Washburn Obs.*, **15**, No. 5, 1933.

The second column of Table 1 gives the line intensities of $H\alpha$ to $H\zeta$, of $N1+N2$, and of λ 3727, expressed in terms of $H\beta$ as unity. These are derived from eleven microphotometer tracings of various portions of the seven spectra. The mean error of each determination and the number of measures available are given in the third and fourth columns. It should be noted that $N1+N2$ varies strongly in intensity with apparent distance from the center of the nebula. It is six times as strong as $H\beta$ near the exciting star and is weaker than $H\beta$ at a distance of 10′ from it. On the other hand, there is a slight tendency for λ 3727 to become strengthened relative to $H\beta$ at large distances from the center. No significant change in the Balmer decrement can be found. The lines of *He* I, λ 5876 and λ 4471, of *He* II, λ 4686, and of [*Ne*III], λ 3869, are highly concentrated toward the center of the nebula. A peculiarity of the Balmer decrement is obvious at $H\zeta$, which is nearly as strong as $H\epsilon$. It is probable that λ 3888 of *He* I is strong and maintains its strength even in the outer parts of the nebula. H. H. Plaskett has observed, with a carbon arc as standard, the relative line intensities given in the fifth column, at the center of the Orion nebula.[4] The difference between our intensities for $N1 + N2$ arises from its greater strength at the center of the nebula. The sixth column contains the theoretical Balmer decrement for the electron temperature of 5000°, as given by Baker and Menzel[5] in

TABLE 1

LINE INTENSITIES IN NGC 1976

Line	Intensity	m.e.	*n*	Plaskett	Predicted
$H\alpha$	5.0	±0.4	8	4.0	2.4
$N1+N2$	1.6	.2	11	4.6	....
$H\beta$	1.0	....	11	1.0	1.0
$H\gamma$	0.60	.03	11	0.48	0.53
$H\delta$	0.37	.04	8	0.19	0.33
$H\epsilon$	0.20	.01	8	....	0.22
$H\zeta$+λ 3888	0.20	.01	7	....	0.16
λ 3727	2.8	±0.4	7	....	....

---

[4] *Pub. Dom. Ap. Obs. Victoria*, **4**, 187, 1928.

[5] *Ap. J.*, **88**, 52, 1938.

their Table 8. The theoretical decrement is not sensitive to the electron temperature, and the present observations would fit the theoretical predictions over a wide range, except for the excessive strength of $H\alpha$. Dr. W. H. Wright, of the Lick Observatory, has been kind enough to inform Dr. Struve that the [*N* II] doublet at λ 6548 and λ 6584 has a strength comparable to, or greater than, that of $H\alpha$ in some planetary nebulae. Stoy's estimates also indicate[6] a high intensity for these lines, which are blended with $H\alpha$ on our plates. It is possible that they are the principal source of the deviation of $H\alpha$ from the theoretical Balmer decrement. The intensities of these lines should be measured before any interpretation can be made of the great strength of $H\alpha$.

The intensity of the Balmer continuous emission beyond the series limit has been measured on four of the spectra. In the Orion nebula the great strength of the continuous (reflection) spectrum makes it particularly difficult to derive the intensity of the emission continuum. The tracing reproduced in Plate XXIX (facing p. 648) shows the nature of the small discontinuity introduced by emission at the series limit. The possible occurrence of Balmer continuous absorption in the reflection spectrum and in that of the comparison stars introduces further uncertainty. The value found for the ratio of the intensity of $H\beta$ to that of the emission at the series limit per unit wave number is 800 ± 200. Cillié has tabulated values of the ratio[7] for the capture spectrum in a planetary nebula. We have corrected his values by using the more recent computations of the theoretical line intensities by Baker and Menzel.[5] The electron temperature derived is 5000°, with a range of uncertainty of perhaps 2000°.

Another measure of the electron temperature may be derived from the gradient of intensity in the continuous emission beyond the series limit. The uncertainty as to the intensity of the reflection background is most serious in this case, since a small error in the unknown slope of the background enters directly into the derived electron temperature. The data of Table 1 in our study of the reflection spectrum[2] of the Orion nebula can be used to determine the additional intensity in the hydrogen emission spectrum. It can be seen that the nebula is −0.4 mag. brighter than would be expected if it radiated like a black body in the region from λ 3640 as far as λ 3390. The nearly constant excess intensity would indicate little or no gradient of intensity in the Balmer emission spectrum, and therefore a high electron temperature. If the background is drawn arbitrarily so as to make the intensity of the Balmer emission zero at λ 3700 and λ 3400, the derived electron temperature is 1800°, which is very definitely a minimum value. It must be emphasized that the value derived from the actual intensity is more nearly correct.

---

[6] *Lick Obs. Bull.*, **17**, 179, 1935.

[7] *M.N.*, **96**, 771, 1936.

An interesting feature of the nebula is the presence of both a strong reflection spectrum and emission lines. We have evaluated the relative brightness of the sum of the emission lines in the range from $H\beta$ to λ 3727, to the integrated continuous spectrum in that range. Table 2 shows the correlation of the total line intensity, in arbitrary units, with the total continuous intensity at various points in the nebula. It is surprising to find that the intensity of the emission lines, produced by an atomic fluorescence process from the ultraviolet radiation, should be so closely correlated with that of the reflection spectrum, the intensity of which depends on absorbing and scattering coefficients of small particles at wave lengths in the photographic region. The variation of the surface brightness of the nebula depends both on geometrical factors and on the absorption and scattering coefficient. It is possible that the optical depth for ultraviolet radiation is of the same order of magnitude as that in the photographic region.

TABLE 2

RATIO, CONTINUUM TO LINES IN NGC 1976

Continuum	13	18	19	25	28	54	60
Lines	12	13	15	22	20	44	60
Ratio, C/L	1.08	1.38	1.27	1.14	1.40	1.23	1.00

OTHER NEBULAE

The nebular spectrograph at the Yerkes Observatory has been used for a survey of the fainter diffuse nebulae. An attempt has been made to obtain line intensities for these objects, with the same spectrophotometric technique as at the McDonald Observatory, but the sky background introduces more serious difficulties. The emission spectrum of the night sky is considerably stronger at northern latitudes, particularly in the red. Table 3 gives the mean line in-

TABLE 3

Line	Mean Intensity	m.e.	IC 1318 Intensity
$H\alpha$	8	±2	42
N_1+N_2	2.5–0.0	...	...
$H\beta$	1.0	...	1.0
$H\gamma$	0.43	0.07	...
$H\delta$	0.23	0.09	...
λ 3727	2.5	±0.4	3.4

TABLE 4

SPECTRAL CHARACTERISTICS OF THE NEBULAE

Object	Star	Balmer Lines +λ 3727	N_1+N_2	Continuous Spectrum
NGC 1435	B7	A	A	Strong, blue
1499	O7	P	P	
1976	O7	P	P	Strong, blue
1977	B2	P	...	Blue
1982	O7+B8?	P	P	Blue
2023	B2	P	...	
2024	B0	P	...	
2175	O6	P	P	
2237	Oe5	P	P	
2264	O7	P	P	
6559	B5?	P	...	
7000	A2p	P	P	P
7023	B5	A	A	P
IC 405	O9	P	...	P
434	B0	P	...	P
1287	B3	A	A	Blue
1318	F8p	P	A	Red
2118	B8p	A	A	Blue
4603	B3	A	A	P
4604	B4	A	A	Blue
IC 4605	B3	A	A	P

tensities for nine emission nebulae—NGC 1499, 1976, 1977, 1982, 2175, 2237, and 7000, and IC 405 and 434—measured on twelve plates taken at both observatories. The fourth column contains the intensities for the nebula IC 1318, near γ Cygni. The latter spectra were obtained in three of the diffuse patches which nearly surround the star, as well as on a plate centered on it. The strength of *Hα* seems to be significantly greater than that in the other nebulae of higher surface brightness. The Balmer decrement is possibly slightly steeper in all these nebulae than in the Orion nebula, which is the brightest of the objects investigated. Possible variations in the strength of the [*N* II] doublet, as suggested by Dr. Wright, make the interpretation of these results uncertain.

Table 4 presents a résumé of the nebulae so far observed, published[8] or unpublished. The presence of a line is indicated by the symbol (P); its definite absence, by (A). The existence of a continuous reflection spectrum is also noted. The spectral type of the illuminating star is given in the second column.

It should be noted that many nebulae have composite spectra and that reflection continua occur even among the nebulae with high-excitation emission lines. No sharp boundary can properly be drawn between the two types of nebulae, and it seems probable that there exists an intimate connection between the occurrence of gases and dust particles in space. In general, the theoretical intensity of the line fluorescence increases rapidly, compared to the photographic reflection spectrum for the hotter stars. Nebular spectra have generally been obtained with exposures sufficient for the lines, and it is possible that all gaseous nebulae have faint continuous spectra.

McDONALD OBSERVATORY
AND
YERKES OBSERVATORY
March 1939

---

[8] Greenstein and Henyey, *Ap. J.*, **86**, 620, 1937; *Ibid.*, **87**, 79, 1938.

STELLAR VARIABILITY AND RELAXATION OSCILLATIONS

A. J. WESSELINK

ABSTRACT

A phenomenological theory of stellar variability is given. The first part of the paper discusses the different types of maintained oscillations possible in physical systems. Three groups are found: the sinusoidal type, the pure relaxation oscillation, and the induced relaxation oscillation. The second part examines the properties of the light-curves of variable stars. The current theory of Cepheid pulsation assumes the oscillations to be of the sinusoidal type and is unable to explain very skew light-curves or irregularities in period. The pure relaxation oscillations fully account for such irregularities as are shown, for example, by the SS Cygni stars and the long-period variables, whereas the regular variables are interpreted as possessing induced relaxation oscillations. For such variables the period-density law will remain valid, but the light-curves may be skew.

The purpose of the present article is to draw attention to the close analogy which exists between the characteristic features of variable stars and those of relaxation oscillations. No mechanism has been worked out, but it is suggested that an ultimate theory of stellar variability should be based on the idea of relaxation oscillations.

The characteristic features of oscillating systems depend on the variation with time of the oscillation energy. No difficulty arises in defining this energy as long as the system is capable of assuming a stationary state (which may be unstable).

Of the many possible cases, those in which, after a complete cycle, the oscillation energy resumes the original value are of special interest for our purpose. This implies that during a complete cycle the energy supplied to the system is equal to the energy dissipated by it. In these cases the oscillations will be maintained indefinitely. The time interval during which a variable star manifests itself as such is probably very long. One argument in favor of this statement is the very large frequency of cluster variables in some globular clusters; a very considerable fraction of the stars between the appropriate magnitude limits is variable.[1]

It is for this reason that maintained oscillations are of importance for the study of stellar variability. We therefore restrict the discussion to such oscillations.

---

[1] E.g., Messier 3; cf. Greenstein, *A.N.*, **257**, 327, 1935.

In general, energy will be supplied to the system during a whole cycle, and dissipation will take place continuously. But since the rates of supply and dissipation will not be equal, the total oscillation energy will vary.

Let the minimum and maximum values of the oscillation energy be E_m and E_M, respectively. We then have

$$0 < \frac{E_m}{E_M} < 1 .$$

The character of the oscillations depends upon whether the ratio E_m/E_M is comparatively large or small. Oscillations for which E_m/E_M is near unity will be called Type I. Oscillations for which E_m/E_M is near zero will be called Type II. Obviously, the classification into Types I and II does not indicate that there are no intermediate cases; actually a gradual transition exists between them.

We shall now summarize the principal features of both types of oscillations, which, after being illustrated by examples, will be compared with the properties of variable stars.

OSCILLATIONS OF TYPE I

1. Graphs representing oscillations of this type have a sinusoidal form. The harmonic features are the better preserved the less E_m/E_M differs from one, as was shown by Lord Rayleigh.[2]

2. The variations are extremely regular.

3. They show the phenomenon of resonance, that is, they oscillate with the period of the forced vibration only when the forced period differs little from the free period. In other words, the amplitude of the oscillation, oscillating with the period of the forced vibration, depends strongly on whether the free and the forced period differ little or much. As a matter of fact, this amplitude tends rapidly toward zero when the difference between the free and the forced period increases.

Type I has a limit in the case in which the oscillation energy does not vary at all. An example of this case is an oscillating system in which both the dissipation and the supplied energy are zero. Although this case does not exist in nature, it is of importance to consider it because of its mathematical simplicity. The free harmonic oscillator is an example of this kind, and the pendulum of a pendulum clock approaches this system in practice. The sinusoidal form of the displacement as a function of time illustrates the first of the features of the oscillations of Type I.

---

[2] *Phil. Mag.*, **15**, 229, 1883; *Scientific Papers*, **2**, 188.

It is well known that the best clocks have pendulums which are almost entirely free: this illustrates the second feature of the oscillations of Type I (see above).

We shall not give an example of the third feature, viz., that of resonance. The behavior of these oscillations under various circumstances (external periodic effects, combined with other sinusoidal oscillations) has been studied in detail, and the results are well known.[3]

OSCILLATIONS OF TYPE II

1. Graphs representing oscillations of Type II deviate, in general, very markedly from sinusoids. They often show very sudden variations. Sometimes such a sudden variation is followed by a much slower one in the opposite direction, by which the original situation, existing before the abrupt change, is gradually restored.

2. The successive cycles are apt to be of unequal duration. This is a consequence of the extreme sensitivity of the duration of the cycle to small disturbances. The durations of the different cycles are completely independent of each other. In spite of the irregularity in the duration of the different cycles, the amplitude is but little affected.

3. The oscillations of Type II do not show the phenomenon of resonance, that is, the amplitude of the oscillation depends but very little on the value of the forced period; it is about the same as is shown by the free relaxation oscillation. Moreover, the synchronization takes place even when the free and the forced periods are very unequal.

A limiting case of Type II is one in which, during a fraction of the period, the oscillation energy drops to a value very close to zero, while during the remainder of the period the original amount is fully restored by the source ($E_m/E_M = 0$). An example of this kind is an aperiodic galvanometer which receives an impulse whenever it comes back to the zero position. The curve representing the displacement as a function of the time illustrates the first feature of the oscillations of Type II.

---

[3] E. T. Whittaker, *Analytical Dynamics*, chaps vii and viii.

A very slight disturbance near the zero position has obviously a large effect on the time between two successive impulses, since the galvanometer reaches its zero position very slowly. It is clear that the period will not be strictly constant if slight disturbances are present. Moreover, the durations of successive cycles are independent of one another. The amplitude of the galvanometer will not be affected by the disturbances. These facts illustrate the general features mentioned under 2, above.

The third general feature of the oscillations of Type II, namely, the synchronization by a forced period, will be illustrated by another example, which will now be treated.[4]

THE NEON-TUBE OSCILLATOR

Figure 1 shows a neon tube, N, placed parallel to a condenser, C. The condenser is charged by a constant battery, B. Figure 2 shows the charge of the condenser, the current through the neon tube, and the total current through the resistance, R, as functions of the time. They again illustrate the features mentioned under 1, above.

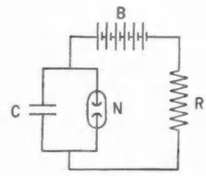

FIG. 1

The phenomenon, which will be treated here in some detail, can be explained on the basis of the "characteristic curve" of the neon tube. This curve gives the relation between the potential difference, V, at the ends of the tube and the current, i_n, passing through it. The full-drawn line in Figure 3 gives a typical characteristic curve. In order that the oscillation phenomenon may set in, it is necessary but not sufficient that the characteristic curve shown in Figure 3 have a part for which dV/di is negative, as we shall see later. We use the following symbols: b, for the potential difference between the poles of the battery; i, for the current through the resistance; i_n, for the current through the neon tube; i_c, for the current through the condenser branch; V, for the potential difference at the condenser or at the ends of the tube; ϵ, for the charge of the condenser; r, for the resistance of the branch including R and B; t, for the time; and τ, for t/rc.

---

[4] B. van der Pol, *Norsk Riks-Kring Kastings Forelesninger*, p. 243, 1934; Ph. le Corbeiller, *Les Systèmes autœntretenus et les oscillations de relaxation*, Paris: Hermann et Cie, 1931.

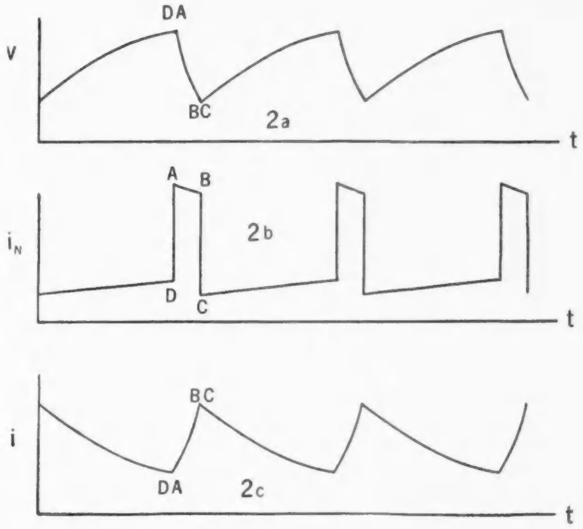

FIG. 2

We then have, by Kirchhoff's laws,

$$V = b - ir \tag{1}$$

$$= b - i_n r - i_c r\,. \tag{1'}$$

Introducing

$$e = b - i_n r \tag{2}$$

and writing

$$ri_c = r\frac{d\epsilon}{dt} = rc\,\frac{dV}{dt} = \frac{dV}{d\tau}\,,$$

Formula (1′) takes the form

$$e - V = \frac{dV}{d\tau}\,. \tag{3}$$

We shall now discuss Figure 3 in more detail. The abscissas are i_n; the ordinates are V. Let the full-drawn characteristic curve be given by $V = f(i_n)$. The quantity e of equation (2) is represented by the straight line bS intersecting the characteristic curve at S. The condition for a stationary state is, by (3), that $e = V$, which corresponds to point S in Figure 3. However, this stationary state is unstable: a slight increase of i_n leads to a value of e which is smaller than the corresponding value of V. Hence, by (3), $dV/d\tau < 0$, and V increases still more.

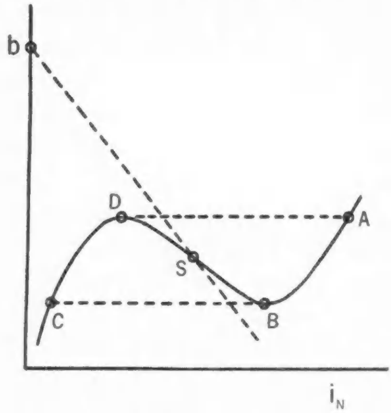

FIG. 3.—The ordinates represent potential differences.

The equilibrium position will, therefore, not be restored. A value of i_n smaller than i_n (S) leads to a further decrease of i_n. There is an unstable stationary state of the system.

In practice the system will, therefore, oscillate indefinitely. The representative point moves along the arcs AB and CD of the characteristic curve, making a jump from B to C and from D to A, practically instantaneously.

We now consider the effect of periodic outside disturbances acting on the system. This case is produced if, at regular intervals, the potential of the condenser is increased for a short time. Suppose that the period of the disturbance is somewhat shorter than that of the freely oscillating system. Then the maximum of the curve in Figure 3 will be reached earlier than is normal; and the discharge will have the period of the disturbance. How much shorter the forced period may be in order that it may still set off a discharge, depends on the amount of the disturbance. It is, however, clear that as a consequence of the form of the electric charge as a function of time, even a small periodic disturbance will make the neon tube synchronize with it, though the forced and the free periods may differ appreciably. This illustrates our statement, made under 3, concerning the synchronization of oscillations of Type II with periodic external disturbances. Our example illustrates the point that the amplitude of the oscillation, when forced by a small periodic disturbance, is about the same as in the free oscillation. One will convince one's self that our example also illustrates statements 1 and 2. Another possibility is that the discharge has a period which is a multiple of the forced one. If the disturbance has a period longer than the free period, it will cause certain discharges to appear out of phase with the others.

One fact of importance just found is this: If the period of the disturbance is shorter than that of the free oscillation and the disturbance is strictly periodic, then the discharge will be strictly periodic too, and the small irregularities which we found to be characteristic of oscillations of Type II will be absent.

The oscillations of Type II have become important only during the last decades. Since the period appears to be determined by a relaxation time (the time of charging, the diffusion time, etc.), they are called "relaxation oscillations," a name introduced by van der Pol.[5]

STELLAR VARIABILITY

A study of the light-curves of different types of variable stars shows striking analogies with oscillations of Type II (relaxation oscillations). We find two distinct groups represented: (*a*) light-curves in which the amplitude remains nearly constant but in which the cycles are of irregular lengths (typical examples are SS Cygni and T Pyxidis [Figs. 4 and 5]);[6] and (*b*) light-curves in which the period, as well as the amplitude, is very nearly constant (examples are δ Cephei and RR Leonis).

In both groups the light-curves may differ strongly from sine-curves. As a matter of fact, they often show the sudden changes (the first property of oscillations of Type II) which are so characteristic for relaxation oscillations. On the basis of these characteristics we may tentatively identify these two groups with the subgroups we found in Type II, namely, the undisturbed free relaxation oscillation (*a*) and the induced type (*b*). This identification accounts for the irregularity of the variables of type (*a*) and for the regularity of those of type (*b*). We shall now explain these analogies in somewhat greater detail.

---

[5] *Phil. Mag.*, 7th ser., **2**, 978, 1926.

[6] *Handb. d. Ap.*, **6**, Part II, 87; L. Campbell, *Pop. Astr.*, **31**, 314, 1923; H. Shapley, *Harvard Bull.*, No. 716, 1920.

As Eddington has shown, oscillations in the interior of a star are, to a high degree of approximation, adiabatic. This implies that the dissipation is small and that a small supply of energy would suffice to maintain them. Oscillations in the interior are thus of the sinusoidal type.

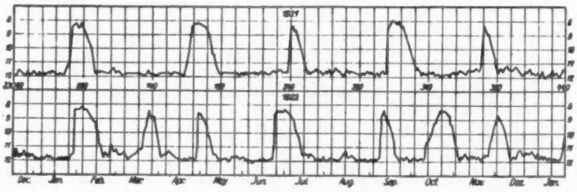

FIG. 4.—Light-curve of SS Cygni in the years 1921–1922, according to Campbell

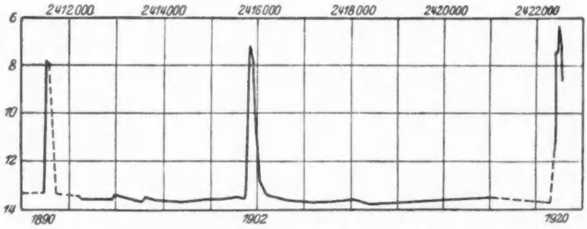

FIG. 5.—Light-curve of T Pyxidis

On the other hand, Eddington has shown that the adiabatic approximation breaks down in the stellar envelope.[7] Empirically we find strong evidence for oscillations of Type II (relaxation oscillations); they must necessarily be located in the envelope.

The light-curve of SS Cygni is shown in Figure 4. The following properties are noted: the light-curve deviates strongly from a sinusoid and shows extremely abrupt changes; and the amplitude is nearly constant, in spite of the fact that the durations of the cycles are very unequal.[8]

Even more striking than the SS Cygni stars is T Pyxidis, which had outbursts in 1890, 1902, and 1920 but which was nearly constant at other times (see Fig. 5). The light-curves of the SS Cygni stars and of T Pyxidis show a strong resemblance to the discharge-curve of the neon tube shown in Fig. 2 (middle curve). This analogy and that of the constancy of the amplitude, combined with a marked irregularity in period, indicate that the accumulation of energy in the stellar envelope and its release are governed by a relaxation phenomenon.

---

[7] *The Internal Constitution of the Stars*, p. 198, 1926.

[8] T. E. Sterne and L. Campbell, "Properties of the Light Curve of SS Cygni," *Harvard Ann.*, **90**, 6, 1934.

The properties of the light-variation of the Cepheids suggest that we are dealing here not with a free relaxation oscillation but with an induced one. Accordingly, we shall have to find a periodic disturbance responsible for the regularity of the period of this oscillation. It may be assumed that the relaxation oscillation takes place in the stellar envelope for which the adiabatic approximation is not valid, but that the periodic disturbance comes from the stellar interior. It seems extremely plausible that radial oscillations of the star as a whole (i.e., oscillations commonly considered in connection with Cepheid variation) are the periodic disturbances which are acting. This explains at once that for Cepheids the period-density relation ($P^2 \cdot \rho$ = Constant) holds, since the period of the internal oscillations and of the relaxation oscillations are the same.[9] In this connection it is important to notice that this period-density relation apparently does not hold for the SS Cygni stars, which have long average periods but probably high mean densities, because of the low luminosity and the high surface temperature. In fact, for these pure relaxation oscillations this relation would not be expected to hold.

On the basis of these considerations we conclude *that the period-density relation should hold for the strictly periodic variables*, since both this relation and the periodicity have the same origin, namely, pulsations of the star as a whole, which govern the period of the relaxation oscillations. But, even if the pulsations of the interior are harmonic, there is no reason for the light-curve to be sinusoidal, this being determined by the relaxation phenomenon. The italicized statement has been confirmed by observation.

---

[9] According to our previous discussion, there is a possibility that the relaxation period is a multiple of the internal pulsation period; however, in that case it is likely that the multiple is small, since large multiples would lead to irregularities in the period if small disturbances are present. According to this view, the period-density law might show a certain dispersion, but hardly enough to be established by means of the crude observational data on densities now available.

An investigation into the details of the relaxation mechanism in the stellar envelope, which is probably related to the ionization of hydrogen and of other abundant elements, is beyond the scope of this paper.

It is a pleasant duty to thank Dr. G. P. Kuiper for his assistance in the preparation of this manuscript.

YERKES OBSERVATORY
February 4, 1939

NOTE

a) In the *Quarterly Journal of Mathematics* of Oxford, October, 1933, E. A. Milne has published an interesting article: "The Energetics of Non-steady Stars with Application to Cepheid Variation." The oscillations discussed by Milne form a particular type of maintained oscillations, namely, the case in which the energy supply is constant. He finds the oscillations nonsinusoidal and ever repeating and identifies Cepheid variation as an oscillation of this type.

b) An instructive example of an induced relaxation oscillation is given by a pendulum clock. Here the relaxation system is formed by the escapement, while the pendulum forms the sinusoidal system. The strict periodicity of the escapement is guaranteed by the pendulum. The behavior of the escapement illustrates its relaxation character.

PHOTOELECTRIC OBSERVATIONS OF ϕ PERSEI

F. E. ROACH

ABSTRACT

Observations of ϕ Persei during the latter part of 1938 do not indicate an eclipse during the abnormal spectroscopic phase, although the star appears to vary in an irregular manner. Changes in the star's color are recorded.

Recent observations of ϕ Persei made with the photoelectric photometer of the Steward Observatory are collected in Table 1.

TABLE 1

Date JD2429+	Δ mag ϕ And−ϕ Per	Δ mag ϕ Per−μ And	Color	Spectral Class (from Color)
194	0.169(3)	....	−0.50	B3.5
200	.165(6)	....	.48	B4.5
201	.177(3)	0.044(1)	.50	B3.5
207	.189(5)	....	.62	O
214	.156(2)	....	....	....
219	.144(3)	....	....	....
221	.156(5)	.054(2)	.41	B8
226	.152(2)	....	....	....
228	.171(2)	....	....	....
229	.154(3)	.052(1)	.39	B9.5
235	0.155(2)	0.035(3)	.66	O
297	....	....	−0.52	B2

Columns 2 and 3 include a correction for extinction according to the formula

$$\text{Differential extinction} = 0.36\Delta \sec z \text{ mag.}$$

Within the parentheses is given the number of sets entering into the mean. A set consists of eight galvanometer readings on the variable and eight on the comparison star.

The color observations of column 4 have been corrected to the zenith by the formula

$$\Delta \text{ color} = -0.072 (\sec z - 1) .$$

A minus color indicates a greater response through the blue filter than through the yellow. The blue filter is gelatin between glass,

TABLE 2

COLORS OF CALIBRATION STARS

H.D.	SPECTRUM	COLOR		H.D.	SPECTRUM	COLOR	
		Steward	Washburn			Steward	Washburn
18,519; 20 . . .	A3s	−0.30	−0.07	76,294	G5	+0.54	+0.52
20,150	A0	− .40	− .10	82,395	G9	+0.62	0.59
48,329	G8	+ .91	+ .82	83,808; 9 . .	F5p	+0.04	0.18
56,986	A7	− .18	+ .07	84,194	M2	+1.14	0.99
57,927	F0	− .18	+ .11	84,441	G0	+0.31	0.39
58,207	G8	+ .50	+ .54	87,837	K5	+0.99	0.89
58,728	F3	− .02	+ .15	89,025	F0	−0.14	0.06
59,294	K3	+ .90	+ .74	89,449	F5	−0.02	0.18
60,522	K6	+ .98	+ .94	91,232	M2	+1.13	1.10
62,345	G7	+ .48	+ .49	96,097	F5	−0.12	0.06
74,739	G5	+ .40	+ .41	99,028	F4	−0.06	0.11
74,874	F9	+0.20	+0.28	102,212	M1	+0.90	+0.90

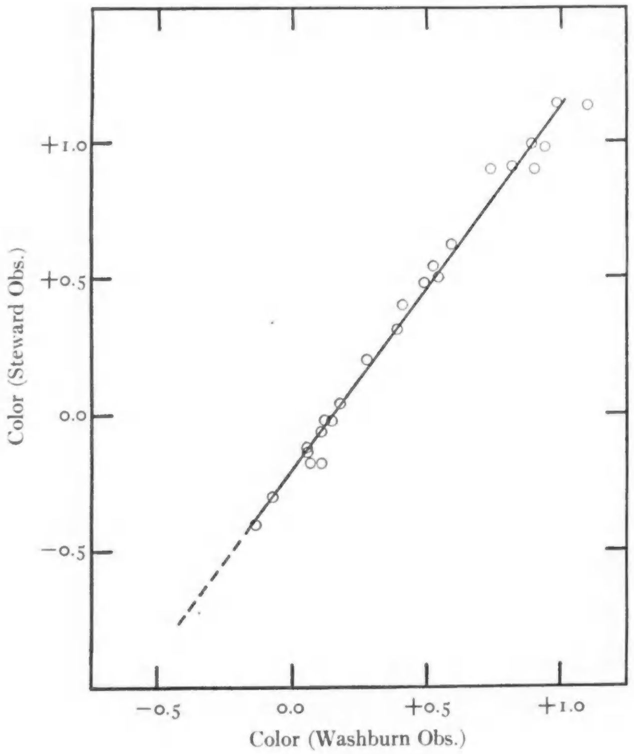

FIG. 1

Wratten No. 35. The yellow filter is the same type, No. 4. The optical path includes one reflection by silver (the main mirror), one reflection by aluminum (the Newtonian flat), the above-mentioned filters, a plate-glass window in the photometer's vacuum chamber, and the quartz bulb of the photoelectric cell. Although the effective wave length of this combination is not known for either filter, an empirical calibration has been made, using a number of the stars in Table 5 of the *Publications of the Washburn Observatory*, Volume **15**, Part V. The calibration data of Table 2 have been plotted in Figures 1 and 2, from which the spectral classes corresponding to the

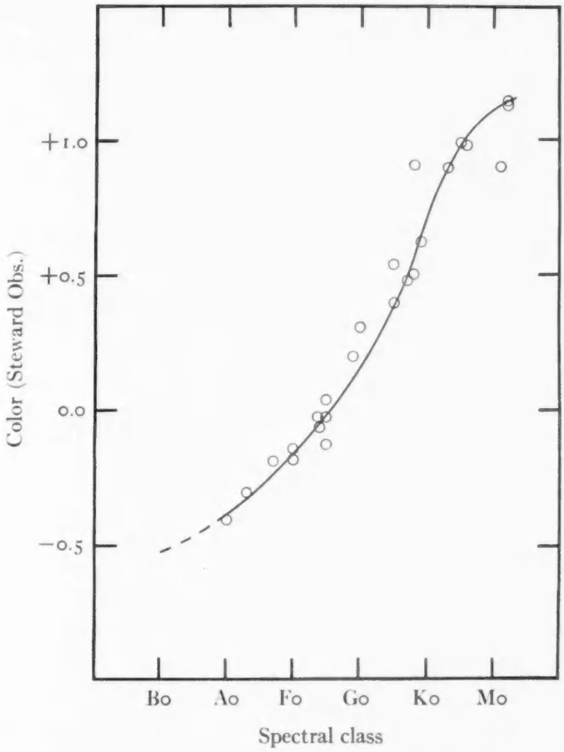

FIG. 2.—Steward Observatory colors plotted against spectral class. The extrapolation is based upon the calibration of Fig. 1 and upon Table 1 of *Pub. Washburn Obs.*, **15**, Part V, 1934.

observed colors of ϕ Persei are determined for column 5 of Table 1. The color changes may, however, be due to variable emission lines rather than to a change in the distribution of light in the continuous spectrum. These observations were made at the suggestion of Dr. Struve and Dr. Elvey. The former has secured a series of spectrographic observations at the Yerkes Observatory, the latter a series of photoelectric observations at the McDonald Observatory.

STEWARD OBSERVATORY
UNIVERSITY OF ARIZONA
February 1939

THE TEMPERATURE OF THE SOLAR CHROMOSPHERE

LEO GOLDBERG

ABSTRACT

The theoretical strengths of the diffuse triplet lines of *He* I have been employed in connection with Menzel and Cillié's measures of 1932 chromospheric lines in an attempt to determine the excitation temperature of the solar chromosphere. The temperature appears to increase with the height, ranging from 4300° for the chromospheric slab 670 km above the solar limb to 6700° for a height of 2330 km.

The diffuse singlet lines of *He* I appear to be anomalously faint relative to the diffuse triplets. The suggestion is made that, in a rarefied chromosphere, the combination of the metastability of the 2^3S level and a possible excess of ultraviolet radiation in the region at 500 A may account for the relative faintness of the singlets.

A great deal of attention has been devoted lately to the determination of ionization and excitation temperatures in the solar atmosphere. Menzel, Baker, and Goldberg[1] and R. B. King[2] have independently arrived at a temperature of 4400° for the reversing layer from studies of metallic absorption lines, while Menzel and Cillié[3] have found evidence for chromospheric temperatures as high as 10,000° from the hydrogen lines and 18,000° from the intensity of λ 4686 of ionized helium. The indications are that the solar radiation deviates from that of a black body at 6000° and that the deviations vary from one spectral region to the other. The temperatures derived from the lines of different elements appear to depend upon the ionization potentials of these elements.

In this note the measures of line intensities in the diffuse series of neutral helium that were obtained by Menzel and Cillié[4] from 1932 eclipse spectra will be utilized in an effort to determine the excitation temperature of the chromosphere and the variations in the temperature with height in the chromosphere. The helium intensities consist of determinations of the energy emitted per second in all directions by a centimeter-wide slice of the chromosphere above the moon's limb. It is understood, of course, that a temperature calculated from such measures represents an average over each chromospheric slab. The observational data for the diffuse series are shown in Table 1 for four different chromospheric heights: 670, 1500, 1730, and 2330 km. The measures were made for two chromospheric regions: region *a*, which is representative of the chromosphere generally, and region *b*, which appears to be one of unusually high excitation.

---

[1] *Ap. J.*, **87**, 81, 1938.

[2] *Ap. J.*, **87**, 40, 1938.

[3] *Harvard Circ.*, No. 410, 1935.

[4] *Ibid.*

TABLE 1

HELIUM LINE-INTENSITIES FOR THE 1932 CHROMOSPHERE
(log E)

λ	670*a*	1500*a*	2330*a*	1730*b*
5876	15.06	14.63	14.11	14.44
4472	14.21	13.84	13.45	....
4026	13.40	13.18	12.87	13.08
3820	12.96	12.81	12.50	12.83
3705	12.77	12.61	....	12.57
3634	12.40	12.21	....	....
4922	12.92	12.84	....	....
4388	12.52	12.17	....	....
4144	12.67	12.26	....	....
4009	12.12	....	....	....

If the possible effects of self-reversal are neglected, the monochromatic energy emitted per second in a chromospheric slab 1 cm wide, as a result of a spontaneous transition from level n to level n', is given by

$$E = N_n A_{nn'} h\nu_{nn'} , \qquad (1)$$

where N_n is the number of atoms in level n, $A_{nn'}$ is the Einstein coefficient in sec^{-1}, and $\nu_{nn'}$ is the frequency, also in sec^{-1}. If we assume that the populations of atoms in the high states of helium follow a Boltzmann distribution, we may write

$$N_n = \text{constant} \times \bar{\omega}_n e^{-\chi_n/kT} , \qquad (2)$$

where $\bar{\omega}_n$ is the weight of level n.

We now substitute (2) in (1) and take the logarithm of the resulting expression, obtaining

$$\log E = \text{constant}' + \log A_{nn'} + \log \bar{\omega}_n + \log \nu_{nn'} - \frac{5040}{T} \chi_n . \qquad (3)$$

If we set

$$\log E' = \log A_{nn'} + \log \bar{\omega}_n + \log \nu_{nn'} , \tag{4}$$

we have

$$\log \frac{E}{E'} = \text{constant}' - \frac{5040}{T} \chi_n . \tag{5}$$

Values of $A_{nn'}$ have been computed by Goldberg.[5] The quantity $\log E/E'$ may, therefore, be calculated from the observed values of $\log E$ and the computed values of $\log E'$. If for each line we then plot $\log E/E'$ against χ_n, the excitation potential of the upper level, the points should fall on a straight line, if the assumption of a Boltzmann distribution is correct. The slope of the line is, of course, $-5040/T$, and, accordingly, the measured slope yields a determination of T, the excitation temperature. The values of $\log E/E'$ for the different heights are shown in Table 2. In Figure 1, the tabulated values of $\log E/E'$ have been plotted against χ_n for each value of the height. The crosses represent the triplets, and the dots the singlets. The triplet points follow the straight-line relationship very well. The singlet lines 4922 and 4388 seem anomalously faint compared with the triplets, while 4144 is too strong. The latter line is, however, badly blended with an *Fe* I line. The straight lines in Figure 1 were fitted to the triplet points by the method of least squares.

TABLE 2

VALUES OF LOG E/E' AND LOG E'

λ	χ_n	$\log E'$	670*a*	1500*a*	2330*a*	1730*b*
5876	23.0	23.70	− 8.64	− 9.07	− 9.59	− 9.26
4472	23.6	23.43	9.22	9.59	9.98	....
4026	23.9	23.16	9.76	9.98	10.29	10.08
3820	24.1	22.90	9.94	10.09	−10.40	10.07
3705	24.2	22.75	9.98	10.14	....	−10.18
3634	24.3	22.56	10.16	10.35	....	....
4922	23.6	22.79	9.87	9.95	....	....
4388	23.9	22.49	9.97	10.32	....	....
4144	24.1	22.22	9.55	− 9.96	....	....
4009	24.2	22.05	− 9.95	....	....	....

---

[5] *Ap. J.*, in press.

The slopes and temperatures deduced from these lines are given in Table 3.

From Table 3 we see that the excitation temperatures increase with height in the chromosphere. The temperature for region *b*, the "superexcited" region, is not too well determined, because of the relative scarcity of line intensities there, but the derived temperature in this region seems to be about 1000° higher than that at the corresponding height in the normal region. The apparent reversal of the temperature gradient is peculiar. The result cannot be attributed to the neglect of self-reversal in the inner chromosphere, for, in applying corrections for this effect, we should have to increase the observed intensities of the strong lines of the diffuse series and therefore to steepen the intensity gradient. Since the temperature depends inversely on the intensity gradient, a correction for the possible effects of self-reversal would decrease the derived temperature in the inner chromosphere and would consequently steepen the negative temperature gradient.

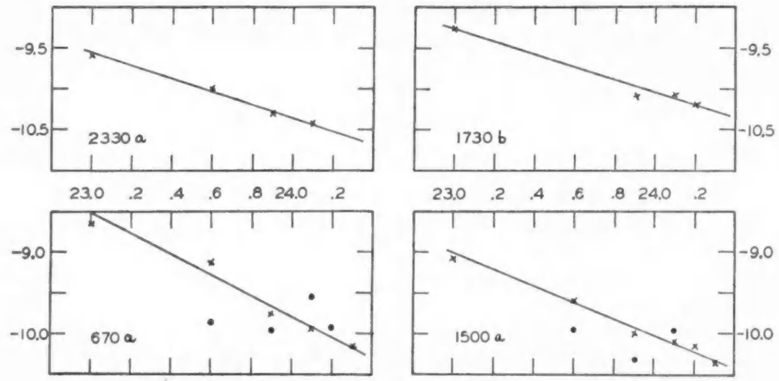

FIG. 1.—Variation of log E/E' with excitation potential. The crosses represent the triplets; the dots, the singlets of the *He* I diffuse series. The ordinates are log E/E'; the abscissas are χ_n.

The neutral helium temperatures are considerably lower than the values of 10,000° and 18,000° found by Menzel and Cillié[6] for hydrogen and ionized helium, respectively. It must be remembered, however, that these temperatures are essentially ionization temperatures, representing the radiation temperatures at 912 A and 243 A necessary to reproduce the observed numbers of ionized hydrogen and doubly ionized helium atoms, whereas the temperatures derived from the neutral helium lines are those necessary to reproduce the observed populations of the neutral helium levels and may perhaps be regarded as electron temperatures.

---

[6] *Op. cit.*

The intensities of the 4922 and 4388 singlet lines are strikingly low. Probably 4144 is likewise too faint, its apparent strength arising from blending with an *Fe* I line. Struve[7] has suggested that the combination of two factors, (*a*) the metastability of the lowest triplet level of helium and (*b*) the great dilution of ionizing radiation in the atmospheres of supergiant O and B stars, may result in an overpopulation of the triplet levels of helium and a consequent relative weakening of the singlet lines. The dilution of radiation in the solar chromosphere cannot, however, be regarded as at all comparable with that prevailing in the distended atmospheres of supergiant stars. It is possible that an excess of ultraviolet solar radiation may be responsible for the faintness of the diffuse singlets. The lowest triplet level of helium is practically stable, in so far as spontaneous radiation is concerned. Once an atom arrives in this level, it can be removed only by excitation to another triplet level, by ionization to the continuum, or by collision. In a rarefied chromosphere collisions are infrequent, and it is possible that two kinds of helium atoms may exist almost independently in such an atmosphere: those in singlet levels and those in triplet levels. The ionization potential from the 2^3S level is about 6 volts; that from the ground state, about 25 volts.

TABLE 3

VARIATION OF TEMPERATURE WITH HEIGHT IN THE CHROMOSPHERE

Height	Slope	*T*
670*a*	1.18	4300° ± 300° (m.e.)
1500*a*	0.956	5300 ± 300
2330*a*	0.754	6700 ± 500
1730*b*	0.770	6500 ± 800

---

[7] *Ap. J.*, **82**, 252, 1935.

These considerations mean that the radiation effective in ionizing the "triplet" helium atoms originates in the spectral region around 2000 A, while the ionizing radiation for the "singlet" atoms comes from the region around 500 A. If, now, the solar spectral energy curve simulates that of a black body at 6000°, the ionization formula shows that the relative populations of 1^1S and 2^3S will be given by a Boltzmann distribution; but, if there exists an excess of ultraviolet radiation in the 500 A region, the relative populations of the singlet levels will be depleted and, consequently, the singlet lines will be weakened with respect to the triplets.

If the foregoing hypothesis is correct, then the relative populations of the excited singlet levels of helium should still follow a Boltzmann distribution at the temperature deduced from the relative populations of the triplet levels. The verification of this supposition, as well as of the general conclusions of this paper, must await the completion of the measures of 1936 flash spectra obtained by the Harvard-Massachusetts Institute of Technology expedition to Siberia. It is expected that these measures will include the leading member of the helium diffuse singlet series at λ 6678 and will consequently afford a more reliable basis for studying the behavior of the *He* I singlets.

In conclusion, it is a pleasure to record my appreciation of the many stimulating discussions of chromospheric problems I have had with Dr. Menzel.

Harvard Observatory
December 9, 1938

REVIEWS

Stellar Dynamics. By W. M. Smart. Cambridge University Press, 1938. Pp. viii+434. Figs. 75. 30*s*.

Our knowledge of the kinematics and dynamics of stellar motions in the galaxy has increased enormously during the last forty years; and if our present understanding of the state of stellar motions (at least on the kinematical side) has some measure of completeness, it is in a large measure due to the labors of those who have taken upon themselves the immense task of determining the radial velocities, the proper motions, and the parallaxes of the stars. At the same time it would not be fair to minimize the influence which the theoretical interpretations of the observational material has exerted even in the matter of directing the course of the purely observational researches. Indeed, it can well be argued that a clear understanding of the meaning and content of the current theories of stellar kinematics and dynamics is essential for the future progress of the subject, and Professor Smart's book is eminently suitable for providing this background to the student and the investigator.

In the book under review the author has successfully collected together in a coherent form all those theoretical investigations which have bearing on the methods of analysis of the stellar motions. The book can be roughly divided into three parts: the kinematics of the stellar motions of the near-by stars (chaps. ii–v); the applications of the derived kinematics to the other problems of stellar statistics (chaps. vi–viii); and, finally, the dynamics of stellar systems and the theory of the rotation of the galaxy (chaps. ix–xii). Further, there is an introductory chapter which is devoted to a brief outline of the relevant facts of observations (parallaxes, proper motions, radial velocities, Hertzsprung-Russell diagram, the mass-luminosity relation, etc.) and some elementary theoretical developments (equatorial and galactic linear components of a stellar velocity, methods for correcting the observed frequency function for accidental errors, etc.).

The discussion of the kinematics of stellar motions of the near-by stars opens with the consideration of the following fundamental problem. Suppose that the individual motions of the stars with respect to a fixed frame of reference are distributed according to Maxwell's law:

$$dN = \frac{Nh^3}{\pi^{3/2}} e^{-h^2(u^2+v^2+w^2)} du dv dw \; ; \qquad (1)$$

suppose, further, that an observer on one of the stars (the sun) determines the transverse and the radial velocities of the other stars. What would be the systematics of the motions (relative to himself) that he would derive? This question is considered in chapter ii from various angles and leads to the discussion of some of the very characteristic aspects in the analysis of stellar motions: the construction of drift-curves (which give the angular distribution of the proper motions in small regions of the sky), the evaluations of the mean transverse and radial speeds (relative to the observer) for different regions of the sky, etc. All these discussions involve the notion of the "solar motion," i.e., the motion of the observer relative to the frame of reference in which the individual motions of the stars, (u, v, w), have the assumed Maxwellian distribution.

The notion of the solar motion already introduced in chapter ii is seen to be quite fundamental. If we consider a group of stars, then the specification of the geometrical centroid of their motions is quite elementary. The motion of the sun with respect to the corresponding frame of reference is the solar motion. Strictly speaking, therefore, solar motion is defined only with reference to a specified set of objects. However, the significance of this notion arises from the circumstance that the near-by stars apparently seem to define (approximately) a unique local standard of rest with respect to which the sun has a definite velocity (19.4 km/sec). (It should be pointed out, even at this stage, that it is very well possible for the local standard of rest to have a motion with respect to a more fundamental standard of rest; but these are questions which are considered at a later stage of the book.)

In chapter iii the various methods that have been used for the practical determination of the solar motion with respect to the near-by stars are considered at length. The methods of Bravis and of Airy (based on the knowledge of the proper motions only) are described, and the appropriate equations of condition are set up. The method based on the radial velocities (described later in the chapter) should really take precedence over the other methods, since it is direct and elucidates the fundamental nature of the problem more explicitly. After the consideration of these methods, a discussion of the υ and the τ components of the proper motions (toward and at right angles to the direction of the antapex) follows. The chapter concludes with the description of a method for combining the motions in quite large regions of the sky (900–1200 square degrees) and correcting suitably for the practical determination of the solar motion. This method (due to Smart himself) has already come into general use.

Chapters iv and v are concerned with the phenomenon of star-streaming. The situation that is encountered here can perhaps be best described as follows: With respect to the local centroid, the motions of the near-by stars have a random character, i.e., in any given direction the number of stars with positive velocities equals the number of stars with negative velocities (in any specified range of velocities $|dv|$). On the other hand, the mean speed $\bar{R}$ is a function of the direction considered. The direction of the maximum mean speed $\bar{R}_{\max}$ defines the vertex of star-streaming. Further, the direction of the vertex of star-streaming is (approximately) an axis of symmetry, i.e., the mean speed $\bar{R}$ in any given direction depends only on the angle χ which this direction makes with the direction of the vertex. This state of affairs can be described in one of the two following ways.

In the first method (due originally to Kapteyn) we assume that the stars can be formally regarded as belonging to one of two groups. Each group by itself will define a standard of rest—the centroid of the motions of each of the two groups. The definition of the local standard of rest, however, requires that with respect to this standard of rest (defined by all the stars) the centroids of the motions of the two groups move in opposite directions with velocities u_1 and u_2 such that $N_1u_1 + N_2u_2 = 0$, where N_1 and N_2 are the numbers of stars in the two groups. The direction of u_1 (or u_2) will define the direction of the vertex of star-streaming. On this interpretation the mean speed $\bar{R}$ in a direction making an angle χ with the direction of the vertex is given by (§ 4.82)

$$\bar{R}(\chi) = \frac{1}{h\sqrt{\pi}} \{\alpha_1 F(hu_1 \cos \chi) + (1 - \alpha) F(hu_2 \cos \chi)\} , \qquad (2)$$

where

$$F(x) = e^{-x^2} + 2x \int_0^x e^{-x^2}\, dx , \qquad (3)$$

$1/h$ is the dispersion of the velocities (assumed to be equal for the two groups), and α is the fraction of the number of stars that belongs to group 1. As is to be expected, $\bar{R}$ has the maximum for $\chi = 0$ (and 180°) and the minimum for $\chi = 90°$ (and 270°). An analysis of the observed motions of the stars on the basis of this interpretation will lead to a determination of the vertex of star-streaming, the direction and magnitude of the solar motion, u_1, u_2, and $1/h$. The methods that have been developed by Eddington and Smart for the practical determination of the quantities referred to are described in detail in chapter iv. A noteworthy feature is the illustration of these methods by the actual working-out of numerical examples.

In the second method (due to Schwarzschild) of interpreting the motions of the near-by stars we argue as follows: Since in any specified direction we have a random distribution of velocities, we may anticipate a Gaussian distribution of velocities:

$$f(\rho) = \frac{j}{\sqrt{\pi}} e^{-j^2\rho^2}, \tag{4}$$

where $f(\rho)$ defines the frequency function of the velocities ρ in the specified direction. The mean speed in the direction considered is

$$\bar{R} = \frac{1}{j\sqrt{\pi}}. \tag{5}$$

The existence of star-streaming requires that $1/j$ is a function of direction and that it has a maximum in the direction of the vertex and a minimum at right angles to this direction. A simple formula which suggests itself is

$$\frac{1}{j^2} = \frac{1}{H^2} \sin^2 \chi + \frac{1}{K^2} \cos^2 \chi \qquad (H > K). \tag{6}$$

Equation (6) gives a very simple variation of the dispersion of the velocities with direction. This is the basis of Schwarzschild's spheroidal theory. Equation (6) is equivalent to the assumption

$$f(u, v, w) = \frac{KH^2}{\pi^{3/2}} e^{-K^2u^2-H^2(v^2+w^2)}, \tag{7}$$

where the direction of u is assumed to be in the direction of the vertex of star-streaming.

A numerical comparison of (2) and (6) shows that any "smooth" variation of $\bar{R}$ with χ can be represented adequately by either of these two equations. Equation (2) has, however, a greater degree of flexibility. This arises chiefly from the fact that in equation (2) we have three disposable constants (namely, h, u_1, and a), while in equation (6) we have only two disposable constants (namely, H and K). But, as Professor Smart shows, the observations are unable to decide between the alternative interpretations. Schwarzschild's method is, however, characterized by greater simplicity and, as such, has been the basis for most of the subsequent dynamical investigations.

In chapter v the methods for determining the direction of star-streaming, the ratio of the axes, K/H, the magnitude and direction of the solar motion, and H (or K) are fully explained. In this chapter (as in the preceding one) two methods—a trial-and-error and an analytical method—are described and illustrated by numerical examples. These chapters (ii–v) on stellar kinematics are, in many ways, the most attractive in the whole book.

We may notice that on the basis of equation (7) it is customary to adopt for f the more general expression

$$f(u, v, w) \equiv f(au^2 + bv^2 + cw^2 + 2fvw + 2gwu + 2huv) \,, \qquad (8)$$

where f is an arbitrary function of the argument on the right-hand side of (8). In equation (8), a, b, c, f, g, and h are the so-called "coefficients of the velocity ellipsoid." For most practical purposes it would be sufficient to use

$$f = \text{constant} \cdot e^{-(au^2+bv^2+cw^2+2fvw+2gwu+2huv)} \,. \qquad (9)$$

This more general case is also considered in chapter v, and the methods to be used for the practical determination of the coefficients of the velocity ellipsoid are also outlined. The spheroidal theory (based on eq. [7]) appears, however, to be quite sufficient for the adequate representation of the observational material.

Chapter vii, on "Statistical Parallaxes," is mainly concerned with the application of the kinematics derived in the two earlier chapters to this problem. Thus, if $\bar{\tau}$ is the mean arithmetical value of the τ-component of the proper motions of a group of stars (either in a small region of the sky or distributed uniformly over the whole sky), we have

$$p = 4.74 \, \frac{\bar{\tau}}{\bar{R}} \,, \qquad (10)$$

where $\bar{R}$ is the mean radial speed (in km sec^{-1}) for the stars which are considered. If there were no star-streaming, $\bar{R}$ would be the same for all regions of the sky. But the existence of star-streaming makes $\bar{R}$ a function of the angular distance of the region considered from the vertex. This variation can be taken into account by the so-called "factor of exaggeration," defined suitably. These factors for a uniform distribution over the whole sky, over the galactic equator, and over the parallel of galactic latitude are conveniently tabulated in this chapter. There exist similar considerations when the υ-components are used. The chapter concludes with a discussion of "the correction to absolute magnitude," "the period luminosity relation of the Cepheids," and the methods (due to van Rhijn and Smart) for correcting the accidental errors in the proper motions.

Chapter vii, on the space distributions of the stars derived from the proper motions, considers the effect of the density variations in the neighborhood of the sun on the angular distribution of the proper motions in small regions of the sky. Most of this chapter is devoted to deriving the consequences of Dyson's density law:

$$D(r) = \frac{D_0}{r} e^{-k^2r^2} . \tag{11}$$

This density law is combined with the Schwarzschild spheroidal law for the distribution of velocities. This chapter is perhaps the weakest in the book, and the criticisms that can be urged are of two kinds. First, the idea of combining a frequency distribution of the velocities with respect to an immediate local standard of rest with a density law intended to take into account the distant stars does not appear to be sound in principle. Second, modern investigations have shown the comparative sterility of the analytical methods in the discussion of the space distribution of the stars in the galaxy. On the other hand, the methods described in this chapter can be regarded as illustrative of general principles, and viewed from this point of view the chapter gains in importance.

In chapter viii the fundamental integral equations of stellar statistics are derived and certain general theorems are proved. The problem here is mainly one of finding the frequency function of an absolute characteristic from the observed frequency function of the apparent characteristic; the latter is obtained by effecting a suitable integration over the former, taking into account the effect of distance, density variations, and space absorption. An example of such an integral relation is the one which expresses the luminosity function in terms of the frequency function of apparent magnitudes. This chapter, while it does not go very far in the discussions of concrete applications of the general theory, is still of considerable value in its clear presentation of the foundations of stellar statistics as laid by Schwarzschild. This chapter also includes an interesting account of an elegant investigation of Ambarzumian on the method of deriving the frequency function of the space velocities of stars from the radial velocities (freed from the solar motion).

Chapter ix, on "Star Clusters," paves the way for the subsequent chapters on dynamical principles. This chapter opens with a description of the method for deriving the convergence point of clusters. After a brief account of Trumpler's researches on star clusters the author passes on to the study of globular clusters. Here the emphasis is mainly on the methods that have been developed by von Zeipel, Plummer, and others for deriving the true density law from the observed star counts. The "analogy" with a gas sphere in equilibrium under its own gravitation is used to derive Plummer's density law, which is equivalent to the Schuster-Emden integral for the polytrope $n = 5$. The reviewer, however, feels that such analogies are misleading; at any rate, there seems to be hardly any reason for arguing in terms of "analogies" when it is perfectly feasible to work out a proper dynamical theory (as is, indeed, done in chap. x of the book).

Chapter x, on "Stellar Dynamics," begins with the theory of stellar encounters. On the basis of this theory the fundamental principle of stellar dynamics is stated as follows: The motions of the individual stars are not appreciably affected by other stars which are temporarily in their neighborhoods but are governed by the general gravitational field due to all the stars. In the dynamical investigations the motions of the individual stars are referred to a fundamental frame of reference defined by the motions of all the stars in the system. From the fundamental principle of stellar dynamics it now follows that the problem of finding the distribution function $f(u, v, w, x, y, z)$ reduces to one of solving the equation of continuity regarded as a partial differential equation for f. Once this is understood, Jeans's theorem that f can be any arbitrary function of the first integrals of the equations of motion is seen to be merely an alternative way of stating Liouville's theorem under the circumstances envisaged in stellar dynamics. The equation of continuity is discussed in greater detail for the cases of stellar systems with spherical and axial symmetries. The discussion of the former case leads directly to a dynamical theory of the globular clusters.

Most of the second half of chapter x (pp. 340–355) is devoted to the consideration of "Eddington's theorem." This "theorem" is based on the notion of the "principal velocity surfaces." It is, however, easy to convince one's self that this notion of the "principal velocity surfaces" introduces restrictions of a purely mathematical character on the physical problem which are wholly irrelevant and certainly unnecessary (cf. the reviewer's paper in a forthcoming issue of the *Journal*).

Chapter x concludes with the derivation of the "hydrodynamical equations" of stellar dynamics. These equations are likely to be the starting-point for future investigations.

Chapter xi, on "Galactic Rotation," gives an interesting account of this subject. When the solar motion with respect to the system of the globular clusters is obtained, it is seen at once that the local standard of rest in the neighborhood of the sun has a predominantly circular motion (of about 300 km/sec^{-1}) about the center of the galaxy. The other evidences (the asymmetric drift and the phenomenon of the high-velocity stars) which support the theory of galactic rotation are adequately reviewed. Oort's interpretation of the double wave in the radial velocities and proper motions and the methods for the practical evaluation of the Oort constants A and B are then outlined. This naturally leads to the consideration of the dynamical consequences which result from the observational values of A and B. It is shown, for instance, that the force per unit mass, $K(\bar{\omega})$, at a distance $\bar{\omega}$ from the center of the galaxy can be written as

$$K(\bar{\omega}) = \frac{C}{\bar{\omega}^2} + D\bar{\omega} , \tag{12}$$

which corresponds to the superposition of the gravitational attraction of a central mass and a quasi-elastic field of force arising from a uniform spheroidal distribution of mass. The constants C and D in equation (12) are also evaluated.

The last chapter (xii), on "The Dynamics of the Galaxy," deals primarily with the relation between the phenomenon of star-streaming and the differential rotation of the galaxy. In the first half of this chapter the discussion centers around the derivation of a relation (due to Oort and Lindblad) between the ratio of the axes of the velocity spheroid, the Oort constant A, and the rotational angular velocity ω. This relation is derived by two independent methods: first, from the general dynamical theory and Jeans's theorem, and, second, on the theory of Lindblad, where the character of the orbits described by the individual stars are considered in great detail. This dynamical discussion is followed by an exposition of the investigations of Ogorodnikoff and Milne on the kinematical interpretation of the double wave in the radial velocities and the proper motions. This kinematical investigation is of particular value since it introduces for the first time the general notion of "differential motions." (This notion has already proved fruitful in certain dynamical investigations.) After this kinematical digression we return to some dynamical investigations which have been attempted to explain a possible deviation of the vertex of star-streaming from the direction of the galactic center. The book concludes with a brief section on Oort's recent work on the accelerations perpendicular to the galactic plane.

This summary of some of the more important topics considered in Smart's *Stellar Dynamics* should be sufficient to indicate the range and magnitude of the book under review. There is only one minor criticism which the reviewer would like to make, and that is that we could have hoped for a more consistent scheme of notations throughout the book. This unfortunate lack of uniformity in the choice of symbols makes the reading of the book needlessly difficult in places. But, apart from this, the book is very attractively written and the style is always clear and lucid. This stimulating book is most definitely a very valuable contribution to the current astronomical literature and will have a profound influence on future theoretical investigations.

S. CHANDRASEKHAR

Variable Stars. By CECILIA PAYNE-GAPOSCHKIN and SERGEI GAPOSCHKIN. Cambridge, Mass.: Harvard Observatory, 1938. Pp. xiv+382. $3.25.

The interpretation of the causes of the various kinds of stellar variability is one of the most difficult problems in astronomy. The spectroscropic and photometric data are so varied that generalization has been possible only for a limited number of objects; for the rest, each star may almost be said to belong to its own class of one member.

There can be no doubt that part of this apparent diversity is due to the low accuracy of the observational material for all but a relatively small number of objects. The stars assigned to the RV Tauri group give a good example of this. The population of the group varies widely among different investigators, and the Gaposchkins actually suggest that the prototype itself does not belong in the group as it has been defined in the past.

In such a situation progress can best be made by the making available of additional good, uniform observational data and by laying special emphasis on certain stars which may be considered as representative of their type. This, in a sentence, is what the authors have attempted to do in the book under discussion. A rather ruthless weeding-out of early material of low accuracy was necessary, but such a procedure is justified when new regularities are brought to light.

After an introductory chapter there is a discussion of eclipsing binaries. This chapter is most useful because of the remarks on individual systems of interest; no attempt is made to present at length the general theory of the determination of the orbits. There is a table containing the elements of well-determined eclipsing systems. There follow discussions of long-period variables, the Cepheids, the semiregular, and the irregular variables. Each chapter contains a catalogue of the principal stars assigned to each class, and a number of light-curves are illustrated.

Next come discussions of the novae, the supernovae, and the SS Cygni and R Coronae Borealis groups. The concluding chapters consider variables associated with nebulosity, spectrum variables, and the technique of observation. A great deal of new material is included, and the results already published are brought together in a way that makes them more significant.

It does not seem too much to say that this will become a sort of source book for investigators in the field of variable stars and in other similar fields. So many avenues for investigation are indicated and so many stimulating suggestions are made that it seems certain to affect the activity and the direction of variable star research for years to come. There is no extended discussion of the theories of the causes of variability; for these it is necessary to look elsewhere. The book, as a whole, derives its value principally from the firsthand acquaintance of the authors with their field and from the multitude of descriptions of the behavior of individual objects. Certain details of the treatment will be questioned by some, but there can be no doubt that in the main the authors have done an excellent job and that the book will be of great value both to the general reader and to the active worker in research.

W. W. Morgan

INDEX TO VOLUME 89

SUBJECTS

PAGE

Absolute Magnitudes, for Stars of Spectral Classes G and K, The Relation between Absolute Magnitude and Reduced Proper Motion, and the Mean Errors in the Spectroscopic. *Gustaf Strömberg* 10

Aluminized Mirrors in Astronomical Use, A Survey of the Durability of. *Robley C. Williams* 611

Antares, Wave Lengths in the Spectrum of. *Dorothy N. Davis* . . . 41

B Stars, Note on Emission. *Carl K. Seyfert* 138

Brown, Ernest William, 1866–1938. *Frank Schlesinger* 152

Campbell, William Wallace, 1862–1938. *J. H. Moore* 143

β Capricorni, Spectrographic Elements for. *Roscoe F. Sanford* . . . 333

γ Cassiopeiae, Photoelectric Measures of. *C. M. Huffer* 139

γ Cassiopeiae in the Photographic Region, The Spectrum of. *Ralph B. Baldwin* 255

Chromospheric Eruptions from λ 3300 to λ 11500, The Spectra of Bright. *R. S. Richardson and R. Minkowski* 347

Cluster NGC 752, Proper Motions in the Galactic. *E. G. Ebbighausen* . 431

CN, C_2, *CH*, *NH*, and *OH* in the Solar Reversing Layer, On the Relative Abundance of. *F. E. Roach* 99

Comets and Their Forms, On the Interpretation of the Spectra of. *K. Wurm* 312

Corona Photographs of June 8, 1937, An Optical Study of Solar. *Brian O'Brien, H. S Stewart, Jr., and C. J. Aronson* 26

P Cygni, On the Color of. *Frances Sherman and W. W. Morgan* . . . 509

D-Lines in the Spectrum of the Night Sky, Note on the Explanation of the. *James Franck and Carol Anger Rieke* 463

Diffraction at the Moon's Limb, Photoelectric Observation of. *A. E. Whitford* 472

Eclipsing Binary Systems, The Temperatures of Secondary Components in. *Zdeněk Kopal* 594

Eclipsing Variable of Large Mass, A New. *Sergei Gaposchkin* 125

PAGE

Eclipsing Variable of Large Mass," Note on the Paper "A New. *Sergei Gaposchkin* 322

Electron Affinity in Astrophysics. *Rupert Wildt* 295

Erratum. *Otto Struve and C. T. Elvey* 554

Europium Lines, Temperature Classification of. *Arthur S. King* 377

Gravity at One Place, Variations of. *O. H. Truman* 445

He I λ 5015 in ζ Tauri and φ Persei, The Behavior of. *J. A. Hynek* 552

Helium Lines in Early-Type Stars, A Study of the Equivalent Width of. *Leo Goldberg* 623

Hydrogen, The Physical State of Interstellar. *Bengt Strömgren* 526

Infrared Solar Radiation at the Lowell Observatory. I. Atmospheric Absorption of. *Arthur Adel* 1

Lane-Emden Function $\theta_{3.25}$, The. *S. Chandrasekhar* 116

McDonald Observatory, The 82-Inch Mirror of the. *J. S. Plaskett* 84

Molecular Bands as Indicators of Stellar Temperatures and Luminosities. *W. W. Morgan* 310

Molecular Bands in Stellar Spectra. *N. T. Bobrovnikoff* 301

Molecular Spectra, Intensities of Electronic Transitions in. *Robert S. Mulliken* 283

Molecules, Dissociation, Predissociation, and Recombination of Diatomic. *G. Herzberg* 290

Molecules, Forbidden Transitions in Diatomic. *G. Herzberg* 288

S Monocerotis, The Nebulosity near. *W. W. Morgan and Frances Sherman* 553

S Monocerotis, The Nebulosity near. *G. Van Biesbroeck* 554

N I, Pressure Shifts of Lines of. *Paul W. Merrill* 321

Nebula in Orion, Photograph of a Diffuse. *John A. O'Keefe* 554

Nebula, Second Report on the Expansion of the Crab. *John C. Duncan* 482

Nebulae. VI. The Equations of Radiative Transfer, Physical Processes in the Gaseous. *Lawrence H. Aller, James G. Baker, and Donald H. Menzel* 587

Nebulae, The Spectra of Two Reflection. *J. L. Greenstein and L. G. Henyey* 647

Nebulae, Studies of Diffuse. *J. L. Greenstein and L. G. Henyey* 653

Nebular Spectrograph of the McDonald Observatory, Observations Made with the. *Otto Struve and C. T. Elvey* 119

PAGE

Nebular Spectrograph of the McDonald Observatory. II. Observations Made with the. *Otto Struve and C. T. Elvey* 517

Nebulosities, Photographs of Diffuse. *H. A. Lower* 137

Nebulosities, Photographs of Two Diffuse. *John A. O'Keefe* 136

Period-Luminosity Curve, The Zero Point of the. *Ralph E. Wilson* . . 218

ϕ Persei, Photoelectric Observations of. *F. E. Roach* 669

Planetary Atmosphere, Spectroscopic Studies of. *Arthur Adel* . . . 311

Point-Source Model with Constant Opacity, The. *Philip C. Keenan* . . 499

Prominences and the Sunspot Cycle. *Vinicio Barocas* 486

Proper Motion Stars, Two New White Dwarfs; Notes on. *G. P. Kuiper* . 548

Radial Velocity of 59 d Serpentis, The. *Otto Struve and Alice Johnson* . 136

Reflection Effect in Eclipsing Binary Systems, The. *Zdeněk Kopal* . . 323

Reviews:
  Fabry, Charles. *Œuvres choisies* (O. Struve) 465
  Finkelnburg, W. *Kontinuierliche Spektren* (Thornton Page) . . . 465
  Payne-Gaposchkin, Cecilia, and Sergei Gaposchkin. *Variable Stars* (W. W. Morgan) 687
  Russell, N. H., R. S. Dugan, and J. Q. Stewart. *Astronomy*, Vol. II (O. Struve) 142
  Smart, W. M. *Stellar Dynamics* (S. Chandrasekhar) 679

Rotation Effects, Interstellar Absorption, and Certain Dynamical Constants of the Galaxy Determined from Cepheid Variables. *Alfred H. Joy* 356

59 d Serpentis, The Radial Velocity of. *Otto Struve and Alice Johnson* . 136

Sodium, The Identification and the Origin of Atmospheric. *René Bernard* 133

Solar Chromosphere, The Temperature of the. *Leo Goldberg* 673

Solar Granules, Photometry of the. *Philip C. Keenan* 604

Solar Radiation at the Lowell Observatory. I. Atmospheric Absorption of Infrared. *Arthur Adel* 1

Solar Reversing Layer, On the Relative Abundance of *CN*, C_2, *CH*, *NH*, and *OH* in the. *F. E. Roach* 99

Solar Spectrum, New Lines in the Rock-Salt Prismatic. *Arthur Adel* . . 320

Spectra, Continuous. *George H. Shortley* 295

Spectral Lines, Influence of Pressure and Temperature upon the Absorption and Fluorescence of. *H. Beutler* 294

PAGE

Stars of Spectral Classes G and K, The Relation between Absolute Magnitude and Reduced Proper Motion, and the Mean Errors in the Spectroscopic Absolute Magnitudes, for. *Gustaf Strömberg* 10

Stellar Diameters, A Method for the Determination of. *J. D. Williams* . 467

Stellar Model, The Shell-Source. *C. L. Critchfield and G. Gamow* . . . 244

Stellar Variability and Relaxation Oscillations. *A. J. Wesselink* . . . 659

Sun, The Energy-producing Reaction in the. *G. Gamow* 130

Sunspots, The Relations between Eruptions and. *R. G. Giovanelli* . . 555

Supernovae in IC 4182 and in NGC 1003, The Spectra of the. *R. Minkowski* 156

Taurus. II. The Space Distribution of the Stars, The Galactic Structure in. *S. W. McCuskey* 568

Water Vapor, The Infrared Spectrum of. *David M. Dennison* 292

White Dwarfs: Notes on Proper Motion Stars, Two New. *G. P. Kuiper* . 548

AUTHORS

ADEL, ARTHUR. Atmospheric Absorption of Infrared Solar Radiation at the Lowell Observatory. I 1

ADEL, ARTHUR. New Lines in the Rock-Salt Prismatic Solar Spectrum . 320

ADEL, ARTHUR. Spectroscopic Studies of Planetary Atmospheres . . 311

ALLER, LAWRENCE H., JAMES G. BAKER, and DONALD H. MENZEL. Physical Processes in the Gaseous Nebulae. VI. The Equations of Radiative Transfer 587

ARONSON, C. J., BRIAN O'BRIEN, and H. S. STEWART, JR. An Optical Study of Solar Corona Photographs of June 8, 1937 26

BAKER, JAMES G., DONALD H. MENZEL, and LAWRENCE H. ALLER. Physical Processes in the Gaseous Nebulae. VI. The Equations of Radiative Transfer 587

BALDWIN, RALPH B. The Spectrum of γ Cassiopeiae in the Photographic Region 255

BAROCAS, VINICIO. Prominences and the Sunspot Cycle 486

BERNARD, RENÉ. The Identification and the Origin of Atmospheric Sodium 133

BEUTLER, H. Influence of Pressure and Temperature upon the Absorption and Fluorescence of Spectral Lines 294

PAGE

Bobrovnikoff, N. T. Molecular Bands in Stellar Spectra 301

Chandrasekhar, S. The Lane-Emden Function $\theta_{3.25}$ 116

Chandrasekhar, S. Review of: *Stellar Dynamics*, W. W. Smart . . 679

Critchfield, C. L., and G. Gamow. The Shell-Source Stellar Model . 244

Davis, Dorothy N. Wave Lengths in the Spectrum of Antares . . . 41

Dennison, David M. The Infrared Spectrum of Water Vapor . . . 292

Duncan, John C. Second Report on the Expansion of the Crab Nebula 482

Ebbighausen, E. G. Proper Motions in the Galactic Cluster NGC 752 . 431

Elvey, C. T., and Otto Struve. Erratum 554

Elvey, C. T., and Otto Struve. Observations Made with the Nebular Spectrograph of the McDonald Observatory 119

Elvey, C. T., and Otto Struve. Observations Made with the Nebular Spectrograph of the McDonald Observatory. II 517

Franck, James, and Carol Anger Rieke. Note on the Explanation of the D-Lines in the Spectrum of the Night Sky 463

Gamow, G. The Energy-producing Reaction in the Sun 130

Gamow, G., and C. L. Critchfield. The Shell-Source Stellar Model . 244

Gaposchkin, Sergei. A New Eclipsing Variable of Large Mass . . . 125

Gaposchkin, Sergei. Note on the Paper "A New Eclipsing Variable of Large Mass" 322

Giovanelli, R. G. The Relations between Eruptions and Sunspots . . 555

Goldberg, Leo. A Study of the Equivalent Width of Helium Lines in Early-Type Stars 623

Goldberg, Leo. The Temperature of the Solar Chromosphere . . . 673

Greenstein, J. L., and L. G. Henyey. The Spectra of Two Reflection Nebulae 647

Greenstein, J. L., and L. G. Henyey. Studies of Diffuse Nebulae . . 653

Henyey, L. G., and J. L. Greenstein. The Spectra of Two Reflection Nebulae 647

Henyey, L. G., and J. L. Greenstein. Studies of Diffuse Nebulae . . 653

Herzberg, G. Dissociation, Predissociation, and Recombination of Diatomic Molecules 290

Herzberg, G. Forbidden Transitions in Diatomic Molecules 288

Huffer, C. M. Photoelectric Measures of γ Cassiopeiae 139

PAGE

HYNEK, J. A. The Behavior of *He* I λ 5015 in ζ Tauri and φ Persei . . 552

JOHNSON, ALICE, and OTTO STRUVE. The Radial Velocity of 59 d Serpentis 136

JOY, ALFRED H. Rotation Effects, Interstellar Absorption, and Certain Dynamical Constants of the Galaxy Determined from Cepheid Variables 356

KEENAN, PHILIP C. Photometry of the Solar Granules 604

KEENAN, PHILIP C. The Point-Source Model with Constant Opacity . 499

KING, ARTHUR S. Temperature Classification of Europium Lines . . 377

KOPAL, ZDENĚK. The Reflection Effect in Eclipsing Binary Systems . . 323

KOPAL, ZDENĚK. The Temperatures of Secondary Components in Eclipsing Binary Systems 594

KUIPER, G. P. Two New White Dwarfs; Notes on Proper Motion Stars 548

LOWER, H. A. Photographs of Diffuse Nebulosities 137

MCCUSKEY, S. W. The Galactic Structure in Taurus. II. The Space Distribution of the Stars 568

MENZEL, DONALD H., LAWRENCE H. ALLER, and JAMES G. BAKER. Physical Processes in the Gaseous Nebulae. VI. The Equations of Radiative Transfer 587

MERRILL, PAUL W. Pressure Shifts of Lines of *N* I 321

MINKOWSKI, R. The Spectra of the Supernovae in IC 4182 and in NGC 1003 156

MINKOWSKI, R., and R. S. RICHARDSON. The Spectra of Bright Chromospheric Eruptions from λ 3300 to λ 11500 347

MOORE, J. H. William Wallace Campbell, 1862–1938 143

MORGAN, W. W. Molecular Bands as Indicators of Stellar Temperatures and Luminosities 310

MORGAN, W. W. Review of: *Variable Stars*, Cecelia Payne-Gaposchkin and Sergei Gaposchkin 689

MORGAN, W. W., and FRANCES SHERMAN. On the Color of P Cygni . . 509

MORGAN, W. W., and FRANCES SHERMAN. The Nebulosity near S Monocerotis 553

MULLIKEN, ROBERT S. Intensities of Electronic Transitions in Molecular Spectra 283

O'BRIEN, BRIAN, H. S. STEWART, JR., and C. J. ARONSON. An Optical Study of Solar Corona Photographs of June 8, 1937 26

PAGE

O'KEEFE, JOHN A. Photograph of a Diffuse Nebula in Orion 554

O'KEEFE, JOHN A. Photographs of Two Diffuse Nebulosities 136

PAGE, THORNTON. Review of: *Kontinuierliche Spektren*, W. Finkelnburg 465

PLASKETT, J. S. The 82-Inch Mirror of the McDonald Observatory . . 84

RICHARDSON, R. S., and R. MINKOWSKI. The Spectra of Bright Chromospheric Eruptions from λ 3300 to λ 11500 347

RIEKE, CAROL ANGER, and JAMES FRANCK. Note on the Explanation of D-Lines in the Spectrum of the Night Sky 463

ROACH, F. E. Photoelectric Observations of ϕ Persei 669

ROACH, F. E. On the Relative Abundance of CN, C_2, CH, NH, and OH in the Solar Reversing Layer 99

SANFORD, ROSCOE F. Spectrographic Elements for β Capricorni . . . 333

SCHLESINGER, FRANK. Ernest William Brown, 1866–1938 152

SEYFERT, CARL K. Note on Emission B Stars 138

SHERMAN, FRANCES, and W. W. MORGAN. On the Color of P Cygni . . 509

SHERMAN, FRANCES, and W. W. MORGAN. The Nebulosity near S Monocerotis 553

SHORTLEY, GEORGE H. Continuous Spectra 295

STEWART, H. S., JR., C. J. ARONSON, and BRIAN O'BRIEN. An Optical Study of Solar Corona Photographs of June 8, 1937 26

STRÖMBERG, GUSTAF. The Relation between Absolute Magnitude and Reduced Proper Motion, and the Mean Errors in the Spectroscopic Absolute Magnitudes, for Stars of Spectral Classes G and K . . . 10

STRÖMGREN, BENGT. The Physical State of Interstellar Hydrogen . . 526

STRUVE, O. Review of: *Astronomy*, Vol. II, H. N. Russell, R. S. Dugan, and J. Q. Stewart 142

STRUVE, O. Review of: *Œuvres choisies*, Charles Fabry 465

STRUVE, OTTO, and C. T. ELVEY. Erratum 554

STRUVE, OTTO, and C. T. ELVEY. Observations Made with the Nebular Spectrograph of the McDonald Observatory 119

STRUVE, OTTO, and C. T. ELVEY. Observations Made with the Nebular Spectrograph of the McDonald Observatory. II 517

STRUVE, OTTO, and ALICE JOHNSON. The Radial Velocity of 59 d Serpentis 136

TRUMAN, O. H. Variations of Gravity at One Place 445

PAGE

Van Biesbroeck, G. The Nebulosity near S Monocerotis 554

Wesselink, A. J. Stellar Variability and Relaxation Oscillations . . 659

Whitford, A. E. Photoelectric Observation of Diffraction at the Moon's Limb 472

Wildt, Rupert. Electron Affinity in Astrophysics 295

Williams, J. D. A Method for the Determination of Stellar Diameters . 467

Williams, Robley C. A Survey of the Durability of Aluminized Mirrors in Astronomical Use 611

Wilson, Ralph E. The Zero Point of the Period-Luminosity Curve . 218

Wurm, K. On the Interpretation of the Spectra of Comets and Their Forms 312

Astron. Obs.

JUL 3 1939

JUL 3 1939

VOLUME 89 NUMBER 5

tpi

THE ASTROPHYSICAL JOURNAL

AN INTERNATIONAL REVIEW OF SPECTROSCOPY AND ASTRONOMICAL PHYSICS

Founded in 1895 by GEORGE E. HALE *and* JAMES E. KEELER

Edited by

HENRY G. GALE
Ryerson Physical Laboratory of the
University of Chicago

FREDERICK H. SEARES
Mount Wilson Observatory of the
Carnegie Institution of Washington

OTTO STRUVE
Yerkes Observatory of the
University of Chicago

JUNE 1939

THE RELATIONS BETWEEN ERUPTIONS AND SUNSPOTS - - - *R. G. Giovanelli* 555

THE GALACTIC STRUCTURE IN TAURUS. II. THE SPACE DISTRIBUTION OF THE STARS - *S. W. McCuskey* 568

PHYSICAL PROCESSES IN GASEOUS NEBULAE. VI. THE EQUATIONS OF RADIATIVE TRANSFER - - - *Lawrence H. Aller, James G. Baker, and Donald H. Menzel* 587

THE TEMPERATURES OF SECONDARY COMPONENTS IN ECLIPSING BINARY SYSTEMS - *Zdeněk Kopal* 594

PHOTOMETRY OF THE SOLAR GRANULES - - - - - - - - *Philip C. Keenan* 604

A SURVEY OF THE DURABILITY OF ALUMINIZED MIRRORS IN ASTRONOMICAL USE - *Robley C. Williams* 611

A STUDY OF THE EQUIVALENT WIDTHS OF HELIUM LINES IN EARLY-TYPE STARS *Leo Goldberg* 623

THE SPECTRA OF TWO REFLECTION NEBULAE - *J. L. Greenstein and L. G. Henyey* 647

STUDIES OF DIFFUSE NEBULAE - - - - - - - *J. L. Greenstein and L. G. Henyey* 653

STELLAR VARIABILITY AND RELAXATION OSCILLATIONS - - - *A. J. Wesselink* 659

PHOTOELECTRIC OBSERVATIONS OF ϕ PERSEI - - - - - - - *F. E. Roach* 669

THE TEMPERATURE OF THE SOLAR CHROMOSPHERE - - - - *Leo Goldberg* 673

REVIEWS

Stellar Dynamics, W. M. SMART (S. Chandrasekhar), 679; *Variable Stars*, CECILIA PAYNE-GAPOSCHKIN and SERGEI GAPOSCHKIN (W. W. Morgan), 687.

INDEX - 689

THE UNIVERSITY OF CHICAGO PRESS
CHICAGO, ILLINOIS, U.S.A.

June 1939 Vol. 89, No. 5

THE ASTROPHYSICAL JOURNAL

AN INTERNATIONAL REVIEW OF SPECTROSCOPY AND ASTRONOMICAL PHYSICS

Edited by

HENRY G. GALE
Ryerson Physical Laboratory of the
University of Chicago

FREDERICK H. SEARES
Mount Wilson Observatory of the
Carnegie Institution of Washington

OTTO STRUVE
Yerkes Observatory of the
University of Chicago

WITH THE COLLABORATION OF

WALTER S. ADAMS, Mount Wilson Observatory
JOSEPH S. AMES, Johns Hopkins University
HENRY CREW, Northwestern University
CHARLES FABRY, Université de Paris
ALFRED FOWLER, Imperial College, London
EDWIN HUBBLE, Mount Wilson Observatory
HEINRICH KAYSER, Universität Bonn
ROBERT A. MILLIKAN, Institute of Technology, Pasadena
HUGH F. NEWALL, Cambridge University
FRIEDRICH PASCHEN, Reichsanstalt, Charlottenburg
HENRY N. RUSSELL, Princeton University
FRANK SCHLESINGER, Yale Observatory
HARLOW SHAPLEY, Harvard College Observatory
F. J. M. STRATTON, Cambridge University

Former Editors:

GEORGE E. HALE JAMES E. KEELER EDWIN B. FROST

The Astrophysical Journal is published by the University of Chicago at the University of Chicago Press, 5750 Ellis Avenue, Chicago, Illinois, during each month except February and August. ¶The subscription price is $10.00 a year; the price of single copies is $1.50. Orders for service of less than a full year will be charged at the single-copy rate. ¶Postage is prepaid by the publishers on all orders from the United States, Mexico, Cuba, Puerto Rico, Panama Canal Zone, Republic of Panama, Dominican Republic, Canary Islands, El Salvador, Argentina, Bolivia, Brazil, Colombia, Chile, Costa Rica, Ecuador, Guatemala, Honduras, Nicaragua, Peru, Hayti, Uruguay, Paraguay, Hawaiian Islands, Philippine Islands, Guam, Samoan Islands, Balearic Islands, Spain, and Venezuela. ¶Postage is charged extra as follows: for Canada and Newfoundland, 30 cents on annual subscriptions (total $10.30); on single copies, 3 cents (total $1.53); for all other countries in the Postal Union, 80 cents on annual subscriptions (total $10.80), on single copies, 8 cents (total $1.58). ¶Patrons are requested to make all remittances payable to The University of Chicago Press, in postal or express money orders or bank drafts.

The following are authorized agents:

For the British Empire, except North America, India, and Australasia: The Cambridge University Press, Bentley House, 200 Euston Road, London, N.W. 1, England. Prices of yearly subscriptions and of single copies may be had on application.

For Japan: The Maruzen Company, Ltd., Tokyo.

For China: The Commercial Press, Ltd., 211 Honan Road, Shanghai. Yearly subscriptions, $10.00; single copies, $1.50, or their equivalents in Chinese money. Postage extra, on yearly subscriptions 80 cents, on single copies 8 cents.

Claims for missing numbers should be made within the month following the regular month of publication. The publishers expect to supply missing numbers free only when losses have been sustained in transit, and when the reserve stock will permit.

Business correspondence should be addressed to The University of Chicago Press, Chicago, Illinois.

Communications for the editors and manuscripts should be addressed to: Otto Struve, Editor of THE ASTROPHYSICAL JOURNAL, Yerkes Observatory, Williams Bay, Wisconsin.

The cable address is "Observatory, Williamsbay, Wisconsin."

The articles in this journal are indexed in the *International Index to Periodicals*, New York, N.Y.

Applications for permission to quote from this journal should be addressed to The University of Chicago Press, and will be freely granted.

Entered as second-class matter, January 17, 1895, at the Post-Office, Chicago, Ill., under the act of March 3, 1879.

Acceptance for mailing at special rate of postage provided for in Section 1103, Act of October 3, 1917, authorized on July 15, 1918.

PRINTED IN THE U.S.A.

Astronomical

LANTERN SLIDES

Since 1903, the Yerkes Observatory of the University of Chicago has been reproducing in lantern slides, transparencies, and prints the original astronomical photographs made at Williams Bay.

The lantern slides are uniformly 4×3½ inches in size. The frequent call for small sets of slides for school and lecture purposes has led to the preparation of a list of 100 representative slides (price $62.50), a catalogue of which may be obtained upon request to the University of Chicago Press, 5750 Ellis Avenue, Chicago.

Prints as well as slides can be furnished, and for many subjects window transparencies are also supplied.

For catalogue and further information write

The University of Chicago Press
5750 Ellis Avenue, Chicago, Ill.

19 TRANSPARENCIES
(14X17) from
YERKES OBSERVATORY
at unusual prices

$3.00 each, without ground glass

$4.00 each, with ground glass

POSTAGE AND INSURANCE EXTRA

Professor E. E. Barnard made many of these from photographs obtained by him with the Bruce photographic telescope of Yerkes. Positives, 14×17 inches, enlarged from negatives made with the Bruce photographic telescope of the Yerkes Observatory. These positives are not covered.

α	δ	
2h12m	+57°	Double cluster of Perseus
5 45	+32	Region of Messier 37, in Aurigae
6 2	+24	Region of Messier 35, in Gemini
6 23	+22	In Gemini—M35 and NGC 2175; also trail of Comet 1905 III (Giacobini)
16 20	−23	Region of Rho Ophiuchi
16 55	−32	In Scorpius, near Messier 62; area of dark markings
17 10	−27	In Ophiuchus and Scorpius
17 56	−28	In Sagittarius
17 56	−28	In Sagittarius
17 56	−30	In Sagittarius
18 20	−23	In Sagittarius; area dark markings
18 20	−25	In Sagittarius; area dark markings
18 20	−15	In Aquila and Sagittarius
18 30	−11	In Aquila and Sagittarius
18 40	− 6	Star Cloud in Scutum
18 45	− 6	Star Cloud in Scutum
21 35	+57	In Cepheus
21 36	+56	In Cepheus
21 36	+50	In Cepheus

For complete information on Yerkes material and catalogue, write to:

The University of Chicago Press
5750 Ellis Avenue Chicago, Illinois

POPULAR ASTRONOMY

A magazine now in its forty-sixth year, devoted to the elementary aspects of Astronomy and allied sciences.

Published monthly, except July and September.

Yearly subscription rates: Domestic $4.00; Canadian $4.25; Foreign $4.50.

Address

POPULAR ASTRONOMY
CARLETON COLLEGE
NORTHFIELD, MINNESOTA, U.S.A.

ASTROPHYSICAL MONOGRAPHS

Sponsored by the Editors of the Astrophysical Journal

A series designed to provide a growing library of precise, up-to-date, authoritative material of modern astronomy and astrophysics for astronomers, physicists, mathematicians, and chemists. By combining the advantages of an advanced textbook with the interest of a research narrative, the monographs will serve as reference volumes for astronomers and as manuals for teachers.

Published

AN INTRODUCTION TO THE STUDY OF STELLAR STRUCTURE. By S. CHANDRASEKHAR. 510 pages, 22 pages of engravings, royal 8vo, cloth, $10.00

THE DISTRIBUTION OF THE STARS IN SPACE. By BART J. BOK. 124 pages, royal 8vo, paper bound, $2.50

In Preparation

THE MASSES OF THE STARS. By HENRY NORRIS RUSSELL

SPECTRA OF LONG PERIOD VARIABLE STARS. By P. W. MERRILL

THE UNIVERSITY OF CHICAGO PRESS

CAMBRIDGE
UNIVERSITY PRESS

STELLAR DYNAMICS

***by* W. M. Smart $8.50**

This new book is essentially mathematical in character. After an introductory chapter, the mathematical theory of a single star-drift is given in detail, followed by a chapter on the solar motion. Chapter IV deals with the theory of the two star-streams and Chapter V with Schwarzschild's ellipsoidal hypothesis relating to stellar motions; in these two Sections special attention has been given to the technical methods of analysing the observational material. Chapter VI discusses various methods of deriving mean parallaxes of various groups of stars; this is followed by an examination of the methods of investigating the space-distribution of the stars from a knowledge of their proper motions. The next chapter is devoted to the general theorems of stellar statistics. In Chapter IX various investigations concerning open and globular clusters and the absorbing cloud are given. The last three chapters deal with the dynamics of stellar systems in general, galactic rotation and the dynamics of the Galaxy.

MACMILLAN